COSMOS: Curation Of Scientific MOdelS of the Earth system from publications

Theo Rekatsinas, Shanan Peters, Miron Livny
University of Wisconsin-Madison

$$F_{CaCO_3} = F_{CaCO_3,0}\left(1 + k_{Ca}\left(T - T_0\right)\right)\frac{R}{R_0}\frac{P}{P_0}$$

$$F_{CaSiO_3} = F_{CaSiO_3,0}\, e^{\frac{1000E_a}{RT_0^2}(T-T_0)}\left(\frac{R}{R_0}\right)^{\beta}\frac{P}{P_0}$$

Variables	PICs of PMIP2 and CMIP5–PMIP3
Potential temperature (°C), N. Atlantic	2.9 to 6.4[a]
Potential temperature (°C), S. Atlantic	−1.6 to 2.0[c]
Salinity, N. Atlantic	34.8 to 35.5[a]
Salinity, S. Atlantic AMOC	34.6 to 35.0[c]
($1\,Sv = 10^6\,m^3\,s^{-1}$)	12.64 to 23.02[e]

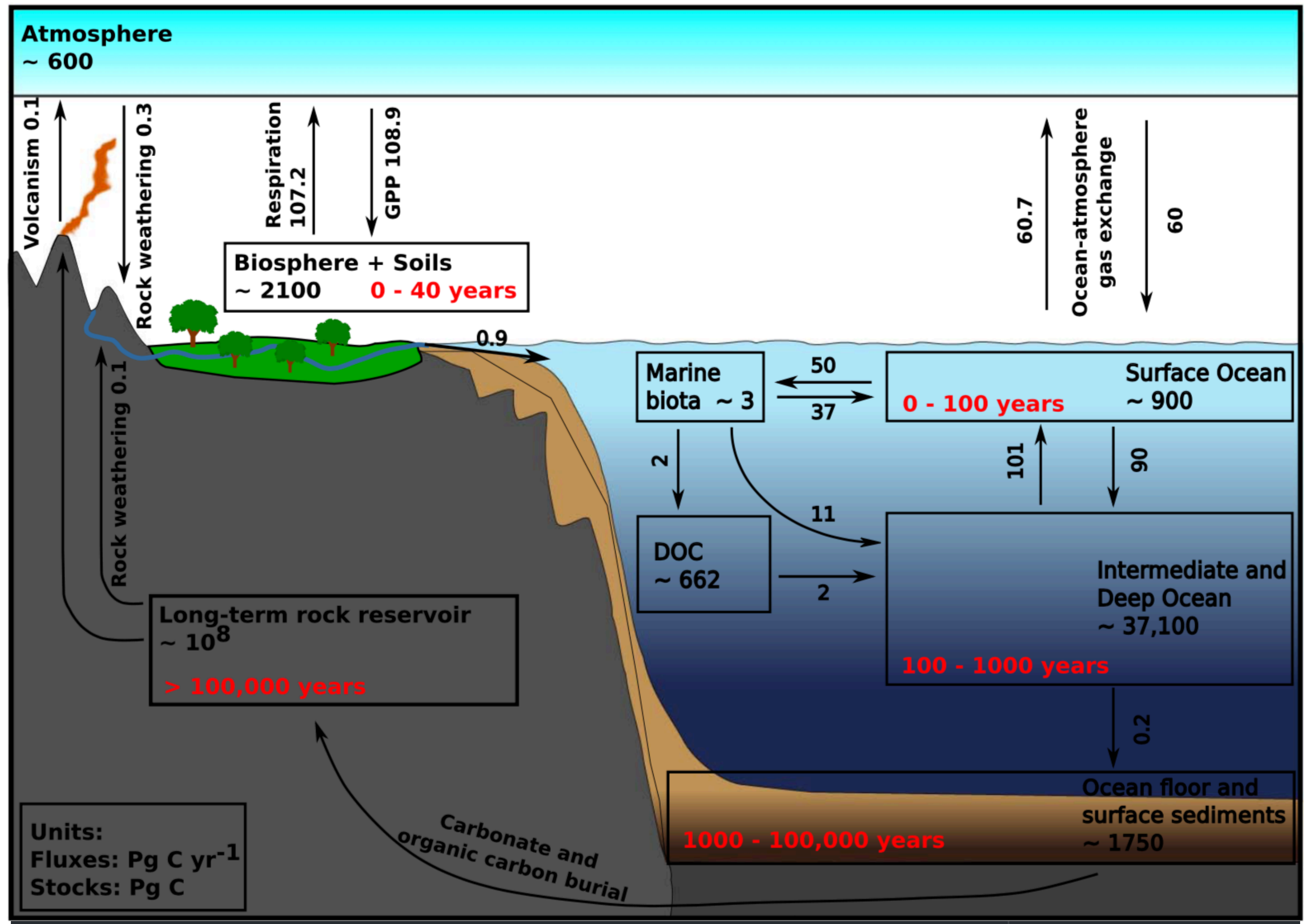


```
Dbio = 5.2*(10.0**(0.7624-0.0003972*dum_D))     !bioturbation coefficient (cm2/yr) - after
Dunbio = 0.01                                   ! "diffusion coefficient" for unbioturbate
tort = 3.0                                      ! tortuosity (-)
irrigationFactor = 1.0

gamma = 0.9                                     ! fraction of NH4 that is oxidised in oxi
gammaH2S = 0.95                                 ! fraction of H2S that is oxidised in oxi
gammaCH4 = 1.0      !0.99                       ! fraction of CH4 that is oxidised at SO4
satSO4 = 0.0                                    ! SO4 saturation
```

GENIE:
Grid ENabled Integrated Earth system model

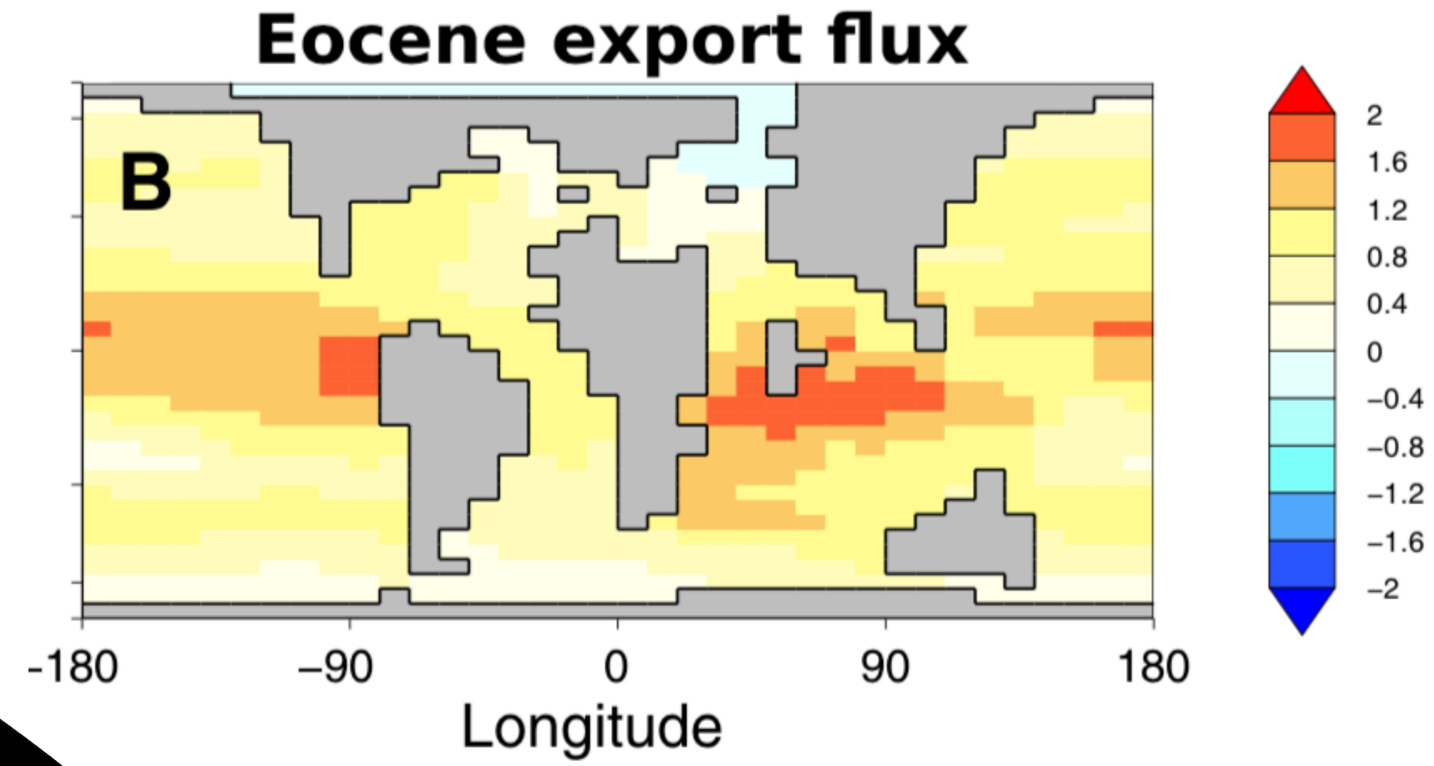

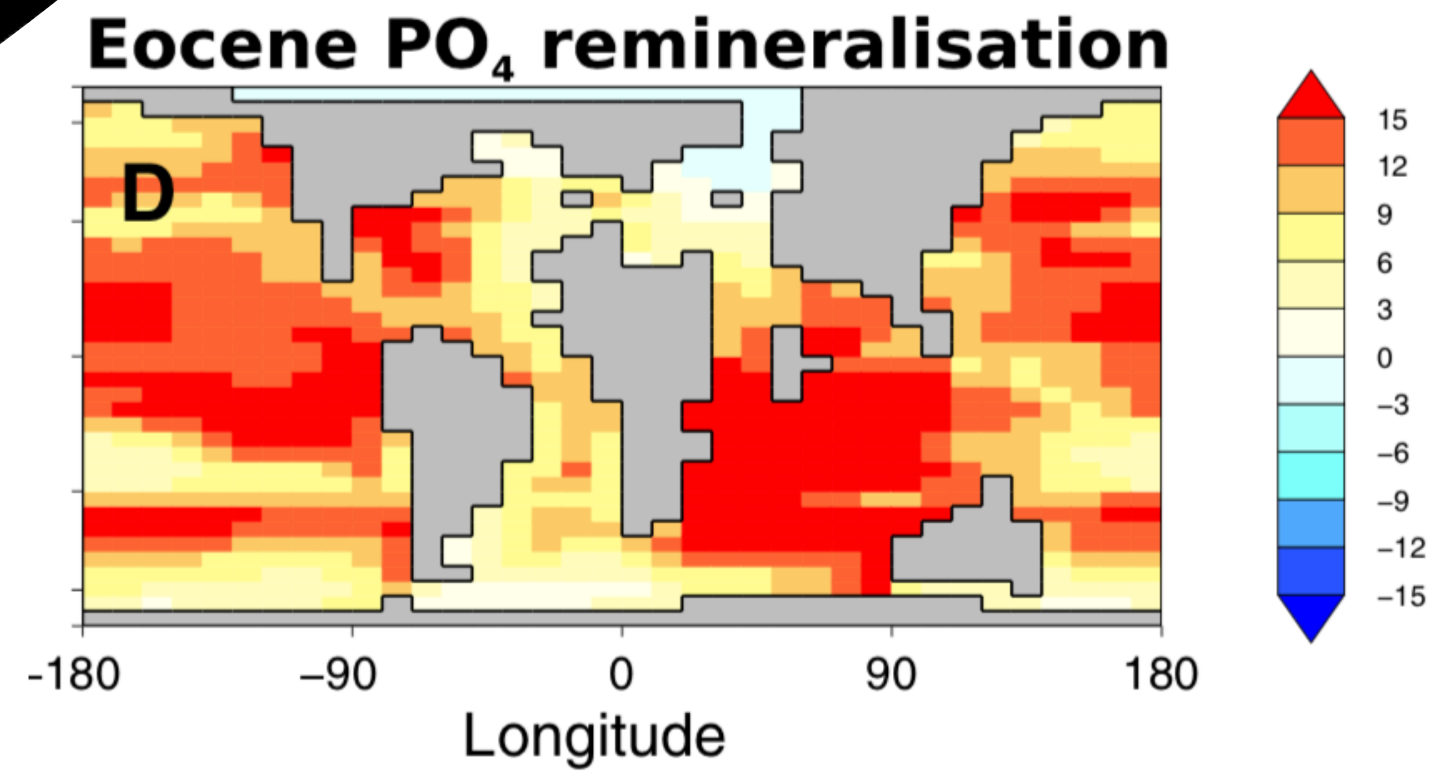

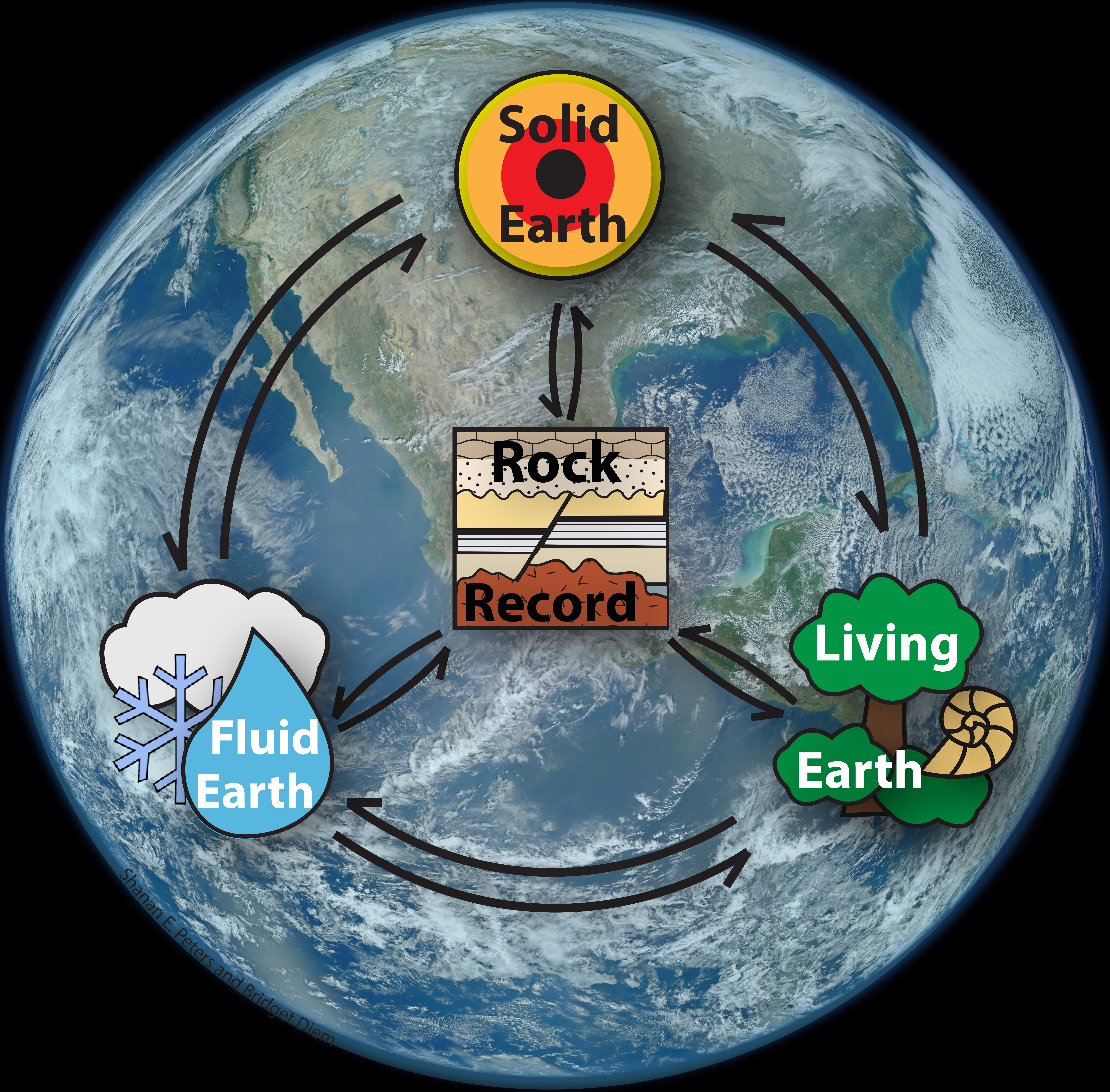
Solid Earth
Rock Record
Fluid Earth
Living Earth
Shanan E. Peters and Bridget Diem

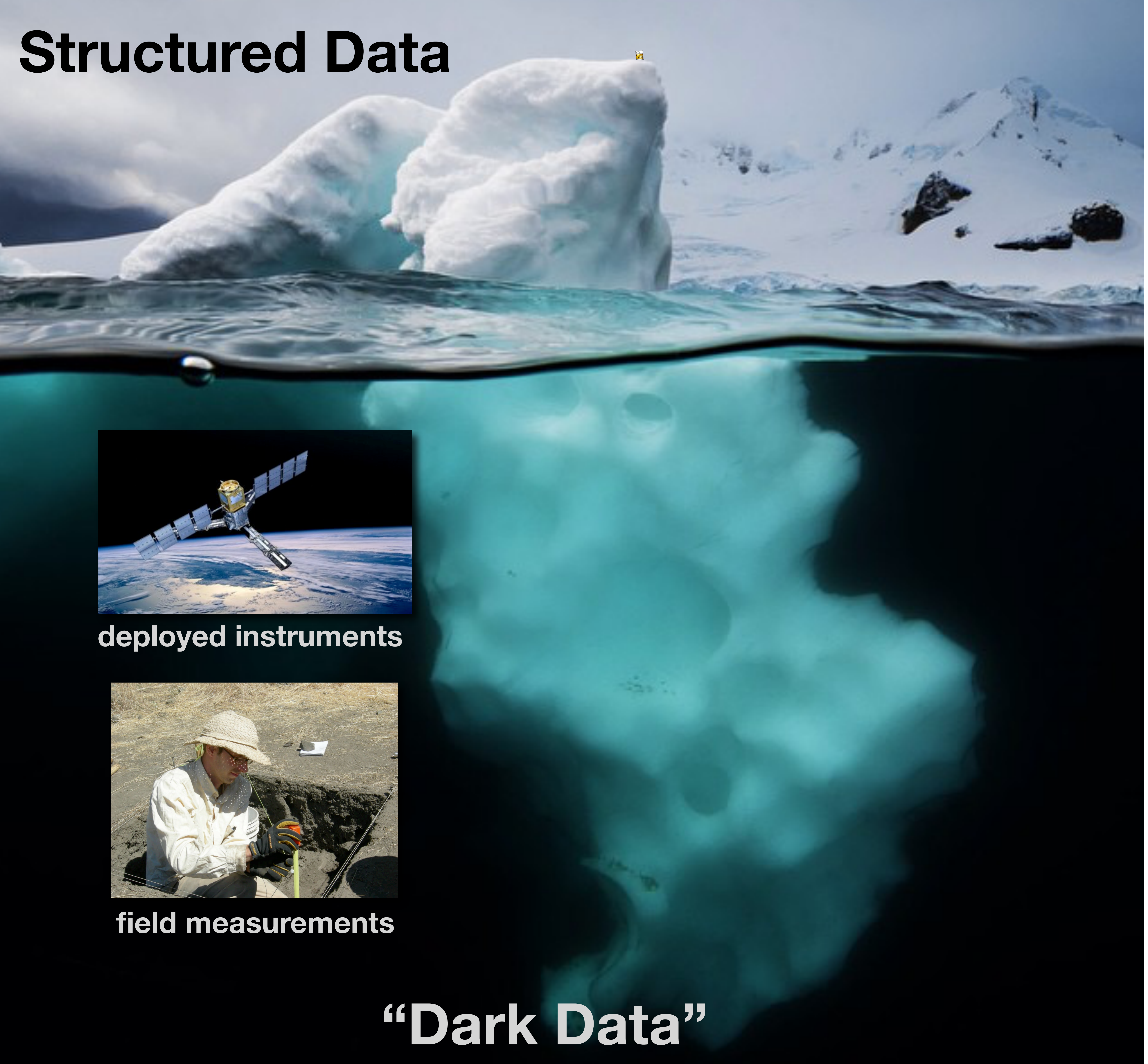
Structured Data
deployed instruments
field measurements
“Dark Data”

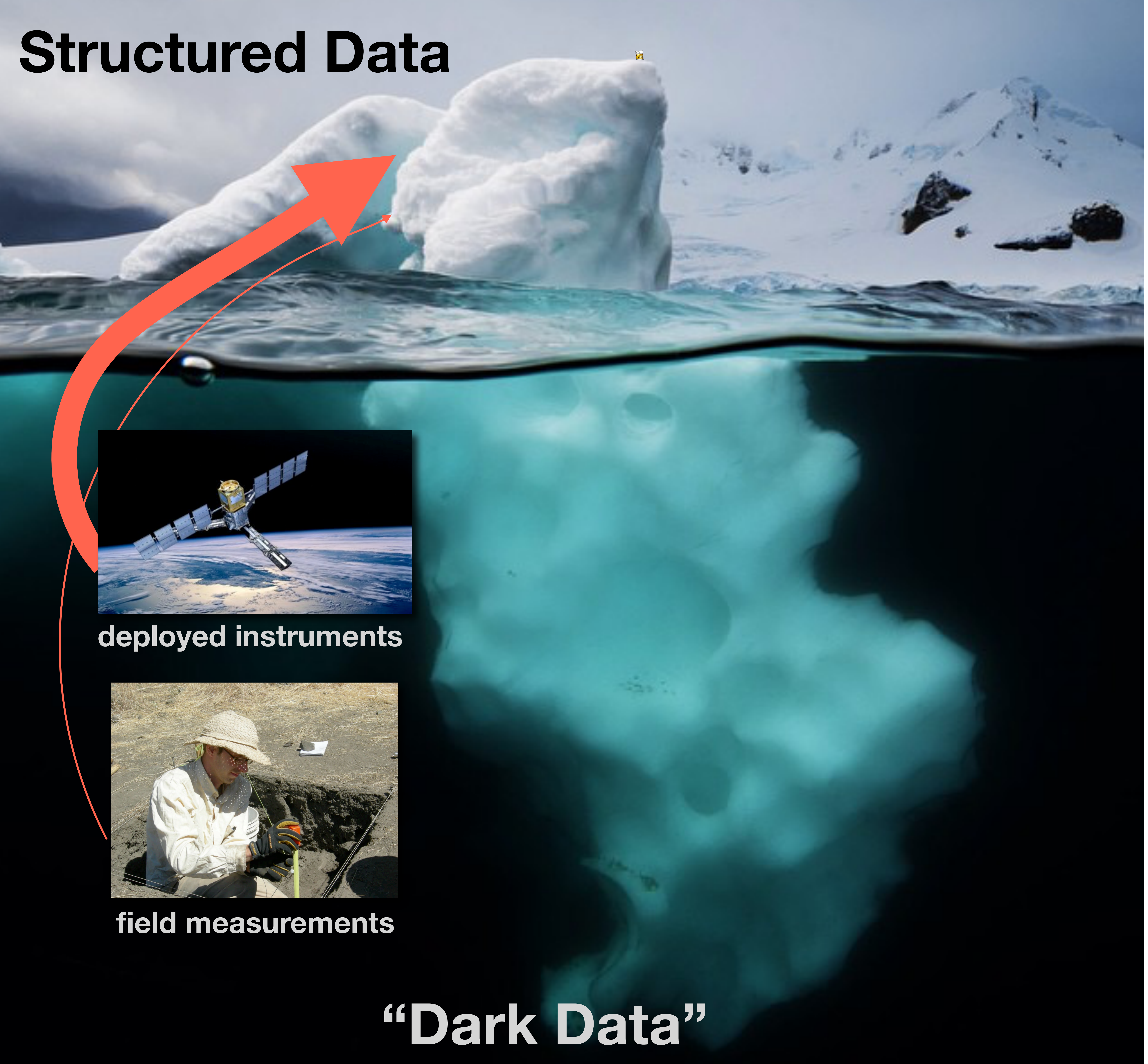
Structured Data
deployed instruments
field measurements
“Dark Data”

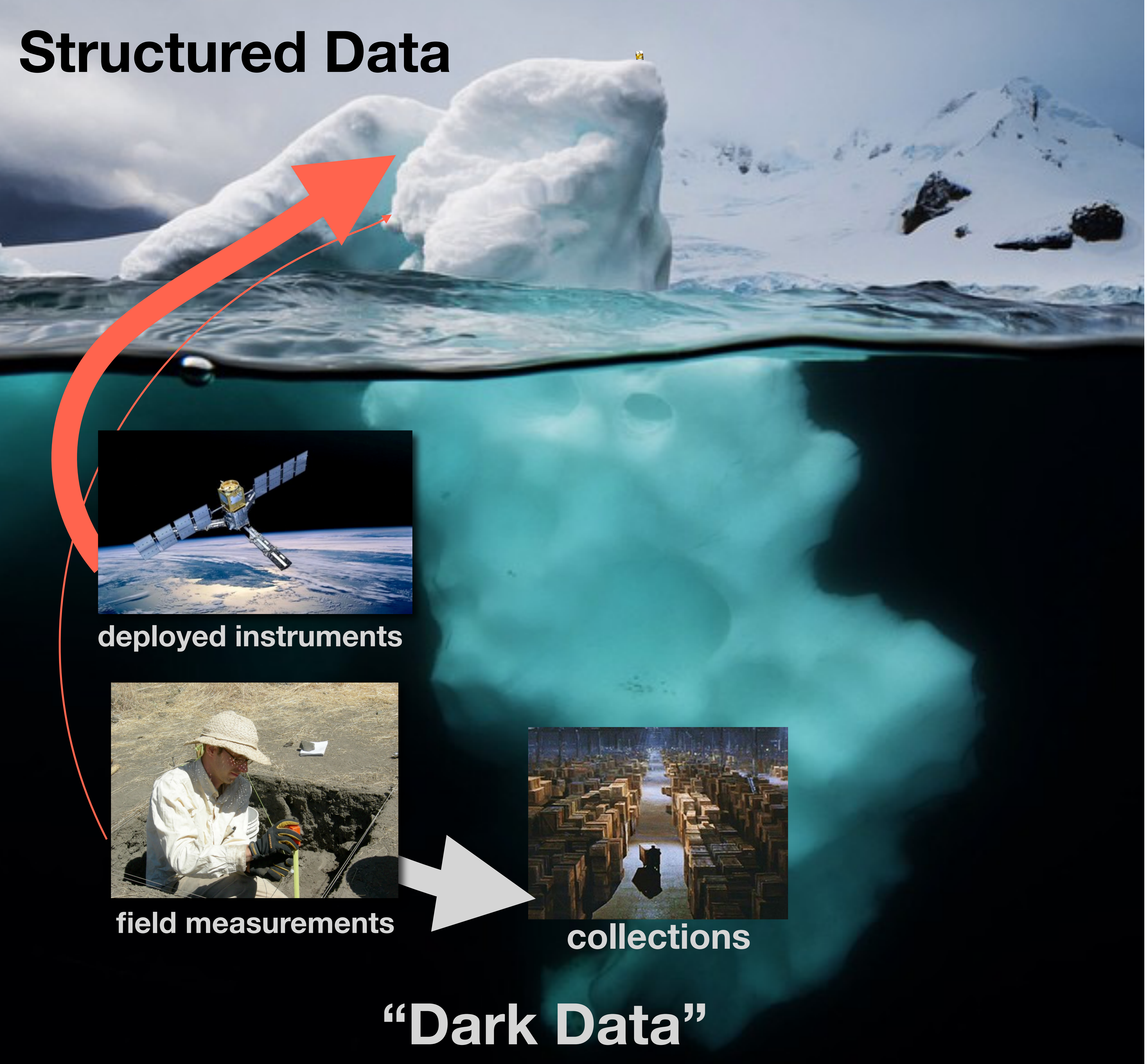
Structured Data
deployed instruments
field measurements
collections
“Dark Data”

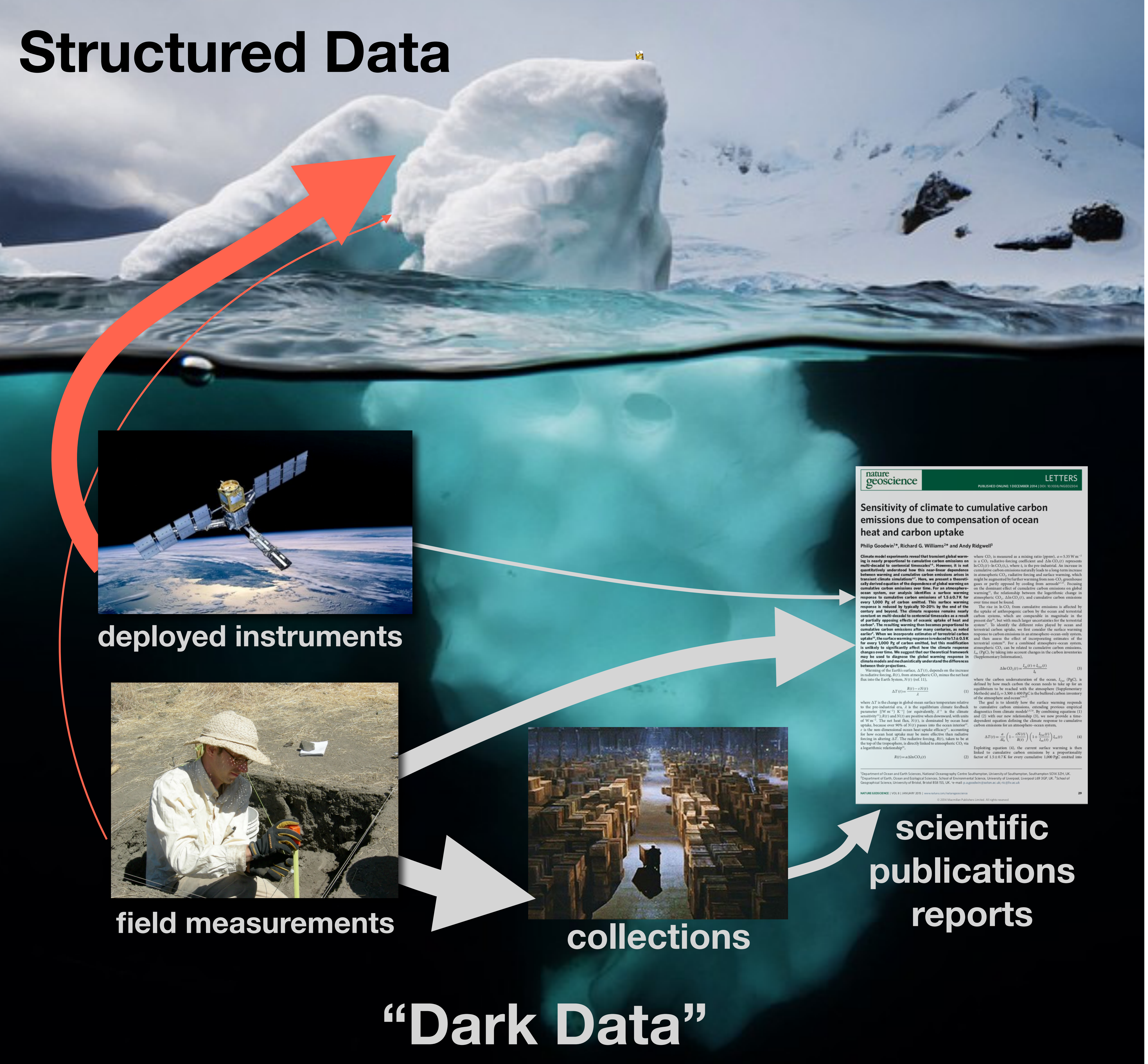
Structured Data
deployed instruments
field measurements
collections
nature geoscience
LETTERS
Sensitivity of climate to cumulative carbon emissions due to compensation of ocean heat and carbon uptake
Philip Goodwin, Richard G. Williams and Andy Ridgwell
scientific publications reports
“Dark Data”


Structured Data
Scientific Models
$$\frac{\partial c}{\partial t} = \nabla \cdot (D \nabla c) - \nabla \cdot (\mathbf{v} c) + R$$
nature geoscience
LETTERS
Sensitivity of climate to cumulative carbon emissions due to compensation of ocean heat and carbon uptake
deployed instruments
field measurements
collections
scientific
publications
reports
“Dark Data”

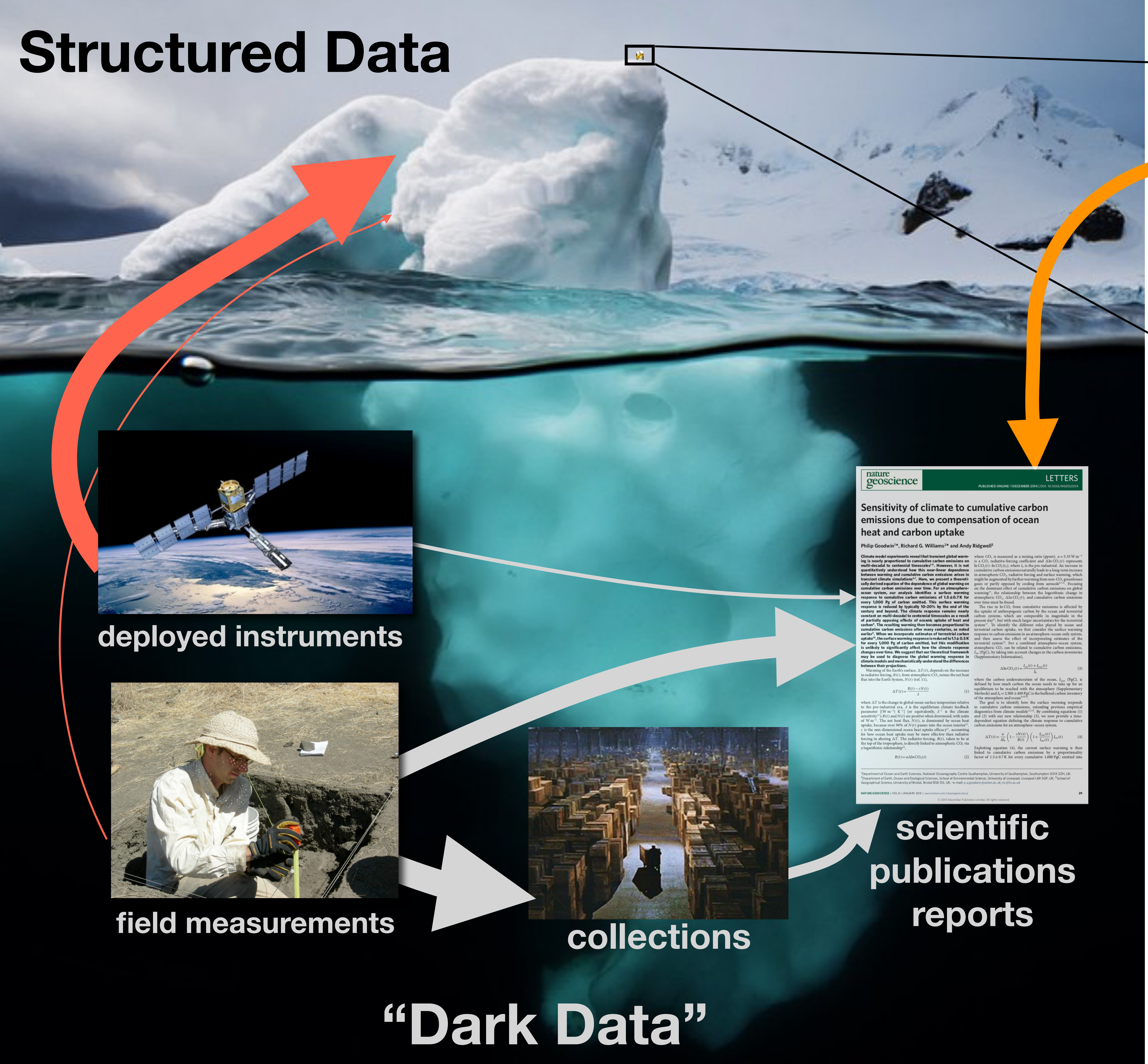

Scientific Models

$$\frac{\partial c}{\partial t} = \nabla \cdot (D \nabla c) - \nabla \cdot (\mathbf{v} c) + R$$


Structured Data
Scientific Models
$$\frac{\partial c}{\partial t} = \nabla \cdot (D \nabla c) - \nabla \cdot (\mathbf{v}c) + R$$
deployed instruments
field measurements
collections
nature geoscience
LETTERS
Sensitivity of climate to cumulative carbon emissions due to compensation of ocean heat and carbon uptake
Philip Goodwin, Richard G. Williams and Andy Ridgwell
scientific
publications
reports
"Dark Data"
Model Predictions

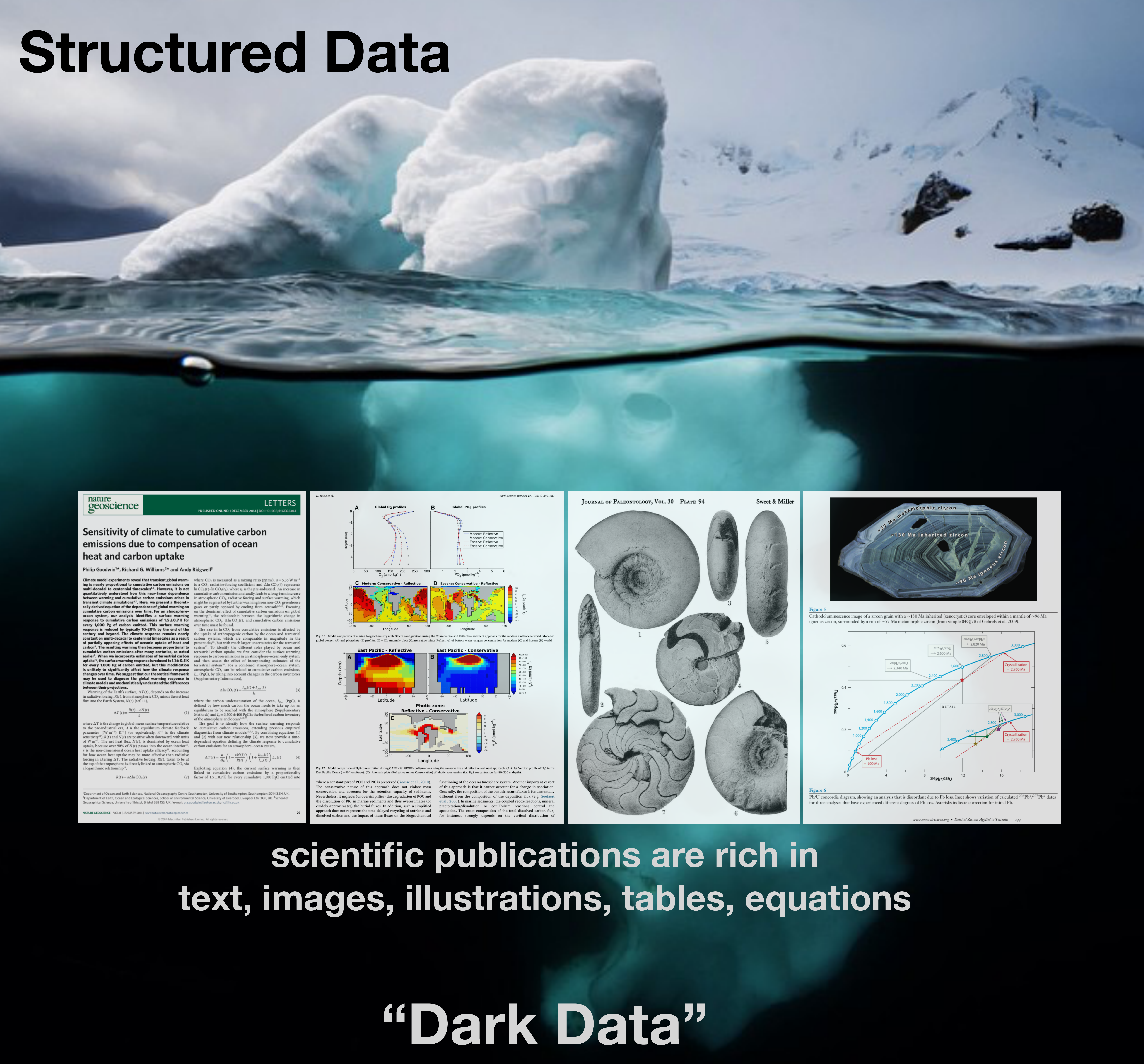
Structured Data
nature geoscience
LETTERS
Sensitivity of climate to cumulative carbon emissions due to compensation of ocean heat and carbon uptake
Journal of Paleontology, Vol. 30 Plate 94
Sweet & Miller
scientific publications are rich in
text, images, illustrations, tables, equations
“Dark Data”

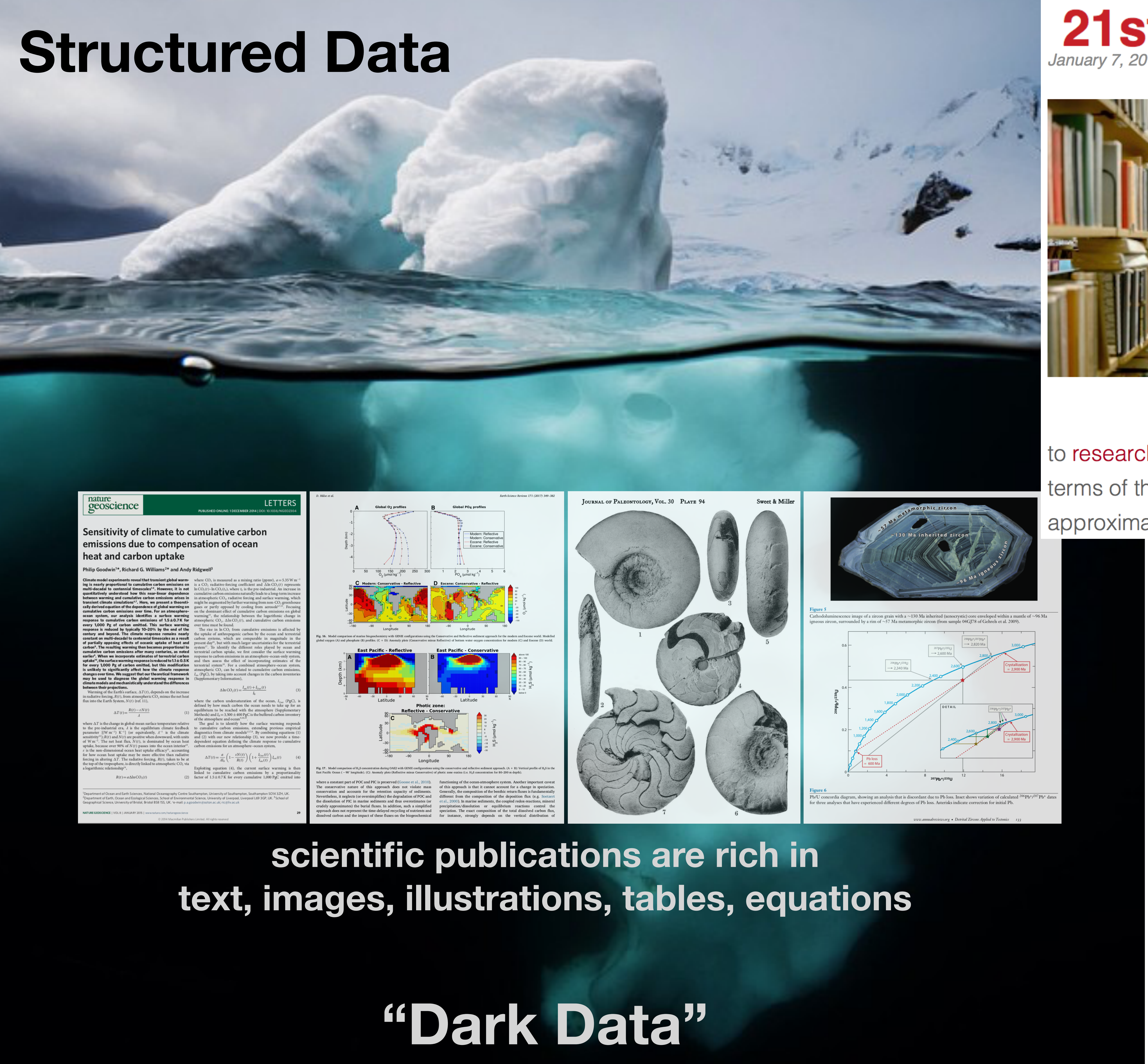

21st Century Science Overload

January 7, 2016

By Sarah Boon, PhD

Do you feel overwhelmed by the number of research papers in your field? Do you wonder if you're missing key ideas that could be critical for your research program? Does it feel like the deluge is only getting worse?

You're not imagining things. According to research from the University of Ottawa, in 2009 we passed the 50 million mark in terms of the total number of science papers published since 1665, and approximately 2.5 million new scientific papers are published each year.

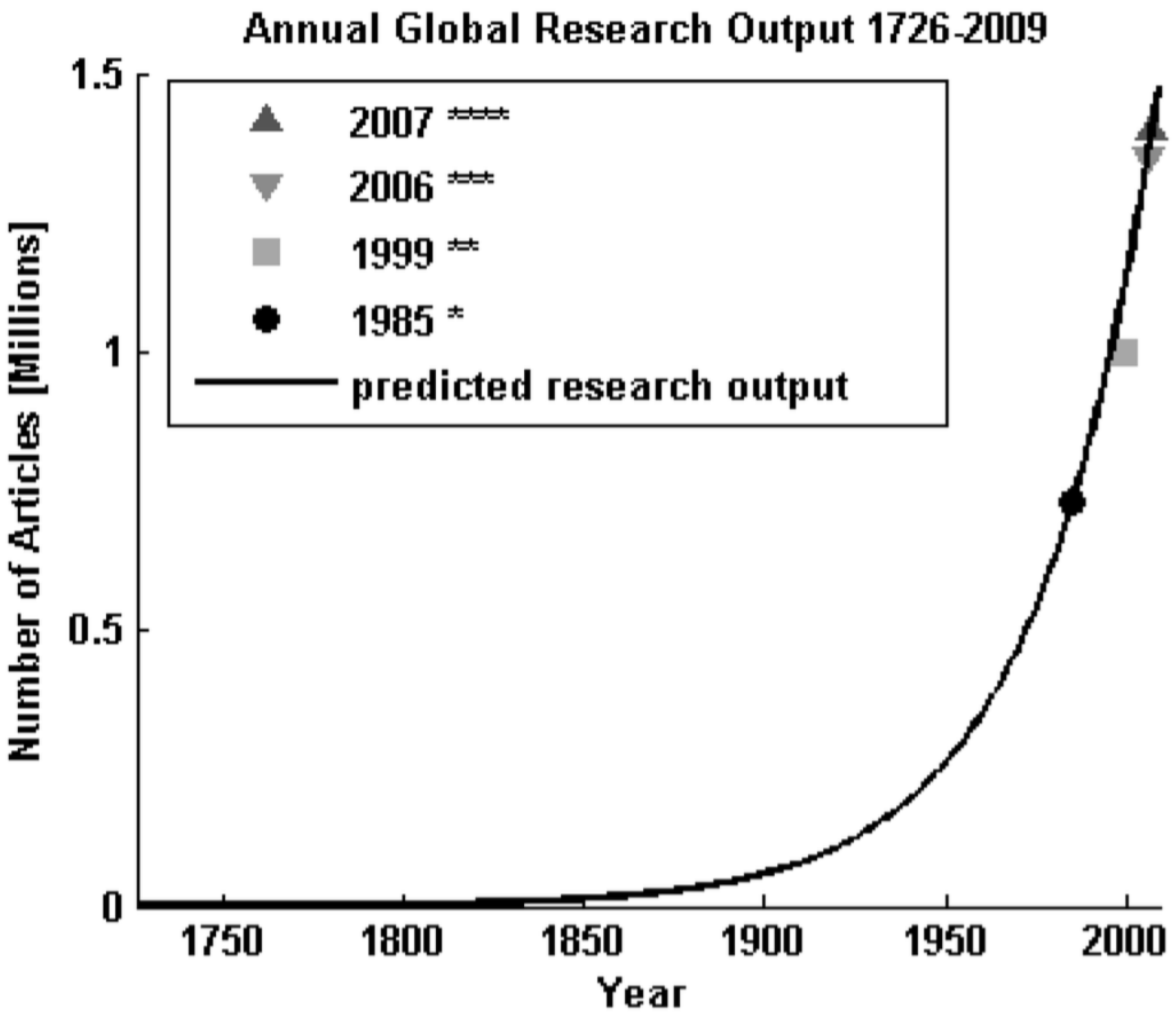

COSMOS: overview of objectives

Biogeosciences, 4, 87–104, 2007
www.biogeosciences.net/4/87/2007/

Biogeosciences

Marine geochemical data assimilation in an efficient Earth System Model of global biogeochemical cycling

A. Ridgwell[1], J. C. Hargreaves[2], N. R. Edwards[3], J. D. Annan[2], T. M. Lenton[4], R. Marsh[5], A. Yool[5], and A. Watson[4]

[1]School of Geographical Sciences, University of Bristol, Bristol, UK
Japan

Table 1. EnKF calibrated biogeochemical parameters in the GENIE-1 model.

Name	Prior assumptions (mean and range[a])	Posterior mean[b]	Description
$u_0^{PO_4}$	1.65 μmol kg^{-1} yr^{-1} (0.3–3.0)	1.91 μmol kg^{-1} yr^{-1}	maximum PO_4 uptake (removal) rate (Eq. 3)
K^{PO_4}	0.2 μmol kg^{-1} (0.1–0.3)	0.21 μmol kg^{-1}	PO_4 Michaelis-Menton half-saturation concentration (Eq. 3)
r^{POC}	0.05 (0.02–0.08)	0.055	initial proportion of POC export as fraction #2 (Eq. 6)
l^{POC}	600 m (200–1000)	556 m	*e*-folding remineralization depth of POC fraction #1 (Eq. 6)
$r_0^{CaCO_3:POC}$	0.036 (0.015–0.088)[c]	0.022[d]	$CaCO_3$:POC: export rain ratio scalar (Eq. 8)
η	1.5 (1.0–2.0)	1.28	thermodynamic calcification rate power (Eq. 9)
r^{CaCO_3}	0.4 (0.2–0.6)	0.489	initial proportion of $CaCO_3$ export as fraction #2 (Eq. 11)
l^{CaCO_3}	600 m (200–1000)	1055	*e*-folding remineralization depth of $CaCO_3$ fraction #1 (Eq. 11)

[a] the range is quoted as 1 standard deviation either side of the mean

udying
ongest

addition of calcium carbonate preservation in
ments and its role in regulating atmospheric C
elsewhere (Ridgwell and Hargreaves, 2007).
We have calibrated the model paramete
ocean carbon cycling in GENIE-1 by assimilat
vational datasets of phosphate and alkalinity u
ble Kalman filter method. The calibrated (me
dicts a global export production of particulate

rti-
ean
cit
of
particulate organic phosphorus ($F^{POP}_{z=h_e}$, in units of mol PO_4 m^{-2} yr^{-1}) is equated directly with PO_4 uptake (Eq. 1):

$$F^{POP}_{z=h_e} = \int_{h_e}^{0} \rho \cdot (1-\nu) \cdot \Gamma \, dz \tag{4}$$

where ρ is the density of seawater and h_e the thickness of the euphotic zone (175 m in the 8-level version of this ocean model).

COSMOS: overview of objectives

1. Automate knowledge base construction (KBC) for equations, parameterizations, and descriptions of scientific models expressed in the published literature.

Biogeosciences, 4, 87–104, 2007
www.biogeosciences.net/4/87/2007/

Biogeosciences

Marine geochemical data assimilation in an efficient Earth System Model of global biogeochemical cycling

A. Ridgwell[1], J. C. Hargreaves[2], N. R. Edwards[3], J. D. Annan[2], T. M. Lenton[4], R. Marsh[5], A. Yool[5], and A. Watson[4]

[1]School of Geographical Sciences, University of Bristol, Bristol, UK

Japan

Table 1. EnKF calibrated biogeochemical parameters in the GENIE-1 model.

Name	Prior assumptions (mean and range[a])	Posterior mean[b]	Description
$u_0^{PO_4}$	1.65 μmol kg^{-1} yr^{-1} (0.3–3.0)	1.91 μmol kg^{-1} yr^{-1}	maximum PO_4 uptake (removal) rate (Eq. 3)
K^{PO_4}	0.2 μmol kg^{-1} (0.1–0.3)	0.21 μmol kg^{-1}	PO_4 Michaelis-Menton half-saturation concentration (Eq. 3)
r^{POC}	0.05 (0.02–0.08)	0.055	initial proportion of POC export as fraction #2 (Eq. 6)
l^{POC}	600 m (200–1000)	556 m	*e*-folding remineralization depth of POC fraction #1 (Eq. 6)
$r_0^{CaCO_3:POC}$	0.036 (0.015–0.088)[c]	0.022[d]	$CaCO_3$:POC: export rain ratio scalar (Eq. 8)
η	1.5 (1.0–2.0)	1.28	thermodynamic calcification rate power (Eq. 9)
r^{CaCO_3}	0.4 (0.2–0.6)	0.489	initial proportion of $CaCO_3$ export as fraction #2 (Eq. 11)
l^{CaCO_3}	600 m (200–1000)	1055	*e*-folding remineralization depth of $CaCO_3$ fraction #1 (Eq. 11)

[a] the range is quoted as 1 standard deviation either side of the mean

udying
ongest

addition of calcium carbonate preservation in
ments and its role in regulating atmospheric C
elsewhere (Ridgwell and Hargreaves, 2007).
We have calibrated the model paramete
ocean carbon cycling in GENIE-1 by assimilat
vational datasets of phosphate and alkalinity u
ble Kalman filter method. The calibrated (me
dicts a global export production of particulate

rti-
ean
cit
of
particulate organic phosphorus ($F^{POP}_{z=h_e}$, in units of mol PO_4 m^{-2} yr^{-1}) is equated directly with PO_4 uptake (Eq. 1):

$$F^{POP}_{z=h_e} = \int_{h_e}^{0} \rho \cdot (1-\nu) \cdot \Gamma \, dz \quad (4)$$

where ρ is the density of seawater and h_e the thickness of the euphotic zone (175 m in the 8-level version of this ocean model).

COSMOS: overview of objectives

1. Automate knowledge base construction (KBC) for equations, parameterizations, and descriptions of scientific models expressed in the published literature.

2. Automate KBC for empirical/experimental data and observations in publications that are semantically related to model inputs and predictions.

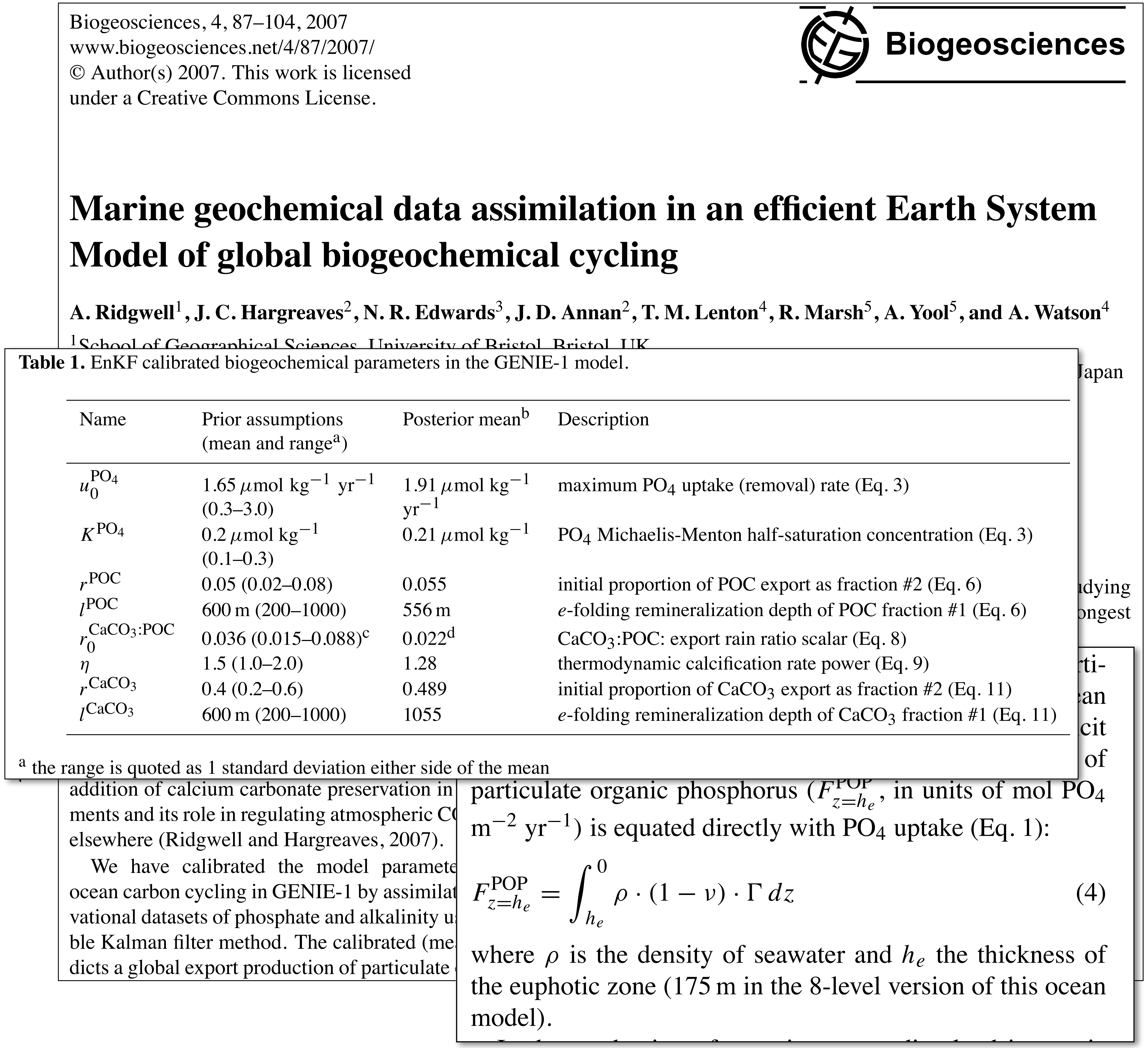

Biogeosciences, 4, 87–104, 2007
www.biogeosciences.net/4/87/2007/
© Author(s) 2007. This work is licensed under a Creative Commons License.

Biogeosciences

Marine geochemical data assimilation in an efficient Earth System Model of global biogeochemical cycling

A. Ridgwell[1], J. C. Hargreaves[2], N. R. Edwards[3], J. D. Annan[2], T. M. Lenton[4], R. Marsh[5], A. Yool[5], and A. Watson[4]

Table 1. EnKF calibrated biogeochemical parameters in the GENIE-1 model.

Name	Prior assumptions (mean and range[a])	Posterior mean[b]	Description
$u_0^{PO_4}$	1.65 μmol kg^{-1} yr^{-1} (0.3–3.0)	1.91 μmol kg^{-1} yr^{-1}	maximum PO_4 uptake (removal) rate (Eq. 3)
K^{PO_4}	0.2 μmol kg^{-1} (0.1–0.3)	0.21 μmol kg^{-1}	PO_4 Michaelis-Menton half-saturation concentration (Eq. 3)
r^{POC}	0.05 (0.02–0.08)	0.055	initial proportion of POC export as fraction #2 (Eq. 6)
l^{POC}	600 m (200–1000)	556 m	*e*-folding remineralization depth of POC fraction #1 (Eq. 6)
$r_0^{CaCO_3:POC}$	0.036 (0.015–0.088)[c]	0.022[d]	$CaCO_3$:POC: export rain ratio scalar (Eq. 8)
η	1.5 (1.0–2.0)	1.28	thermodynamic calcification rate power (Eq. 9)
r^{CaCO_3}	0.4 (0.2–0.6)	0.489	initial proportion of $CaCO_3$ export as fraction #2 (Eq. 11)
l^{CaCO_3}	600 m (200–1000)	1055	*e*-folding remineralization depth of $CaCO_3$ fraction #1 (Eq. 11)

[a] the range is quoted as 1 standard deviation either side of the mean

addition of calcium carbonate preservation in ments and its role in regulating atmospheric C elsewhere (Ridgwell and Hargreaves, 2007).

We have calibrated the model paramete ocean carbon cycling in GENIE-1 by assimilat vational datasets of phosphate and alkalinity u ble Kalman filter method. The calibrated (me dicts a global export production of particulate

particulate organic phosphorus ($F_{z=h_e}^{POP}$, in units of mol PO_4 m^{-2} yr^{-1}) is equated directly with PO_4 uptake (Eq. 1):

$$F_{z=h_e}^{POP} = \int_{h_e}^{0} \rho \cdot (1 - \nu) \cdot \Gamma \, dz \qquad (4)$$

where ρ is the density of seawater and h_e the thickness of the euphotic zone (175 m in the 8-level version of this ocean model).

COSMOS: overview of objectives

1. Automate knowledge base construction (KBC) for equations, parameterizations, and descriptions of scientific models expressed in the published literature.

2. Automate KBC for empirical/experimental data and observations in publications that are semantically related to model inputs and predictions.

3. Remove major pain-point in model-data assimilation and improve pace and completeness of model assessment and improvement.

Biogeosciences, 4, 87–104, 2007
www.biogeosciences.net/4/87/2007/

Biogeosciences

Marine geochemical data assimilation in an efficient Earth System Model of global biogeochemical cycling

A. Ridgwell[1], J. C. Hargreaves[2], N. R. Edwards[3], J. D. Annan[2], T. M. Lenton[4], R. Marsh[5], A. Yool[5], and A. Watson[4]

[1]School of Geographical Sciences, University of Bristol, Bristol, UK
Japan

Table 1. EnKF calibrated biogeochemical parameters in the GENIE-1 model.

Name	Prior assumptions (mean and range[a])	Posterior mean[b]	Description
$u_0^{PO_4}$	1.65 μmol kg^{-1} yr^{-1} (0.3–3.0)	1.91 μmol kg^{-1} yr^{-1}	maximum PO_4 uptake (removal) rate (Eq. 3)
K^{PO_4}	0.2 μmol kg^{-1} (0.1–0.3)	0.21 μmol kg^{-1}	PO_4 Michaelis-Menton half-saturation concentration (Eq. 3)
r^{POC}	0.05 (0.02–0.08)	0.055	initial proportion of POC export as fraction #2 (Eq. 6)
l^{POC}	600 m (200–1000)	556 m	*e*-folding remineralization depth of POC fraction #1 (Eq. 6)
$r_0^{CaCO_3:POC}$	0.036 (0.015–0.088)[c]	0.022[d]	$CaCO_3$:POC: export rain ratio scalar (Eq. 8)
η	1.5 (1.0–2.0)	1.28	thermodynamic calcification rate power (Eq. 9)
r^{CaCO_3}	0.4 (0.2–0.6)	0.489	initial proportion of $CaCO_3$ export as fraction #2 (Eq. 11)
l^{CaCO_3}	600 m (200–1000)	1055	*e*-folding remineralization depth of $CaCO_3$ fraction #1 (Eq. 11)

[a] the range is quoted as 1 standard deviation either side of the mean

udying
ongest

addition of calcium carbonate preservation in
ments and its role in regulating atmospheric C
elsewhere (Ridgwell and Hargreaves, 2007).

We have calibrated the model paramete
ocean carbon cycling in GENIE-1 by assimilat
vational datasets of phosphate and alkalinity u
ble Kalman filter method. The calibrated (me
dicts a global export production of particulate

rti-
ean
cit
of
particulate organic phosphorus ($F_{z=h_e}^{POP}$, in units of mol PO_4 m^{-2} yr^{-1}) is equated directly with PO_4 uptake (Eq. 1):

$$F_{z=h_e}^{POP} = \int_{h_e}^{0} \rho \cdot (1 - \nu) \cdot \Gamma \, dz \qquad (4)$$

where ρ is the density of seawater and h_e the thickness of the euphotic zone (175 m in the 8-level version of this ocean model).

COSMOS: required components

COSMOS: required components

1. Principled, automated access to scientific publications and the computing capacity and infrastructure required to repeatedly analyze them.

COSMOS: required components

1. Principled, automated access to scientific publications and the computing capacity and infrastructure required to repeatedly analyze them.

2. Models and techniques to represent and capture multi-modal data within publications.

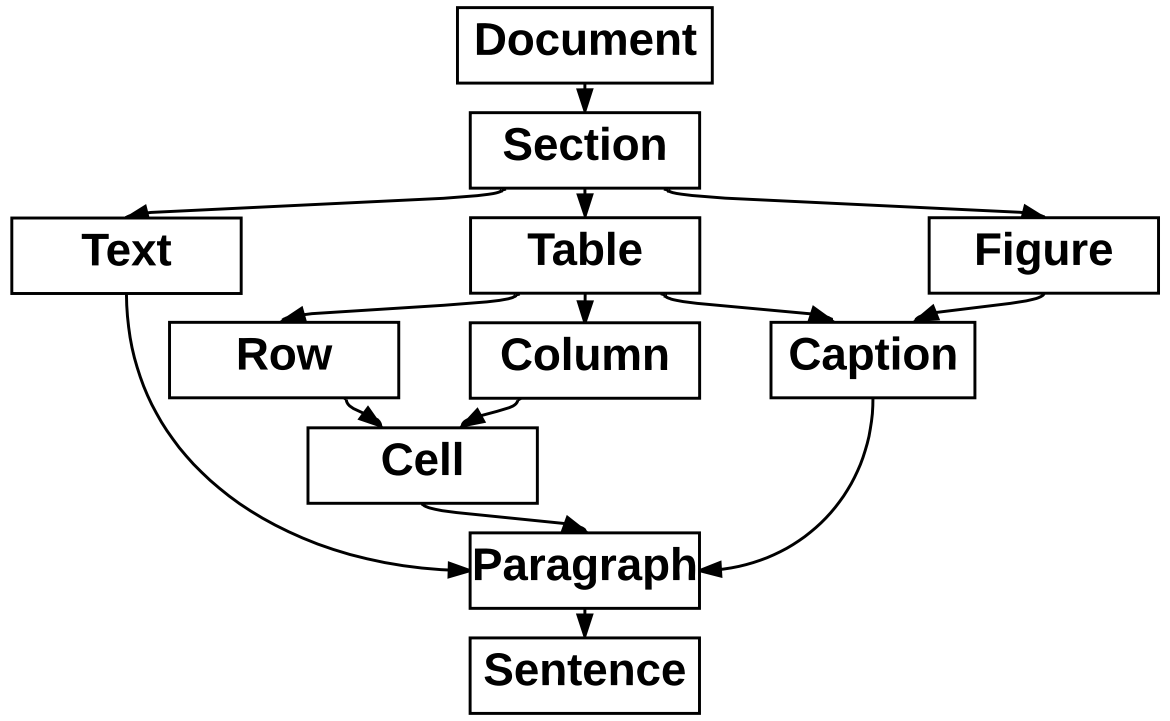

COSMOS: required components

1. Principled, automated access to scientific publications and the computing capacity and infrastructure required to repeatedly analyze them.

2. Models and techniques to represent and capture multi-modal data within publications.

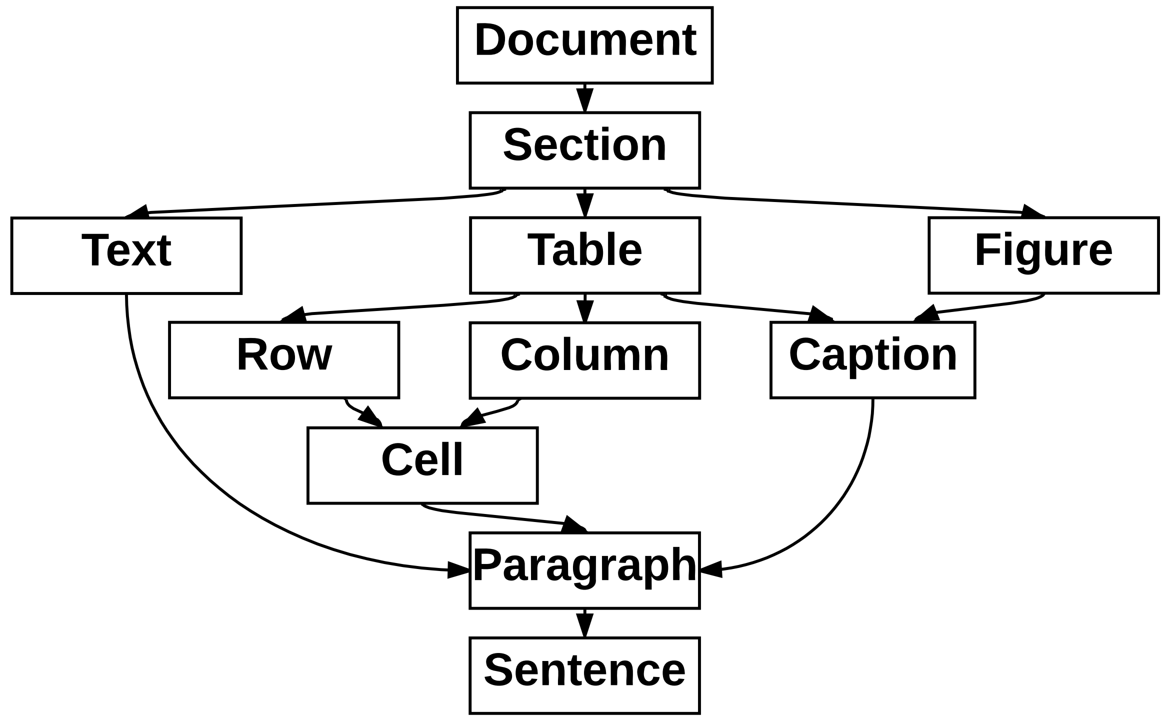

3. Earth system model with parameterizations and predictions that overlap with many different types of empirical data and observations in publications.

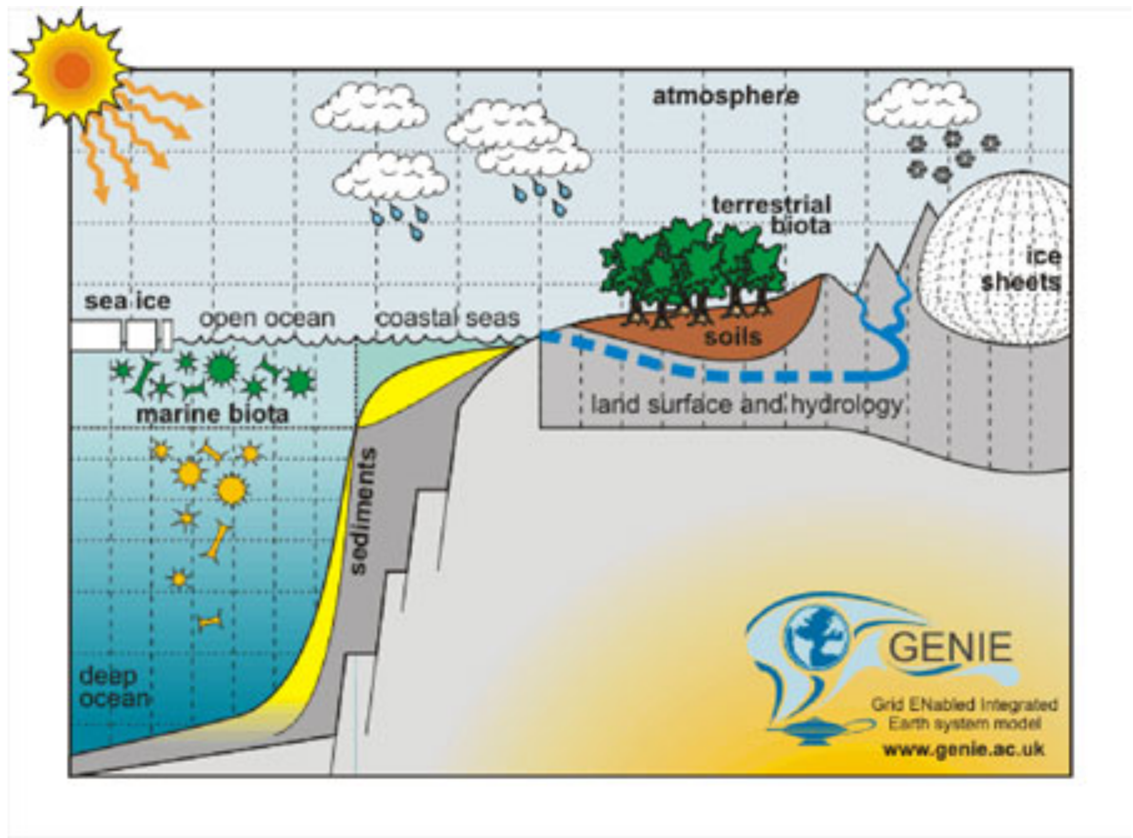

COSMOS: required components

1. Principled, automated access to scientific publications and the computing capacity and infrastructure required to repeatedly analyze them.

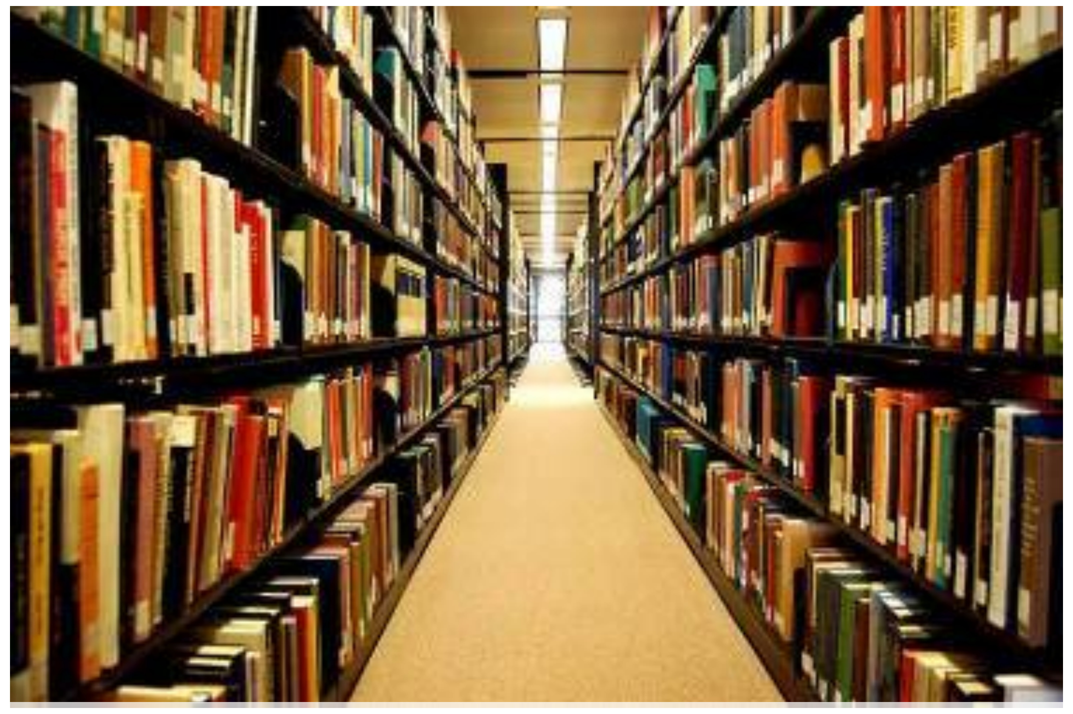

2. Models and techniques to represent and capture multi-modal data within publications.

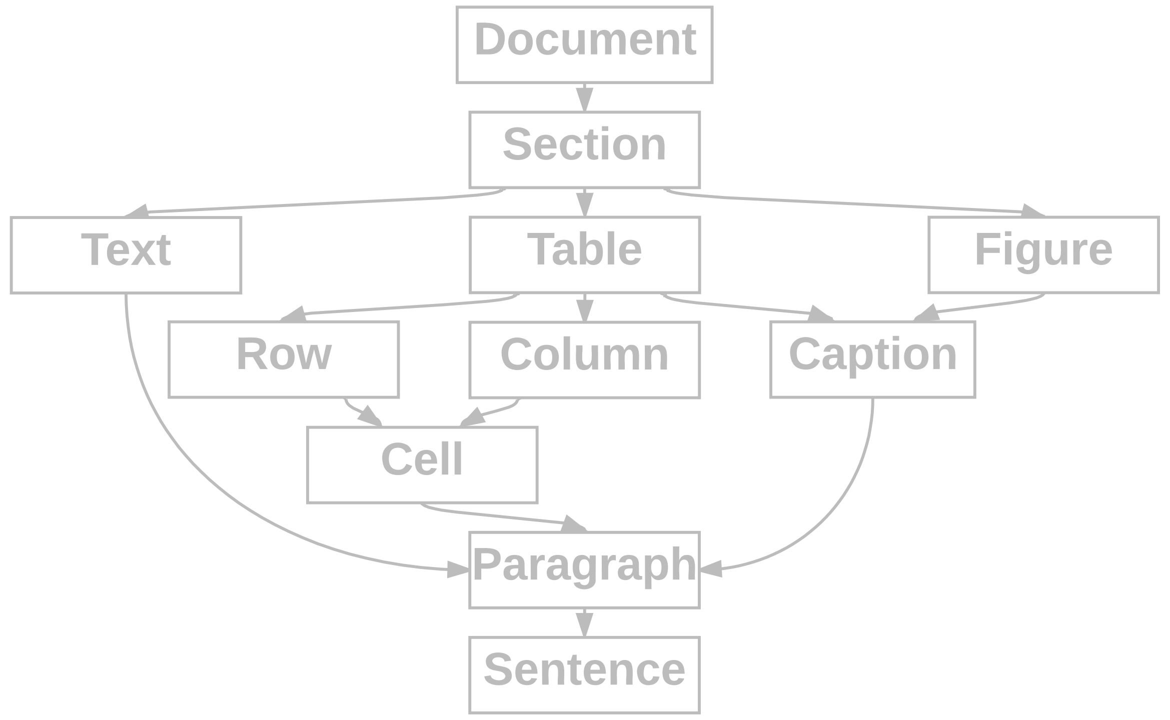

3. Earth system model with parameterizations and predictions that overlap with many different types of empirical data and observations in publications.

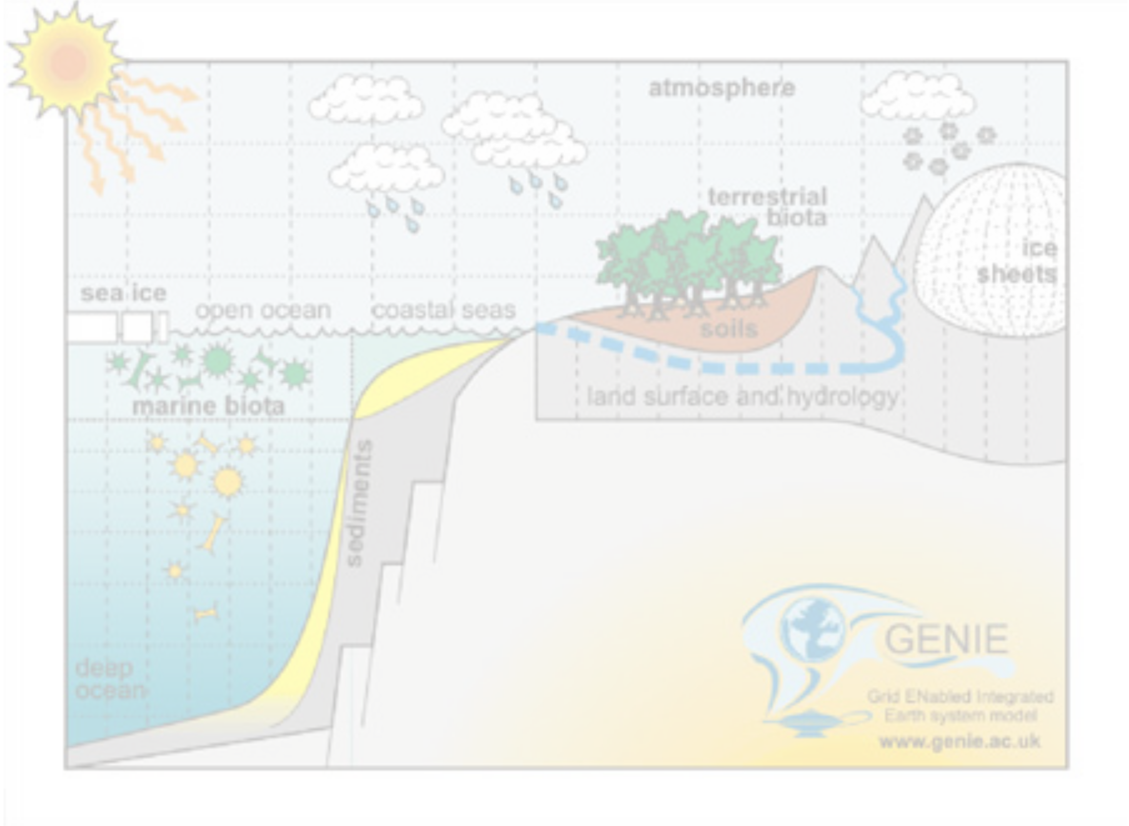

GeoDeepDive

(aka: xDD)

8.3M published documents coupled to *and readable by* a computing infrastructure

HTCondor
High Throughput Computing

CENTER FOR
HIGH THROUGHPUT
COMPUTING

GeoDeepDive Infrastructure Overview

ScienceDirect   Journals   Books

Purchase   Export   Search ScienceDirect   Advanced search

ELSEVIER

Cretaceous Research

Volume 29, Issues 5–6, October–December 2008, Pages 1008–1023

7th International Symposium on the Cretaceous

Organic carbon deposition and phosphorus accumulation during Oceanic Anoxic Event 2 in Tarfaya, Morocco

Haydon P. Mort[a, 1], Thierry Adatte[a, 2], Gerta Keller[b], David Bartels[b], Karl B. Föllmi[a, 2], Philipp Steinmann[a, 2], Zsolt Berner[c], E.H. Chellai[d]

Show more

https://doi.org/10.1016/j.cretres.2008.05.026   Get rights and content

publisher agreements

Libraries UNIVERSITY OF WISCONSIN-MADISON

THE GEOLOGICAL SOCIETY OF AMERICA®

USGS science for a changing world

PLOS ONE

ELSEVIER

WILEY Publishers Since 1807

Canadian Science Publishing

Taylor & Francis Taylor & Francis Group

SEPM

CAMBRIDGE UNIVERSITY PRESS

?

?

GeoDeepDive Infrastructure Overview

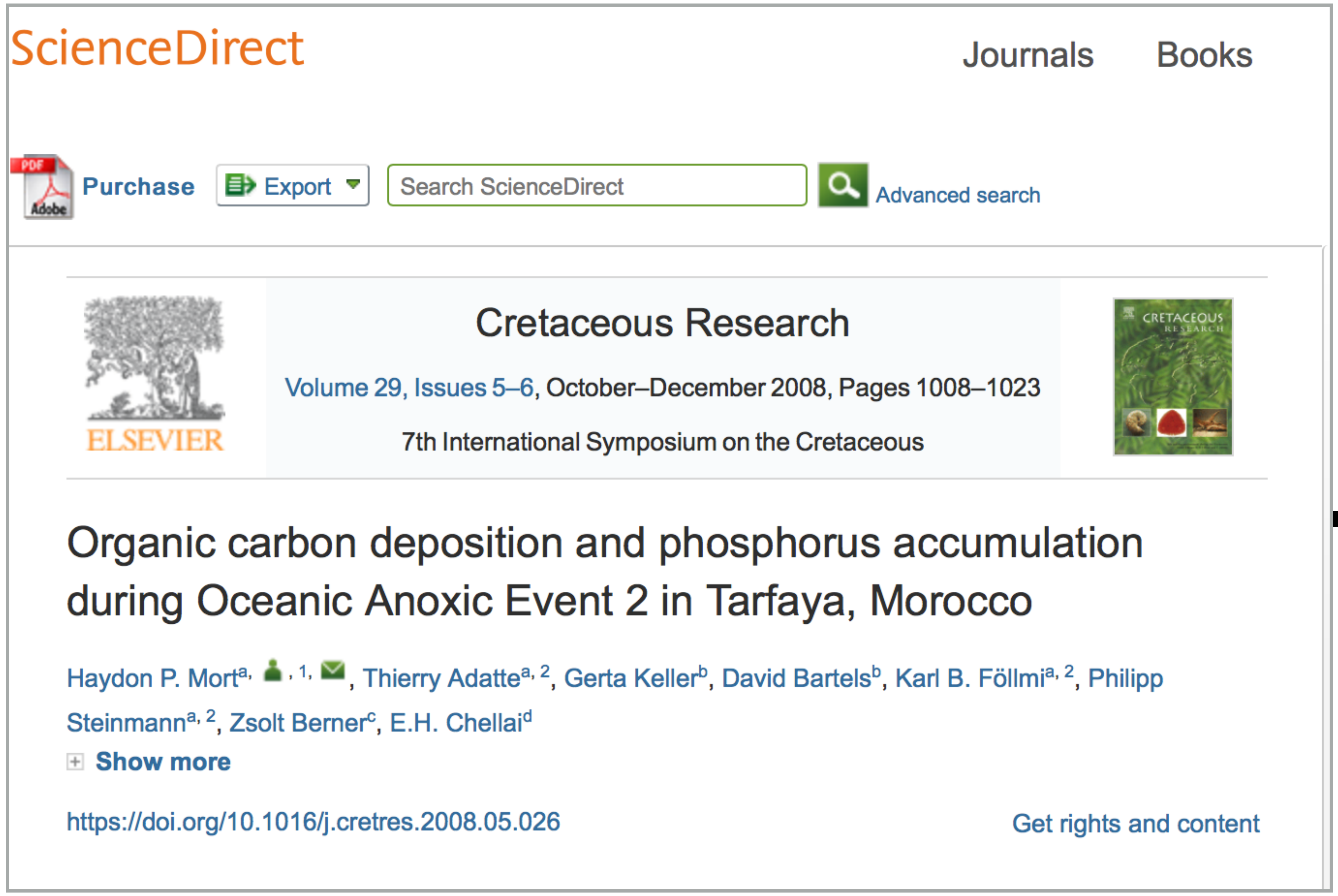

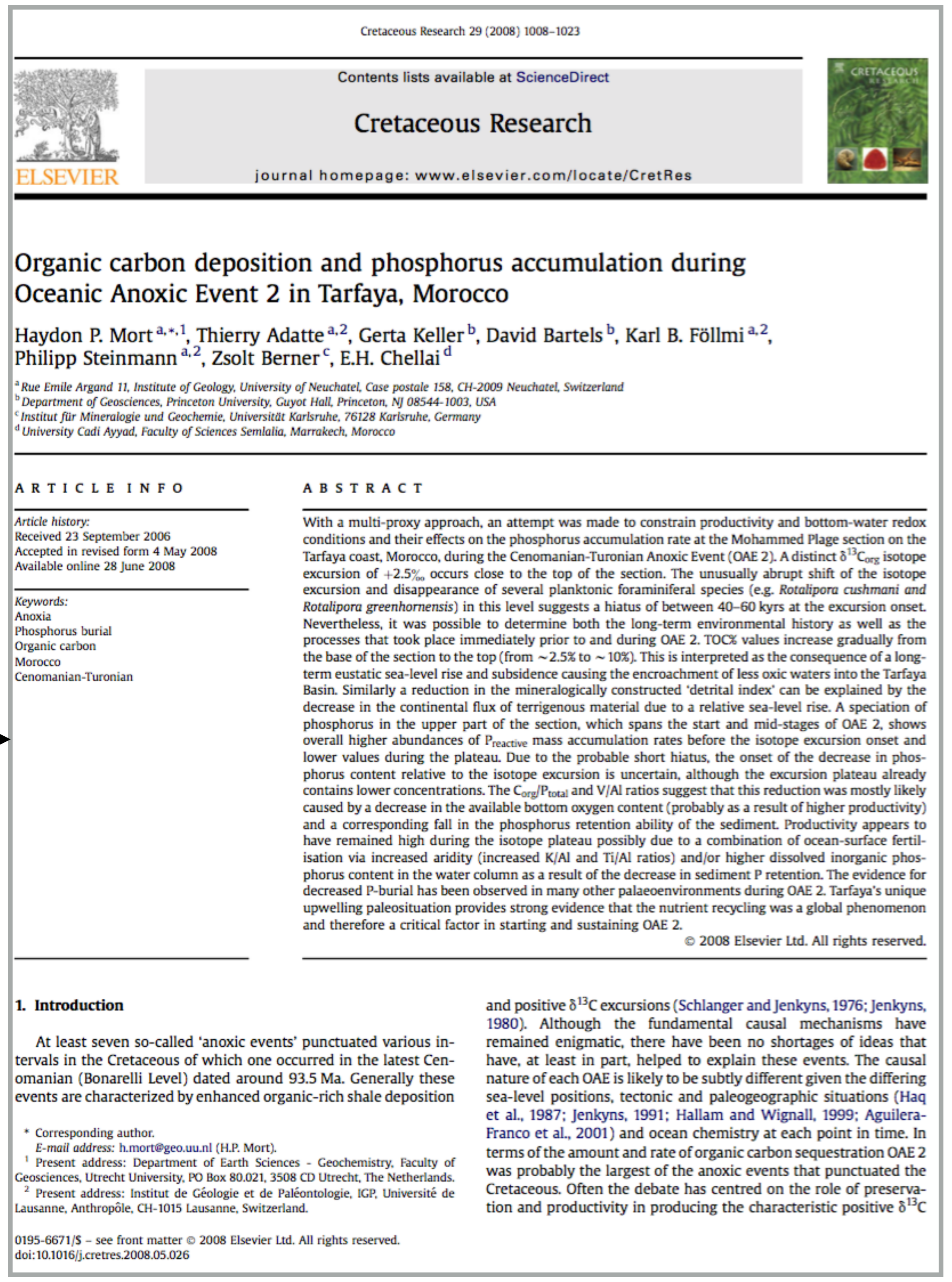

publisher agreements

doc. fetching/storage

?

?

8-12k/day

GeoDeepDive Infrastructure Overview

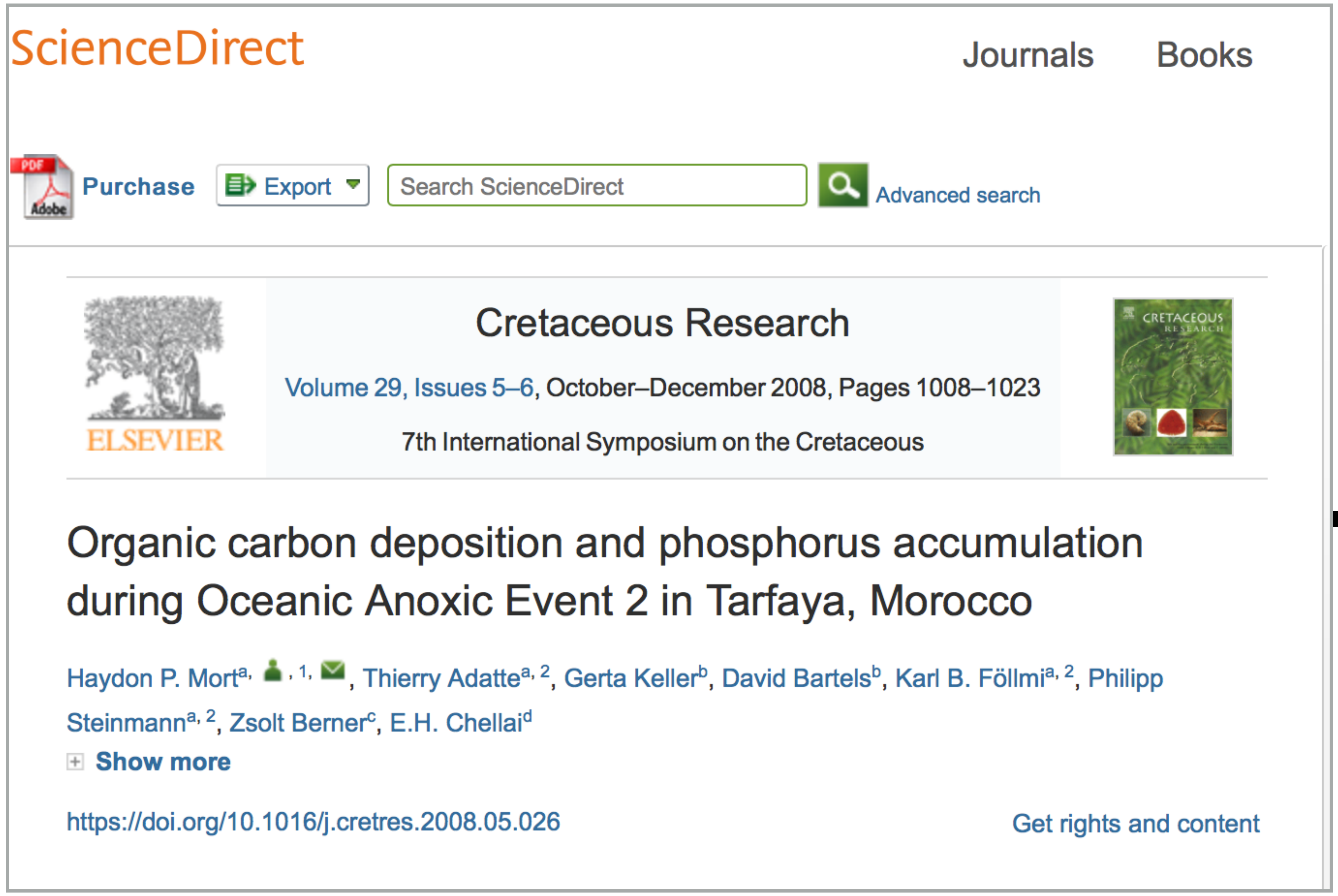

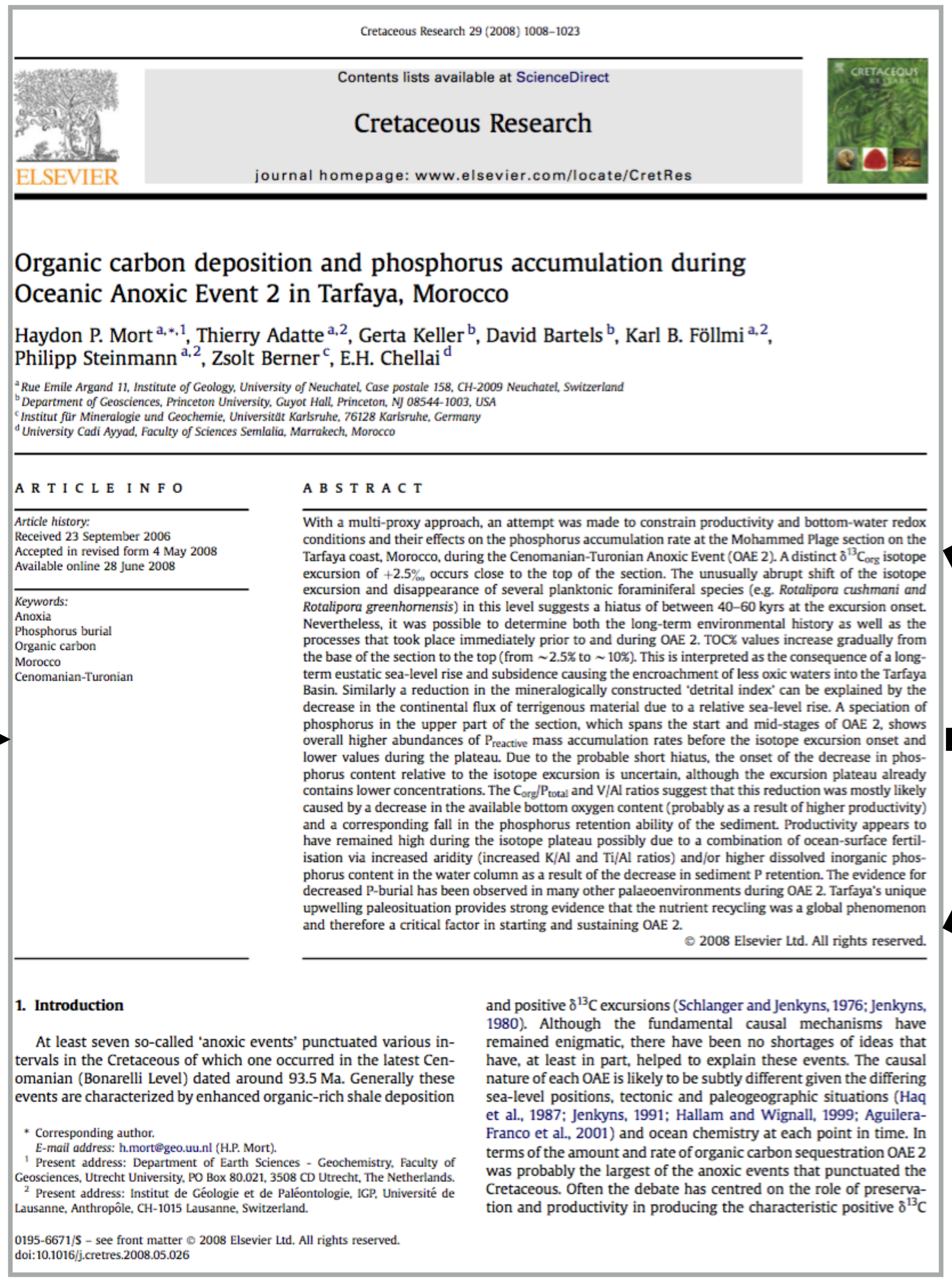

software tools

CoreNLP

OCR

“geoNER”

publisher agreements

doc. fetching/storage

parsing, annotation, labeling

CENTER FOR HIGH THROUGHPUT COMPUTING

?

?

8-12k/day

GeoDeepDive Infrastructure Overview

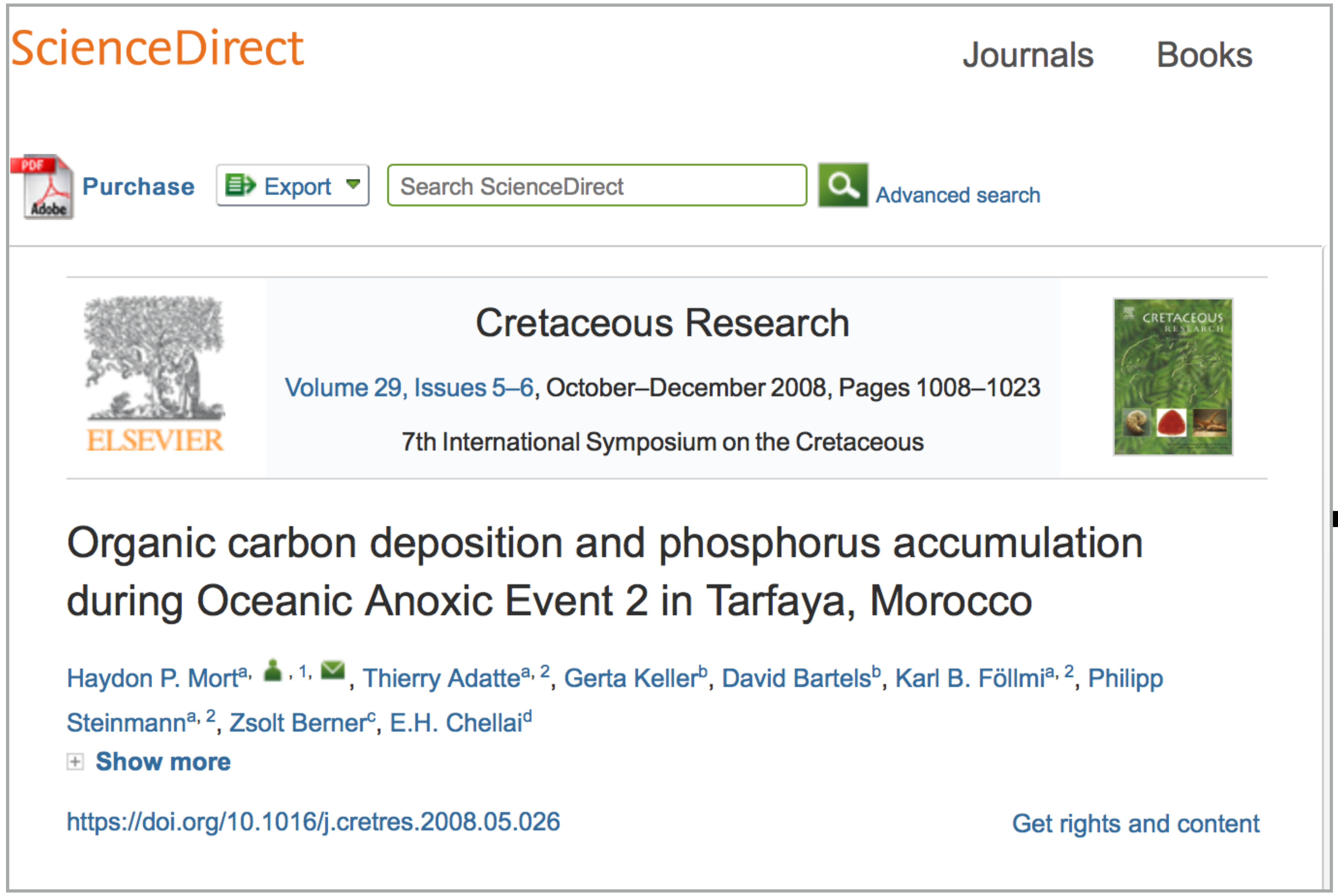

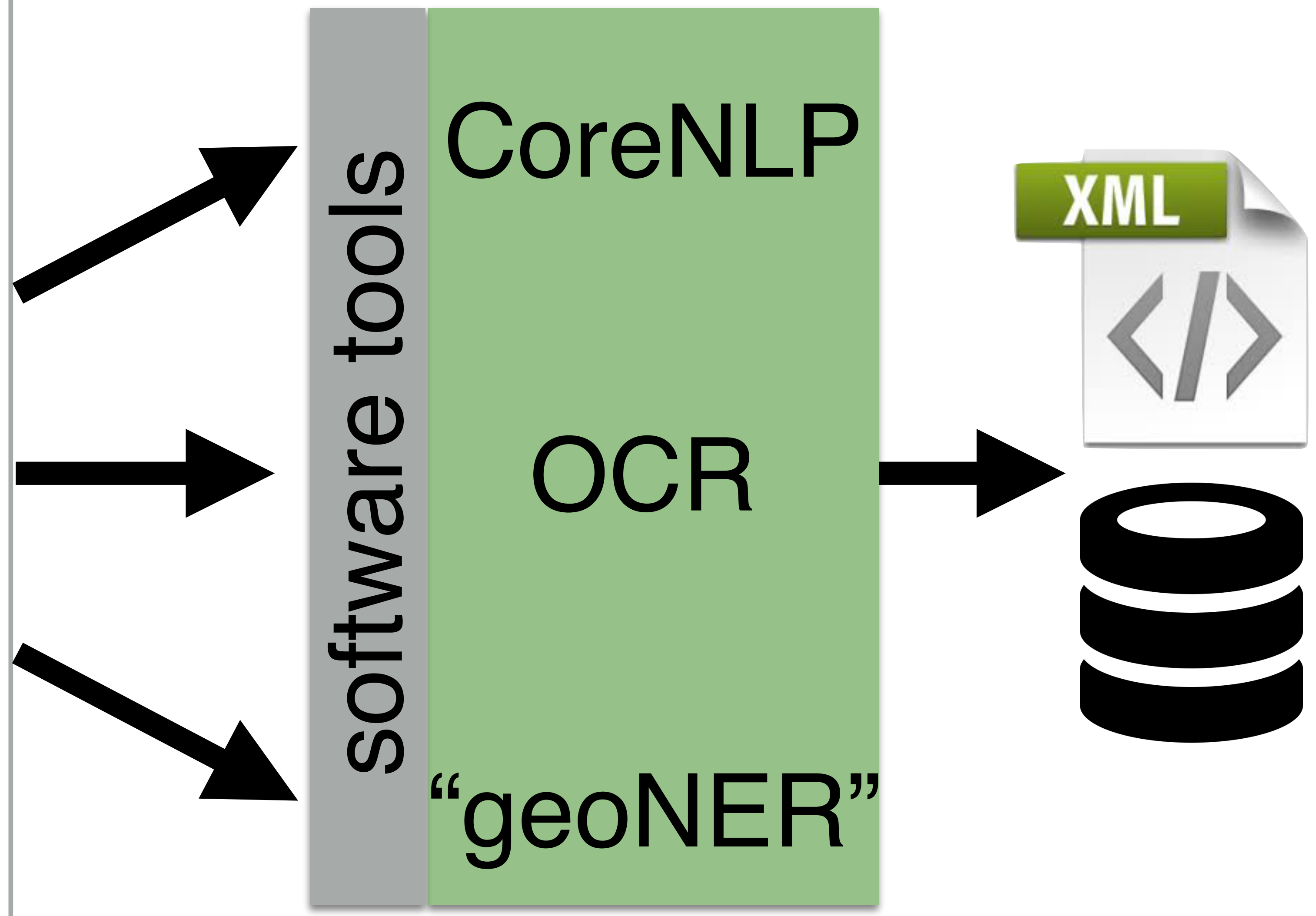

publisher agreements

Libraries
UNIVERSITY OF WISCONSIN-MADISON

USGS
science for a changing world

THE GEOLOGICAL SOCIETY OF AMERICA®

PLOS ONE

ELSEVIER

WILEY
Publishers Since 1807

Canadian Science Publishing

Taylor & Francis
Taylor & Francis Group

SEPM

CAMBRIDGE UNIVERSITY PRESS

?

?

doc. fetching/storage

CENTER FOR HIGH THROUGHPUT COMPUTING

8-12k/day

parsing, annotation, labeling

GeoDeepDive Infrastructure Overview

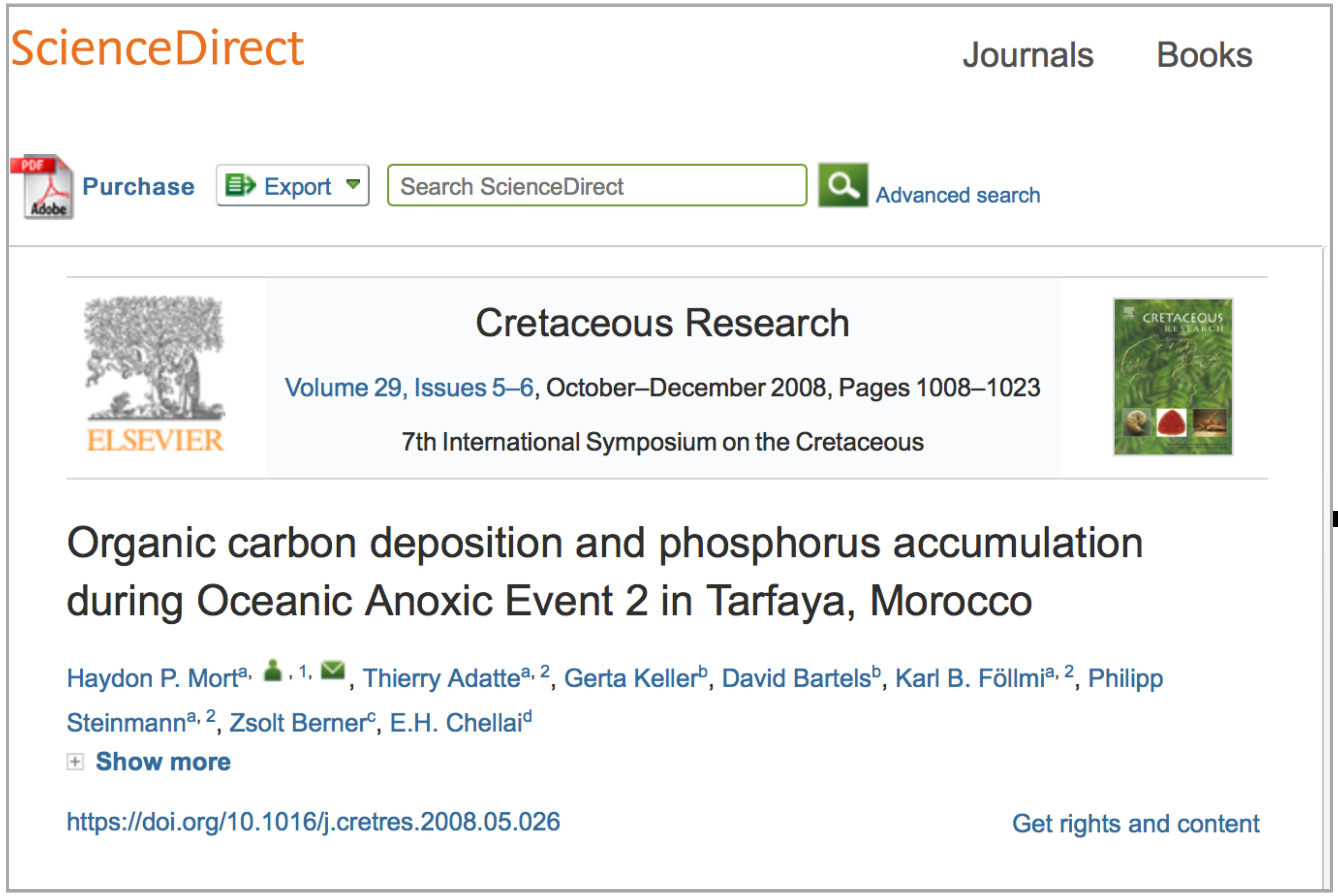
ScienceDirect
Journals
Books
Purchase
Export
Search ScienceDirect
Advanced search
Cretaceous Research
Volume 29, Issues 5–6, October–December 2008, Pages 1008–1023
7th International Symposium on the Cretaceous
Organic carbon deposition and phosphorus accumulation during Oceanic Anoxic Event 2 in Tarfaya, Morocco
Haydon P. Mort[a, 1], Thierry Adatte[a, 2], Gerta Keller[b], David Bartels[b], Karl B. Föllmi[a, 2], Philipp Steinmann[a, 2], Zsolt Berner[c], E.H. Chellai[d]
Show more
https://doi.org/10.1016/j.cretres.2008.05.026
Get rights and content

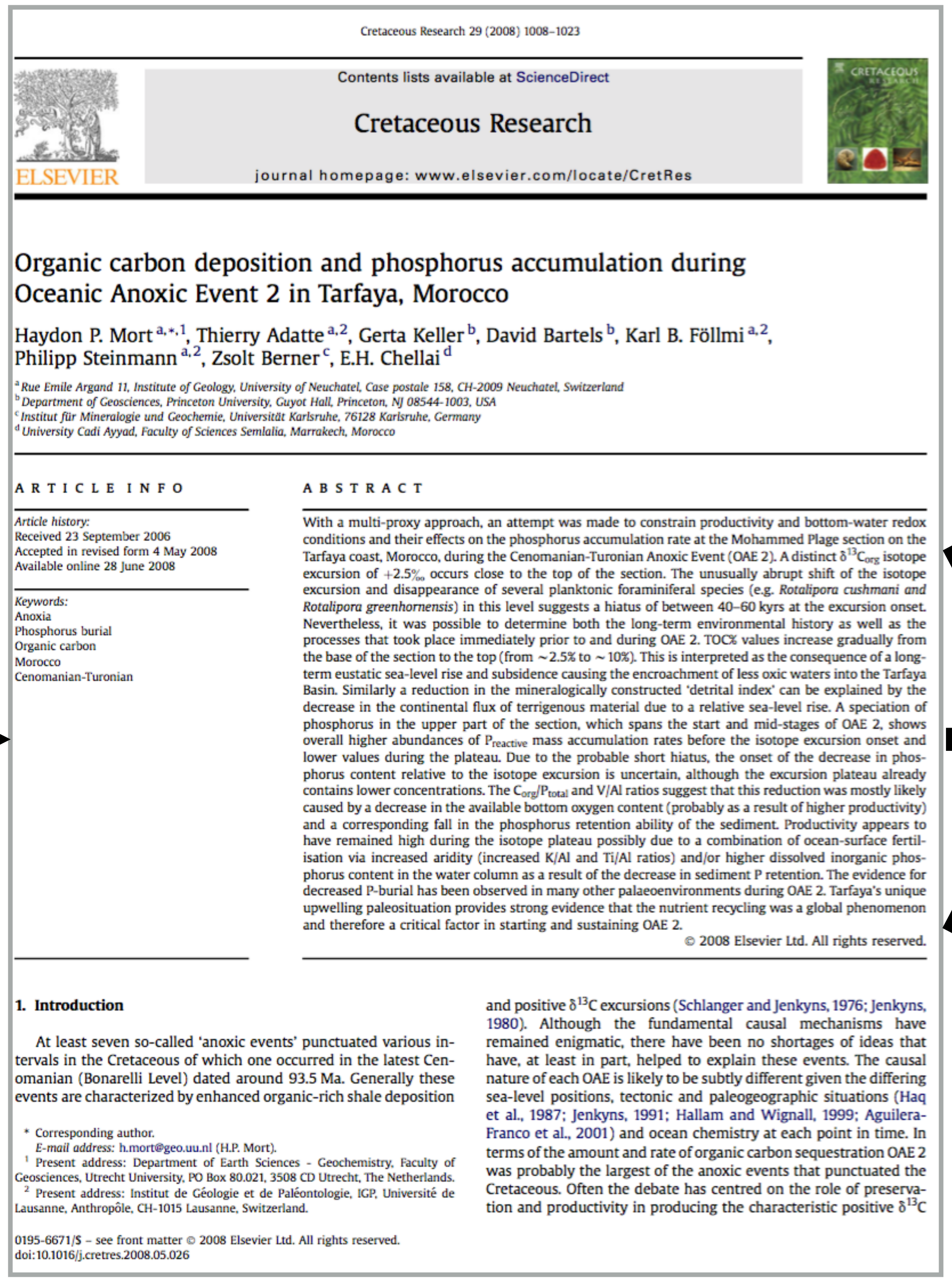
Cretaceous Research 29 (2008) 1008–1023
Contents lists available at ScienceDirect
Cretaceous Research
journal homepage: www.elsevier.com/locate/CretRes
Organic carbon deposition and phosphorus accumulation during Oceanic Anoxic Event 2 in Tarfaya, Morocco
Haydon P. Mort, Thierry Adatte, Gerta Keller, David Bartels, Karl B. Föllmi, Philipp Steinmann, Zsolt Berner, E.H. Chellai
ARTICLE INFO
ABSTRACT
1. Introduction

software tools

- CoreNLP
- OCR
- "geoNER"

publisher agreements

Libraries — University of Wisconsin-Madison; USGS — science for a changing world; The Geological Society of America; PLOS ONE; Elsevier; Wiley — Publishers Since 1807; Canadian Science Publishing; Taylor & Francis — Taylor & Francis Group; SEPM; Cambridge University Press; ?; ?

doc. fetching/storage

Center for High Throughput Computing

8-12k/day

parsing, annotation, labeling

COSMOS

GeoDeepDive Infrastructure Overview

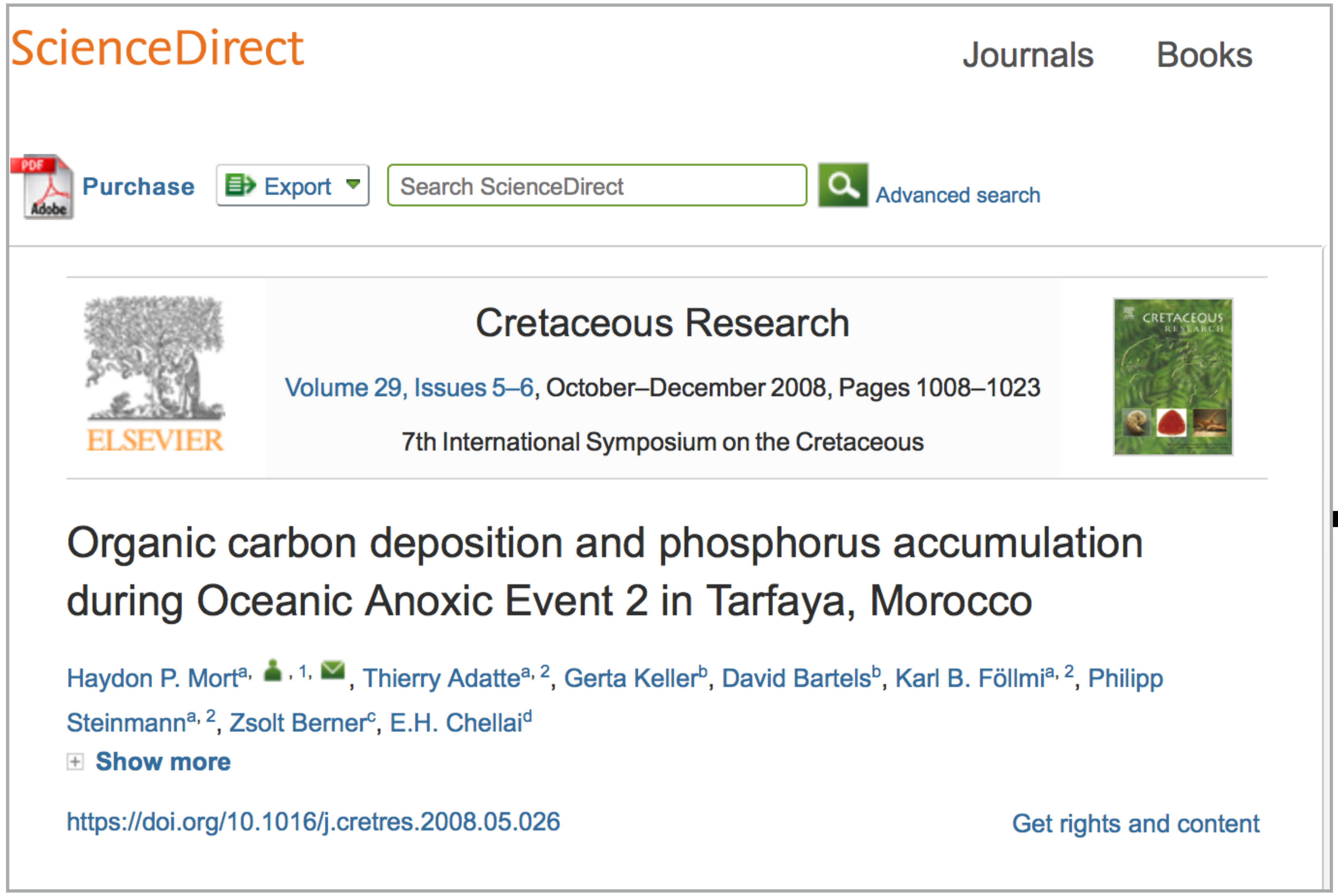
ScienceDirect
Journals Books
Purchase Export
Search ScienceDirect
Advanced search
ELSEVIER
Cretaceous Research
Volume 29, Issues 5–6, October–December 2008, Pages 1008–1023
7th International Symposium on the Cretaceous
CRETACEOUS RESEARCH
Organic carbon deposition and phosphorus accumulation during Oceanic Anoxic Event 2 in Tarfaya, Morocco
Haydon P. Mort[a, 1], Thierry Adatte[a, 2], Gerta Keller[b], David Bartels[b], Karl B. Föllmi[a, 2], Philipp Steinmann[a, 2], Zsolt Berner[c], E.H. Chellai[d]
Show more
https://doi.org/10.1016/j.cretres.2008.05.026
Get rights and content


Cretaceous Research 29 (2008) 1008–1023
Contents lists available at ScienceDirect
Cretaceous Research
journal homepage: www.elsevier.com/locate/CretRes
ELSEVIER

Organic carbon deposition and phosphorus accumulation during Oceanic Anoxic Event 2 in Tarfaya, Morocco

Haydon P. Mort[a,*,1], Thierry Adatte[a,2], Gerta Keller[b], David Bartels[b], Karl B. Föllmi[a,2], Philipp Steinmann[a,2], Zsolt Berner[c], E.H. Chellai[d]

[a] Rue Emile Argand 11, Institute of Geology, University of Neuchatel, Case postale 158, CH-2009 Neuchatel, Switzerland
[b] Department of Geosciences, Princeton University, Guyot Hall, Princeton, NJ 08544-1003, USA
[c] Institut für Mineralogie und Geochemie, Universität Karlsruhe, 76128 Karlsruhe, Germany
[d] University Cadi Ayyad, Faculty of Sciences Semlalia, Marrakech, Morocco

ARTICLE INFO

Article history:
Received 23 September 2006
Accepted in revised form 4 May 2008
Available online 28 June 2008

Keywords:
Anoxia
Phosphorus burial
Organic carbon
Morocco
Cenomanian-Turonian

ABSTRACT

With a multi-proxy approach, an attempt was made to constrain productivity and bottom-water redox conditions and their effects on the phosphorus accumulation rate at the Mohammed Plage section on the Tarfaya coast, Morocco, during the Cenomanian-Turonian Anoxic Event (OAE 2). A distinct $\delta^{13}C_{org}$ isotope excursion of +2.5‰ occurs close to the top of the section. The unusually abrupt shift of the isotope excursion and disappearance of several planktonic foraminiferal species (e.g. *Rotalipora cushmani and Rotalipora greenhornensis*) in this level suggests a hiatus of between 40–60 kyrs at the excursion onset. Nevertheless, it was possible to determine both the long-term environmental history as well as the processes that took place immediately prior to and during OAE 2. TOC% values increase gradually from the base of the section to the top (from ~2.5% to ~10%). This is interpreted as the consequence of a long-term eustatic sea-level rise and subsidence causing the encroachment of less oxic waters into the Tarfaya Basin. Similarly a reduction in the mineralogically constructed 'detrital index' can be explained by the decrease in the continental flux of terrigenous material due to a relative sea-level rise. A speciation of phosphorus in the upper part of the section, which spans the start and mid-stages of OAE 2, shows overall higher abundances of $P_{reactive}$ mass accumulation rates before the isotope excursion onset and lower values during the plateau. Due to the probable short hiatus, the onset of the decrease in phosphorus content relative to the isotope excursion is uncertain, although the excursion plateau already contains lower concentrations. The C_{org}/P_{total} and V/Al ratios suggest that this reduction was mostly likely caused by a decrease in the available bottom oxygen content (probably as a result of higher productivity) and a corresponding fall in the phosphorus retention ability of the sediment. Productivity appears to have remained high during the isotope plateau possibly due to a combination of ocean-surface fertilisation via increased aridity (increased K/Al and Ti/Al ratios) and/or higher dissolved inorganic phosphorus content in the water column as a result of the decrease in sediment P retention. The evidence for decreased P-burial has been observed in many other palaeoenvironments during OAE 2. Tarfaya's unique upwelling paleosituation provides strong evidence that the nutrient recycling was a global phenomenon and therefore a critical factor in starting and sustaining OAE 2.

© 2008 Elsevier Ltd. All rights reserved.

1. Introduction

At least seven so-called 'anoxic events' punctuated various intervals in the Cretaceous of which one occurred in the latest Cenomanian (Bonarelli Level) dated around 93.5 Ma. Generally these events are characterized by enhanced organic-rich shale deposition and positive $\delta^{13}C$ excursions (Schlanger and Jenkyns, 1976; Jenkyns, 1980). Although the fundamental causal mechanisms have remained enigmatic, there have been no shortages of ideas that have, at least in part, helped to explain these events. The causal nature of each OAE is likely to be subtly different given the differing sea-level positions, tectonic and paleogeographic situations (Haq et al., 1987; Jenkyns, 1991; Hallam and Wignall, 1999; Aguilera-Franco et al., 2001) and ocean chemistry at each point in time. In terms of the amount and rate of organic carbon sequestration OAE 2 was probably the largest of the anoxic events that punctuated the Cretaceous. Often the debate has centred on the role of preservation and productivity in producing the characteristic positive $\delta^{13}C$

* Corresponding author.
E-mail address: h.mort@geo.uu.nl (H.P. Mort).
[1] Present address: Department of Earth Sciences - Geochemistry, Faculty of Geosciences, Utrecht University, PO Box 80.021, 3508 CD Utrecht, The Netherlands.
[2] Present address: Institut de Géologie et de Paléontologie, IGP, Université de Lausanne, Anthropôle, CH-1015 Lausanne, Switzerland.

0195-6671/$ – see front matter © 2008 Elsevier Ltd. All rights reserved.
doi:10.1016/j.cretres.2008.05.026

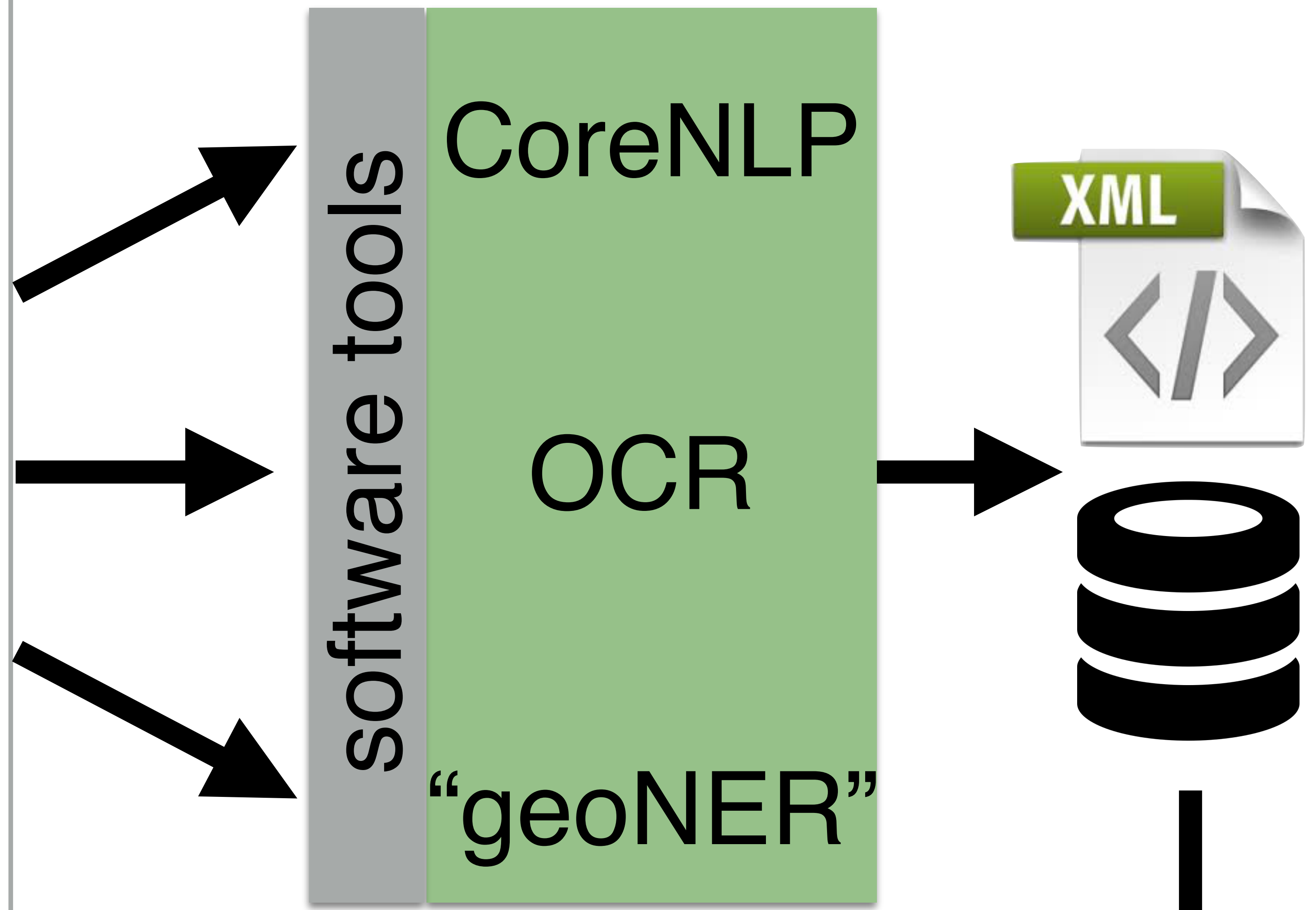

publisher agreements

Libraries
UNIVERSITY OF WISCONSIN-MADISON
THE GEOLOGICAL SOCIETY OF AMERICA®
USGS
science for a changing world
PLOS ONE
ELSEVIER
WILEY
Publishers Since 1807
Canadian Science Publishing
Taylor & Francis
Taylor & Francis Group
SEPM
CAMBRIDGE UNIVERSITY PRESS
?
?

doc. fetching/storage

HT CENTER FOR HIGH THROUGHPUT COMPUTING

8-12k/day

parsing, annotation, labeling

COSMOS

Science!

GeoDeepDive Infrastructure Overview

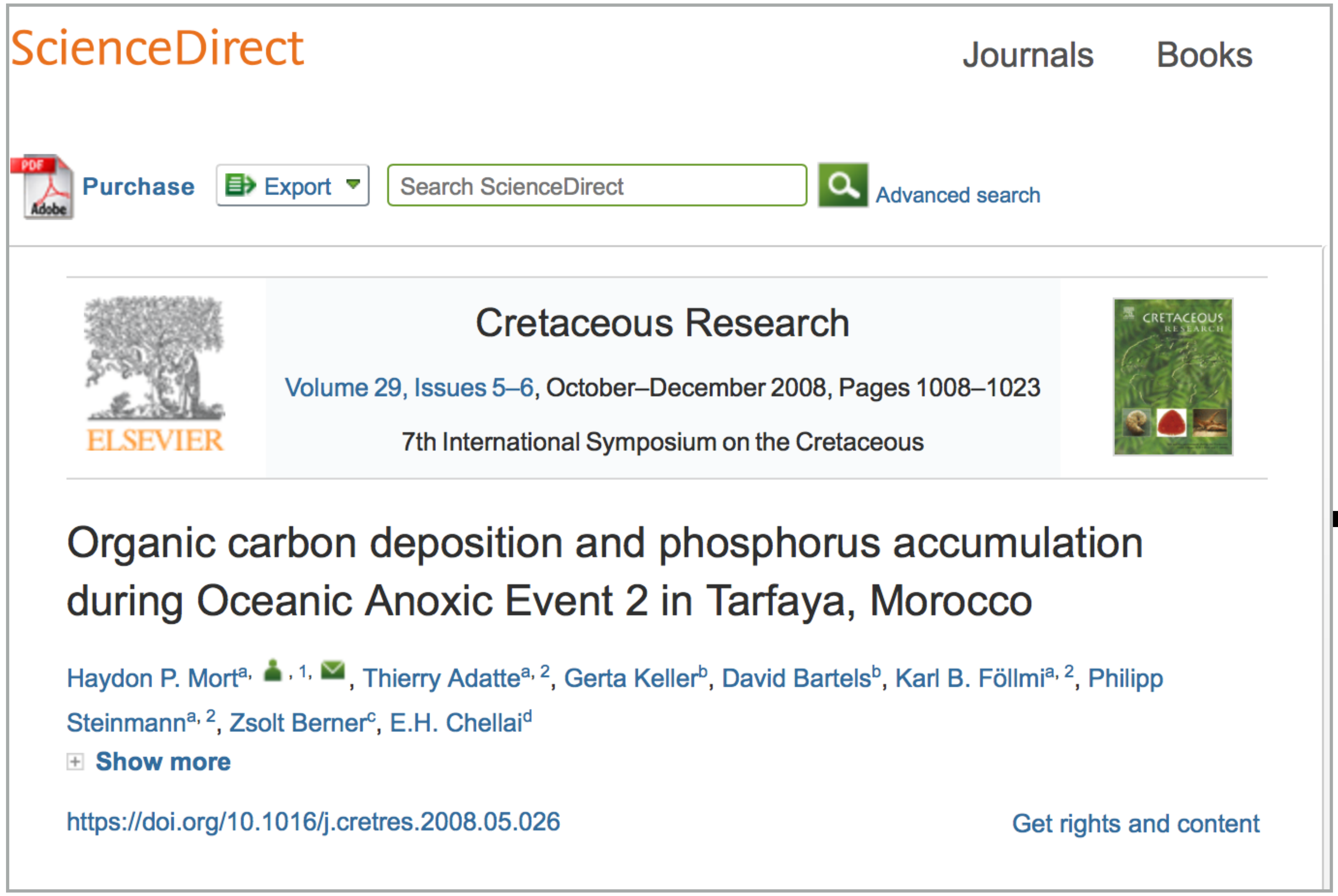

software tools

CoreNLP

OCR

"geoNER"

XML

publisher agreements

Libraries
UNIVERSITY OF WISCONSIN-MADISON

USGS
science for a changing world

THE GEOLOGICAL SOCIETY OF AMERICA®

PLOS ONE

ELSEVIER

WILEY
Publishers Since 1807

Canadian Science Publishing

Taylor & Francis
Taylor & Francis Group

SEPM

CAMBRIDGE
UNIVERSITY PRESS

?

?

doc. fetching/storage

CENTER FOR
HIGH THROUGHPUT
COMPUTING

8-12k/day

parsing, annotation, labeling

COSMOS

Science!

Original document data and metadata curation


```
<doi_record>
<journal_metadata language="en">
<full_title>Annals of the New York Academy of Sciences</full_title>
</journal_metadata>
<journal_issue>
<publication_date media_type="print">
                <month>03</month>
                <year>1956</year>
</publication_date>
<journal_volume>
<volume>63</volume>
<doi_data>
<doi>10.1111/nyas.1956.63.issue-6</doi>
</doi_data>
<titles>
<title>TOPOLOGICAL CYTOCHEMISTRY</title>
</titles>
<contributors>
<person_name contributor_role="author" sequence="first">
<given_name>M. J.</given_name>
<surname>Kopac</surname>
</person_name>
</contributors>
<first_page>1219</first_page>
<last_page>1235</last_page>
</pages>
```


🔒Original PDFs 🔒


```
{u'dc:title': u'Editorial Board',
 u'prism:coverDate': [{u'$': u'2011-01-01', u'@_fa': u'true'}],
 u'prism:coverDisplayDate': u'January\u2013June 2011',
 u'prism:doi': u'10.1016/S0753-3969(11)00046-2',
 u'prism:publicationName': u'Annales de Pal\xe9ontologie',
 u'prism:startingPage': u'i',
u'prism:volume': u'97'}
```

Original document data and metadata curation

WILEY Publishers Since 1807


```
<doi_record>
<journal_metadata language="en">
<full_title>Annals of the New York Academy of Sciences</full_title>
</journal_metadata>
<journal_issue>
<publication_date media_type="print">
              <month>03</month>
              <year>1956</year>
</publication_date>
<journal_volume>
<volume>63</volume>
<doi_data>
<doi>10.1111/nyas.1956.63.issue-6</doi>
</doi_data>
<titles>
<title>TOPOLOGICAL CYTOCHEMISTRY</title>
</titles>
<contributors>
<person_name contributor_role="author" sequence="first">
<given_name>M. J.</given_name>
<surname>Kopac</surname>
</person_name>
</contributors>
<first_page>1219</first_page>
<last_page>1235</last_page>
</pages>
```


ELSEVIER


```
{u'dc:title': u'Editorial Board’,
 u'prism:coverDate': [{u'$':
u'2011-01-01', u'@_fa':
u'true'}],
 u'prism:coverDisplayDate':
u'January\u2013June 2011',
 u'prism:doi': u'10.1016/
S0753-3969(11)00046-2’,
 u'prism:publicationName':
u'Annales de Pal\xe9ontologie',
 u'prism:startingPage': u'i’,
u'prism:volume': u'97'}
```


Original PDFs

Fetched by GDD

Harmonized
Document Metadata (bibJSON files + mongoDB)


```
{"authors":"Kopac, M. J.",
"coverDate":"March 1956",
"publication_date":{"month":3,"year":1956},
"publisher":"Wiley-Blackwell",
"pubname":"Annals of the New York Academy of Sciences",
"sha1":"01b2fcc8a94a2bfbe785812aab28e45fcbe02d3f",
"startingPage":"1219",
"time":["2016-03-17T08:39:22.532-05:00"]
"title":"TOPOLOGICAL CYTOCHEMISTRY",
"vol":"63",
"doi":"10.1111/j.1749-6632.1956.tb32132.x",
"url":"http://doi.wiley.com/10.1111/j.
1749-6632.1956.tb32132.x"
…}

{
"coverDate":"January—June 2011",
"publication_date":{"month":6,"year":2011},
"publisher":"Elsevier",
"pubname":"Annales de Paléontologie",
"sha1":"6ee25a57571021e45faa1b545a5c59b9748ada7b",
"startingPage":"i",
"time":"2015-07-09T15:00:17.875-05:00",
"title":"Editorial Board",
"vol":"97",
"doi": "10.1016/S0753-3969(11)00046-2",
"url":"http://www.sciencedirect.com/science/article/pii/
S0753396911000462"
…
}
```

Vocabulary ingestion and labeling

geodeepdive.org/api/dictionaries

curated lists of terms
with hierarchy/context:

The Paleobiology Database
revealing the history of life

→ 350k
taxonomic names/
bio classification

mindat.org

→ 6k
mineral names/
chemistry

Macrostrat

→ 45k
stratigraphic names/
hierarchy, rock types

Vocabulary ingestion and labeling

geodeepdive.org/api/dictionaries

curated lists of terms
with hierarchy/context:

The Paleobiology Database
revealing the history of life

→ 350k
taxonomic names/
bio classification

mindat.org

→ 6k
mineral names/
chemistry

Macrostrat

→ 45k
stratigraphic names/
hierarchy, rock types

GDD-supplied full text
and citation info.

Pyritization of soft-bodied fossils: Beecher's Trilobite Bed, Upper Ordovician, New York State

Derek E.G. Briggs
Department of Geology, University of Bristol, Wills Memorial Building, Queen's Road
Bristol BS8 1RJ, England
Simon H. Bottrell, Robert Raiswell
Department of Earth Sciences, University of Leeds, Leeds LS2 9JT, England

ABSTRACT

Although pyrite is ubiquitous in fine-grained, organic, carbon-bearing marine sediments, it is only rarely involved in the preservation of soft-bodied organisms. Beecher's Trilobite Bed in Upper Ordovician strata of New York State is an exception—it is a classic locality for trilobites having appendages and other soft tissues preserved in pyrite. The relative timing and duration of the formation of pyrite associated with the fossils and their host sediments were determined by use of sulfur isotope ratios. The exoskeleton and appendages of the trilobites show relatively light sulfur isotope values in contrast to the enclosing sediment, which is characterized by a substantial excursion to heavy isotope values. Preservation of soft parts requires rapid burial of carcasses in sediments otherwise low in metabolizable organic matter. In these circumstances, pyrite formation within the sediments is suppressed; thus, concentrations of sulfate and reactive iron are initially high enough to promote early, rapid, and extensive pyritization of nonmineralized tissue.

INTRODUCTION

Fossils that preserve soft tissues provide critical evidence of the morphology and paleobiology of extinct organisms—in contrast to normal shelly fossil assemblages, which yield only limited information. Soft tissues (i.e., those lacking any mineral component in life) may be preserved in a variety of ways. Those that are particularly decay resistant (cuticles composed of lignin, sporopollenin, cutan, sclerotized chitin, for example) may become fossilized as stable kerogen compounds in certain environments (Tegelaar et al., 1989; Jeram et al., 1990). Tissues more susceptible to bacterial breakdown (e.g., muscles, internal organs, thin cuticles) survive only where they are replicated by very early authigenic mineralization (Allison, 1988b). This normally involves one of three groups of diagenetic minerals: phosphate, carbonate, or pyrite. Pyrite is commonly a component of fine-grained, organic-rich marine sediments, forming by reactions between detrital iron minerals and the H_2S generated by anaerobic sulfate-reducing bacteria (Goldhaber and Kaplan, 1974). In marine sediments, iron and seawater sulfate are normally present in abundance, and pyrite formation is apparently controlled by the concentration of metabolizable organic carbon (Berner, 1970, 1984).

Although pyrite is widespread in marine sediments, and commonly is found in association with fossils, these are usually the remains of mineralized (Hudson, 1982), or at least refractory, tissues (e.g., in plants; Kenrick and Edwards, 1988). Beecher's Trilobite Bed (named after the Yale paleontologist who worked extensively on the trilobites in the 1890s) is one of the very rare examples where pyrite formed early enough to contribute to the preservation of soft tissues. Only the Devonian (lower Emsian) Hunsrückschiefer of western Germany (Stürmer et al., 1980; Kott and Wuttke, 1987; Bartels and Brassel, 1990), which preserves the soft tissues of trilobites (Stürmer and Bergström, 1973), cephalopods (Stürmer, 1985), and ctenophores (Stanley and Stürmer, 1987), for example, is comparable.

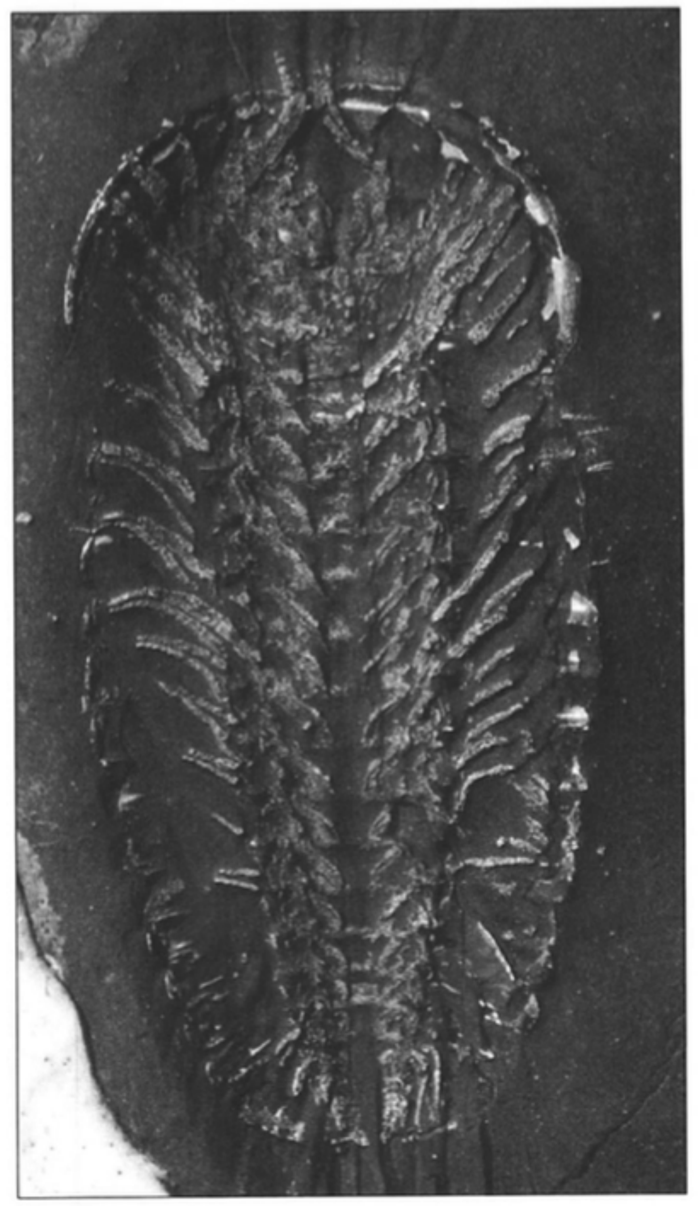

Figure 1. ***Triarthrus eatoni*, ~30 mm long, from Beecher's Trilobite Bed (photograph by J. E. Almond, provided by H. B. Whittington).**

Beecher's Bed is additionally important as the only major occurrence of soft-bodied organisms (Konservat-Lagerstätte) known from the Ordovician (Allison and Briggs, 1991). In this paper we analyze the mineralization of the trilobites in Beecher's Bed and present a model for the pyritization of soft tissues in the fossil record.

GEOLOGY, v. 19, p. 1221–1224, December 1991

Vocabulary ingestion and labeling

geodeepdive.org/api/dictionaries

curated lists of terms
with hierarchy/context:

The Paleobiology Database
revealing the history of life

→ 350k
taxonomic names/
bio classification

mindat.org

→ 6k
mineral names/
chemistry

Macrostrat

→ 45k
stratigraphic names/
hierarchy, rock types

GDD-supplied full text
and citation info.

Pyritization of soft-bodied fossils: Beecher's Trilobite Bed, Upper Ordovician, New York State

Derek E.G. Briggs
Department of Geology, University of Bristol, Wills Memorial Building, Queen's Road
Bristol BS8 1RJ, England
Simon H. Bottrell, Robert Raiswell
Department of Earth Sciences, University of Leeds, Leeds LS2 9JT, England

ABSTRACT

Although pyrite is ubiquitous in fine-grained, organic, carbon-bearing marine sediments, it is only rarely involved in the preservation of soft-bodied organisms. Beecher's Trilobite Bed in Upper Ordovician strata of New York State is an exception—it is a classic locality for trilobites having appendages and other soft tissues preserved in pyrite. The relative timing and duration of the formation of pyrite associated with the fossils and their host sediments were determined by use of sulfur isotope ratios. The exoskeleton and appendages of the trilobites show relatively light sulfur isotope values in contrast to the enclosing sediment, which is characterized by a substantial excursion to heavy isotope values. Preservation of soft parts requires rapid burial of carcasses in sediments otherwise low in metabolizable organic matter. In these circumstances, pyrite formation within the sediments is suppressed; thus, concentrations of sulfate and reactive iron are initially high enough to promote early, rapid, and extensive pyritization of nonmineralized tissue.

INTRODUCTION

Fossils that preserve soft tissues provide critical evidence of the morphology and paleobiology of extinct organisms—in contrast to normal shelly fossil assemblages, which yield only limited information. Soft tissues (i.e., those lacking any mineral component in life) may be preserved in a variety of ways. Those that are particularly decay resistant (cuticles composed of lignin, sporopollenin, cutan, sclerotized chitin, for example) may become fossilized as stable kerogen compounds in certain environments (Tegelaar et al., 1989; Jeram et al., 1990). Tissues more susceptible to bacterial breakdown (e.g., muscles, internal organs, thin cuticles) survive only where they are replicated by very early authigenic mineralization (Allison, 1988b). This normally involves one of three groups of diagenetic minerals: phosphate, carbonate, or pyrite. Pyrite is commonly a component of fine-grained, organic-rich marine sediments, forming by reactions between detrital iron minerals and the H_2S generated by anaerobic sulfate-reducing bacteria (Goldhaber and Kaplan, 1974). In marine sediments, iron and seawater sulfate are normally present in abundance, and pyrite formation is apparently controlled by the concentration of metabolizable organic carbon (Berner, 1970, 1984).

Although pyrite is widespread in marine sediments, and commonly is found in association with fossils, these are usually the remains of mineralized (Hudson, 1982), or at least refractory, tissues (e.g., in plants; Kenrick and Edwards, 1988). Beecher's Trilobite Bed (named after the Yale paleontologist who worked extensively on the trilobites in the 1890s) is one of the very rare examples where pyrite formed early enough to contribute to the preservation of soft tissues. Only the Devonian (lower Emsian) Hunsrückschiefer of western Germany (Stürmer et al., 1980; Kott and Wuttke, 1987; Bartels and Brassel, 1990), which preserves the soft tissues of trilobites (Stürmer and Bergström, 1973), cephalopods (Stürmer, 1985), and ctenophores (Stanley and Stürmer, 1987), for example, is comparable.

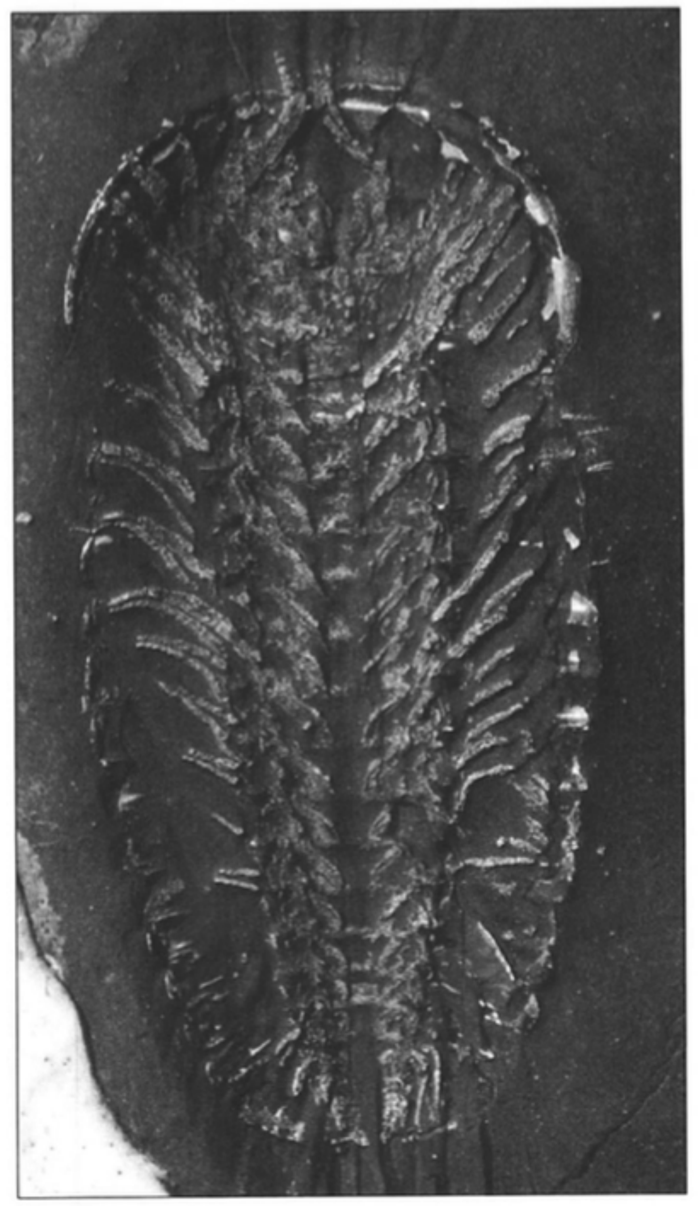

Figure 1. ***Triarthrus eatoni*****, ~30 mm long, from Beecher's Trilobite Bed (photograph by J. E. Almond, provided by H. B. Whittington).**

Beecher's Bed is additionally important as the only major occurrence of soft-bodied organisms (Konservat-Lagerstätte) known from the Ordovician (Allison and Briggs, 1991). In this paper we analyze the mineralization of the trilobites in Beecher's Bed and present a model for the pyritization of soft tissues in the fossil record.

GEOLOGY, v. 19, p. 1221–1224, December 1991

labeled
entities, tuples

Trilobita
Triarthrus
Climacograptus

pyrite

Frankfort Shale

exposed
via API

```
"term_hits": { ▼ 189470 properties, 6 MB
  "Navajosuchus novomexicanus": 7,
  "Ptilocolepidae": 2,
  "Geotrupidae": 652,
  "Macropoma lewesiensis": 11,
  "Simia morio": 7,
  "Anhanguera robustus": 4,
  "Montipora verrilli": 36,
  "Geffenina wangi": 6,
  "Shuvosaurus": 198,
  "Dryorhizopsidae": 1,
  "Ostrea antarctica": 12,
  "Pholidophorus dentatus": 10,
  "Oochorista": 6,
  "Sciurus arizonensis": 18,
  "Prosbole biexcisa": 3,
  "Toxopatagus": 271,
  "Sulcavitus": 169,
  "Brontops amplus": 2,
  "Melonella": 1087,
  "Bathrotomaria": 688,
  "Placochelyanus": 64,
  "Iliochione": 555,
  "Attenosaurus subulensis": 10,
  "Miccylotyrans": 4,
```

```
  "Deryeuma": 4,
  "Chaetabraeus": 2,
  "Cardinalis cardinalis": 1113,
  "Odontaster": 2532,
  "Coeloma": 384,
  "Megatrema": 36,
  "Xinjiangtitan": 4,
  "Tephrodytes brassicarvalis": 74,
  "Prolagus crusafonti": 42,
  "Streblascopora germana": 2,
  "Dichobunoidea": 11,
  "Cetotherium hupschi": 1,
  "Hauericeras (Gardeniceras) gardeni": 10,
  "Parevania": 15,
  "Histriobdellidae": 130,
  "Berosus (Berosus)": 13,
  "Dinornis elephantopus": 8,
  "Sternoxi": 11,
  "Bellimurina (Bellimurina)": 4,
  "Raphignathoidea": 76,
  "Cybelurus occidentalis": 4,
```


Define your own dictionaries:
https://github.com/UW-Deepdive-Infrastructure/dictionary_example

"term_hits": { ▼ 189470
"Navajosuchus novomex
"Ptilocolepidae": 2,
"Geotrupidae": 652,
"Macropoma lewesiensis
"Simia morio": 7,
"Anhanguera robustus":
"Montipora verrilli":
"Geffenina wangi": 6,
"Shuvosaurus": 198,
"Dryorhizopsidae": 1,
"Ostrea antarctica": 1
"Pholidophorus dentatu
"Oochorista": 6,
"Sciurus arizonensis":
"Prosbole biexcisa": 3
"Toxopatagus": 271,
"Sulcavitus": 169,
"Brontops amplus": 2,
"Melonella": 1087,
"Bathrotomaria": 688,
"Placochelyanus": 64,
"Iliochione": 555,
"Attenosaurus subulensis": 10,
"Miccylotyrans": 4,

"pubname": "Earth-Science Reviews",
"publisher": "Elsevier",
"title": "The Cambrian palaeontological record of the Indian subcontinent",
"coverDate": "Available online 11 June 2016",
"URL": "http://www.sciencedirect.com/science/article/pii/S0012825216301179",
"authors": "Hughes, Nigel C.",
"hits": 4,
"highlight": [▼ 4 items, 411 bytes
" represented is the hyolithimorph Sulcavitus wynnei (Waagen, 1885) collected from several horizons within",
") Hy Sulcavitus wynnei (Waagen), dorsum, Khussak Formation, Salt Range, SH, GSI 4118 (CMCIP 71490",
",) Kruse and Hughes in press, fig. 5C, scale bar: 2.5 mm; T) Hy Sulcavitus wynnei (Waagen), venter",
" 71490), Kruse and Hughes in press, fig. 5A, scale bar: 2.5 mm; U) Hy Sulcavitus wynnei (Waagen"
]
},
{ ▼ 8 properties, 431 bytes
"pubname": "Alcheringa: An Australasian Journal of Palaeontology",
"publisher": "Taylor and Francis",
"title": "Biostratigraphic potential of Middle Cambrian hyoliths from the eastern Georgina Basin",
"coverDate": "2002 01",
"URL": "http://www.tandfonline.com/doi/abs/10.1080/03115510208619263",
"authors": "Kruse, Peter D.",
"hits": 1,
"highlight": [▼ 1 item, 94 bytes
",it is noteworthy that Sulcavitus possesses a distinctive deep median sulcus on the dorsum"

Define your own dictionaries:
https://github.com/UW-Deepdive-Infrastructure/dictionary_example

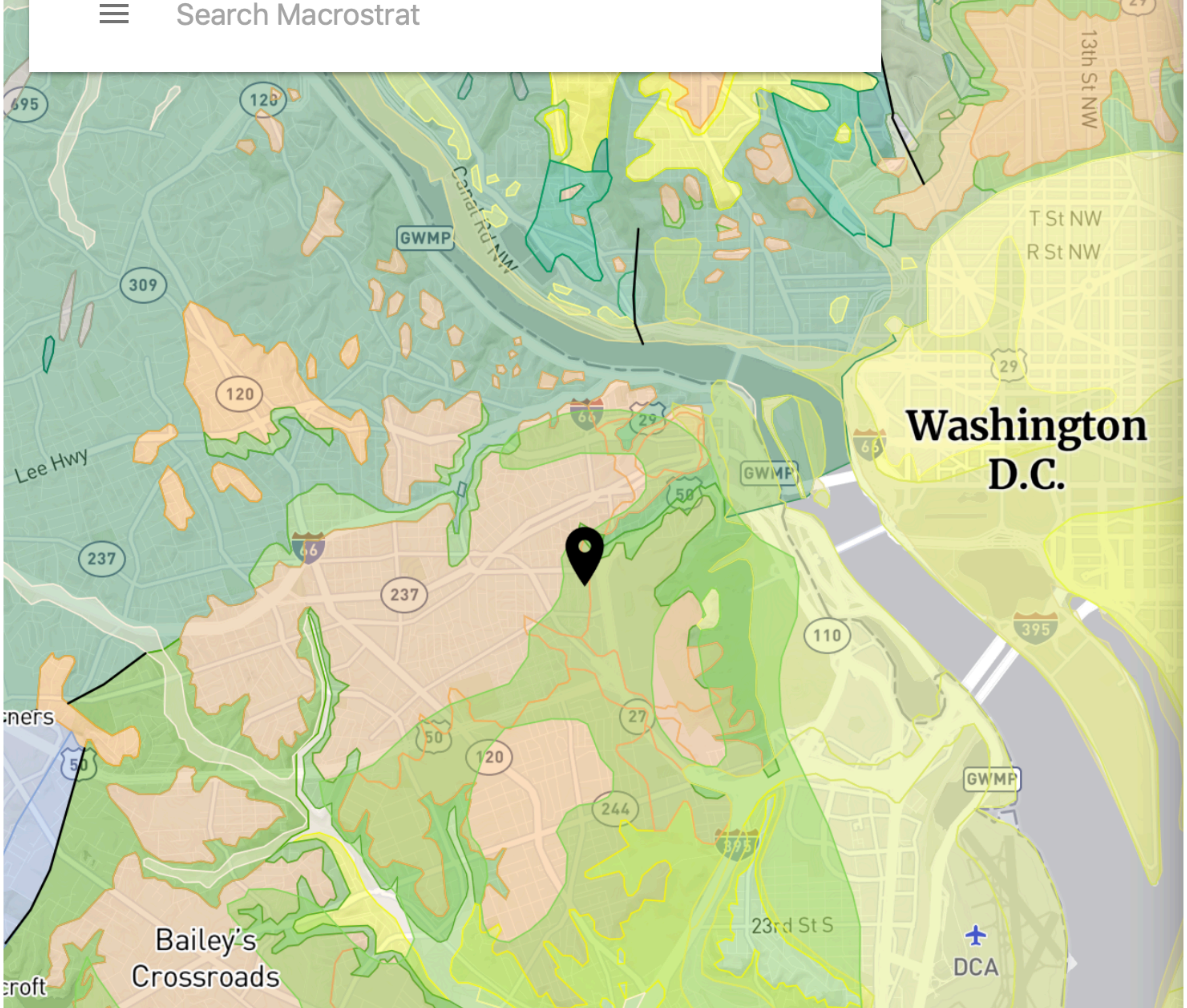

Primary Literature via GeoDeepDive

Palaeogeography, Palaeoclimatology, Palaeoecology Elsevier

Wolfe, Jack A., Upchurch, Garland R., 1987. **North American nonmarine climates and vegetation during the Late Cretaceous.**

...First , toothed angiosperm leaves appear by the Aptian (e.g. , Quercophyllum in Zone I of the **Potomac Group** ; Hickey and Doyle , 1977) , and virtually all other major physiognomic types of dicotyledonous leaves appeared by the early Cenomanian (Zone III of the **Potomac Group** ; Upchurch and Wolfe , 1987) ....

Uličný, David, Kvaček, Jiří, Svobodová, Marcela, Špičáková, Lenka, 1997. **High-frequency sea-level fluctuations and plant habitats in Cenomanian fluvial**

GeoDeepDive: key components

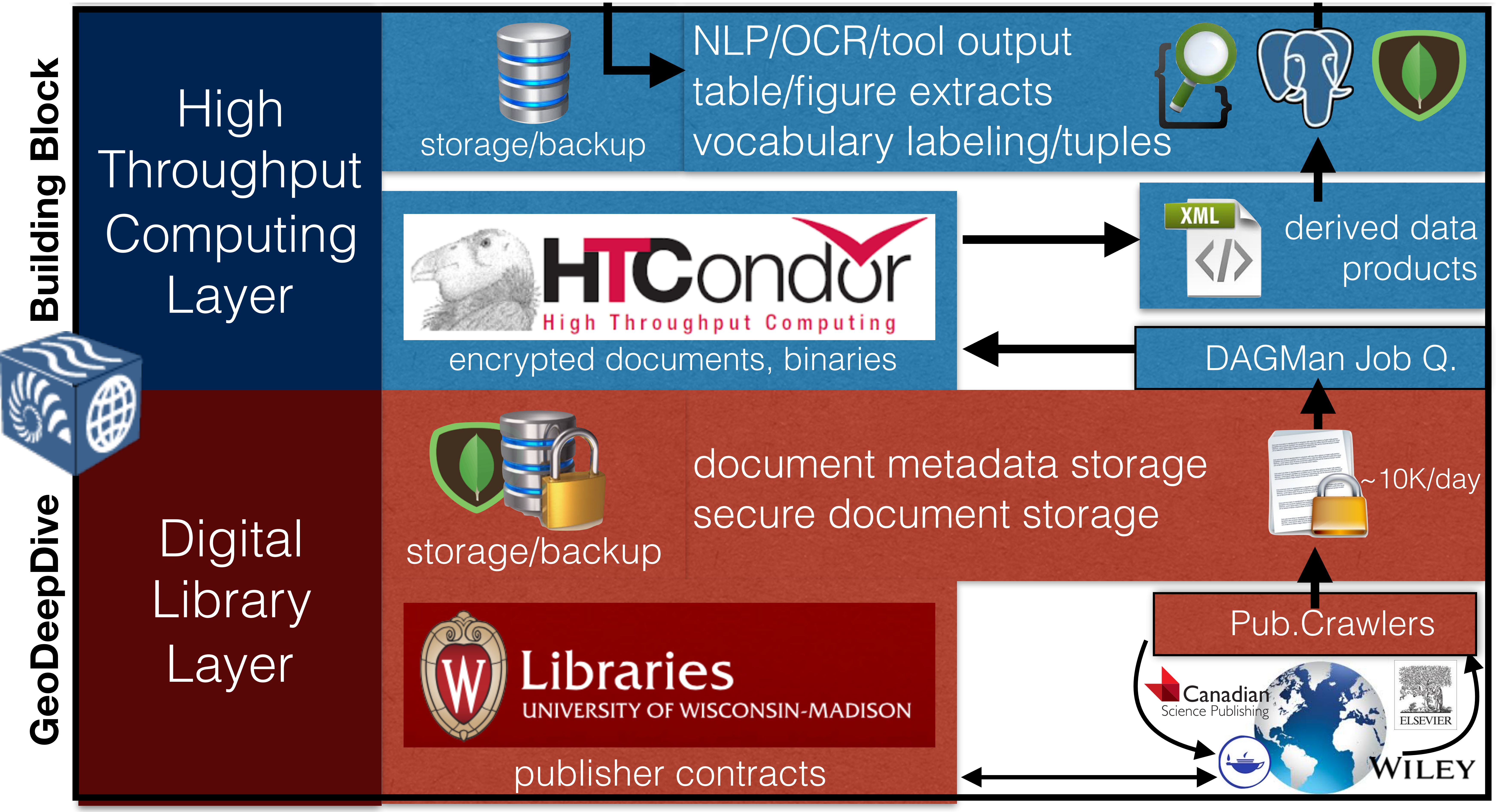

- Permissive, custom agreements with content owners that enable local storage, collaborative use.
- Automated system for acquiring documents and metadata from multiple providers.
- ElasticSearch for simple full-text word/phrase matching, cached results for large vocabularies.
- Harmonized document metadata for citation & linking to original content.
- Computing resources to rapidly re-analyze all documents.

NSF
USGS
science for a changing world
support 2014-2018 by NSF-ICER 1343760
partial current support from USGS

✓Principled access to scientific literature

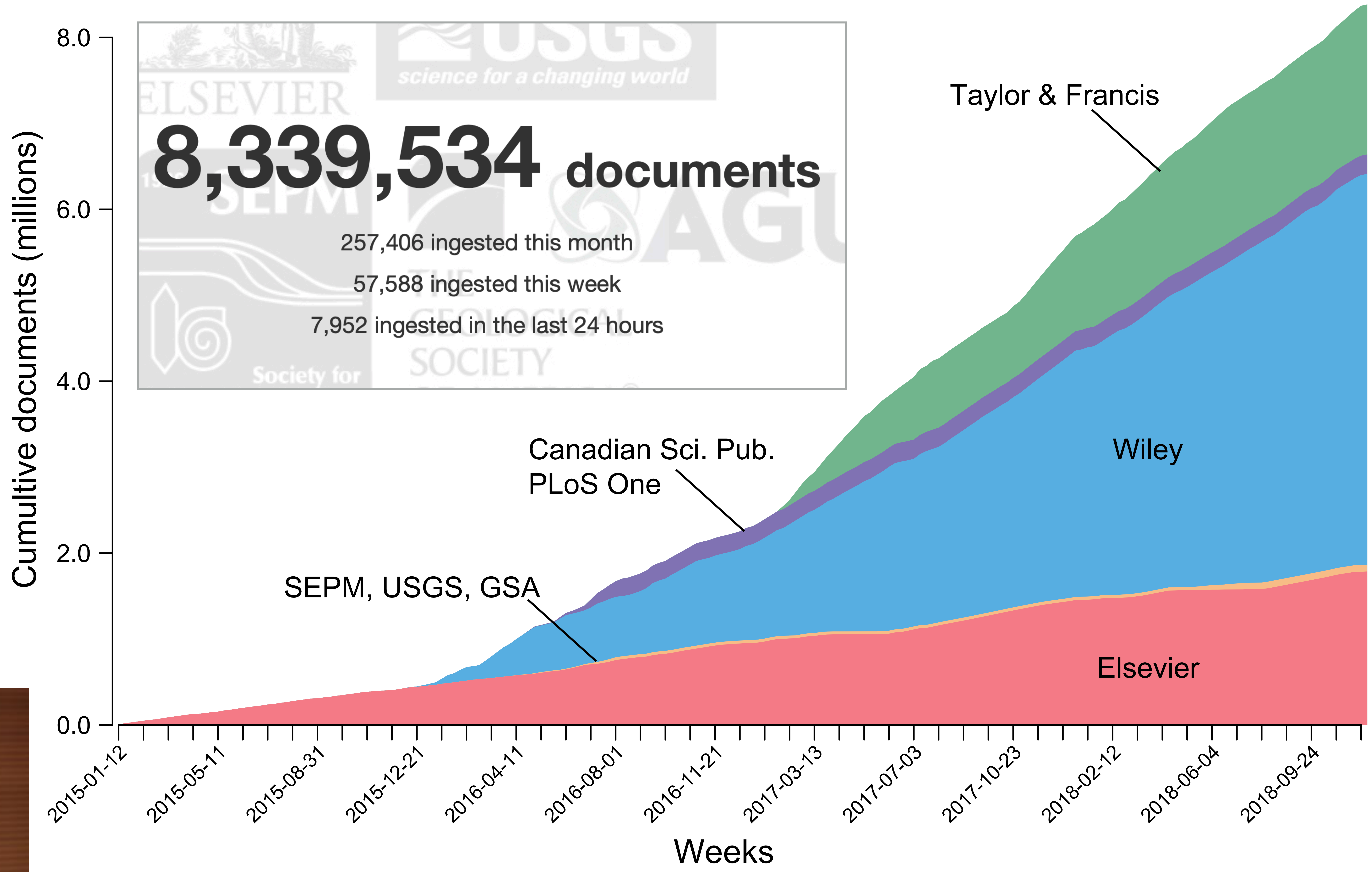

Miron Livny
Computer Sciences Dept.

Ian Ross
Computer Sciences Dept.

COSMOS: required components

1. Principled, automated access to scientific publications and the computing capacity and infrastructure required to repeatedly analyze them.

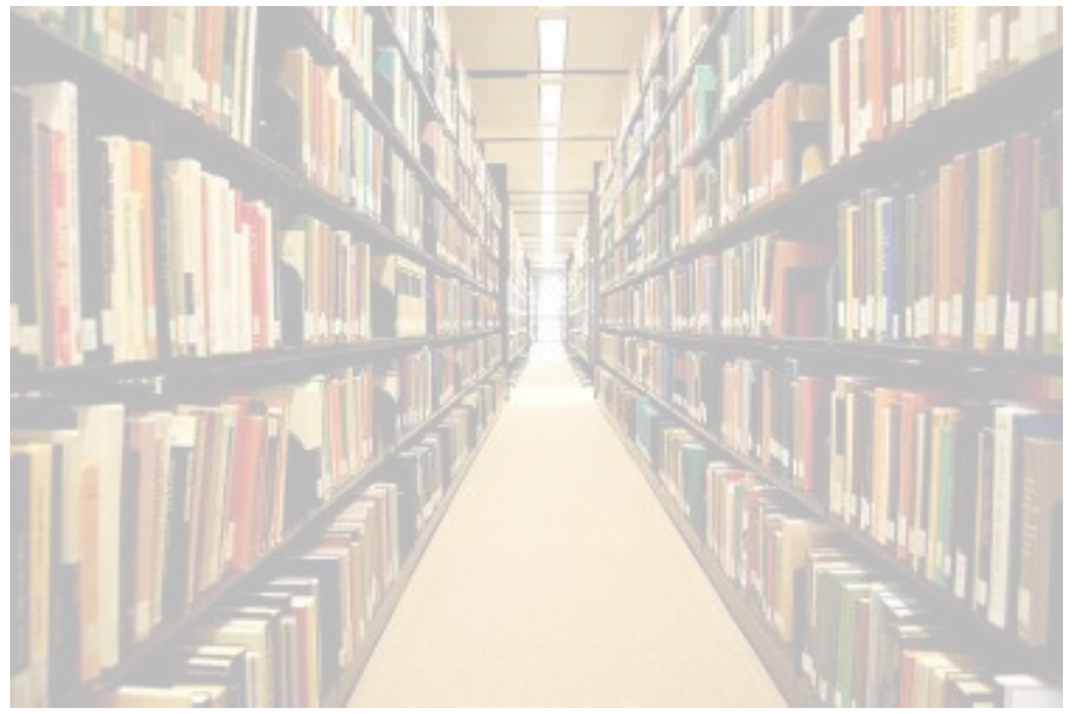

2. Models and techniques to represent and capture multi-modal data within publications.

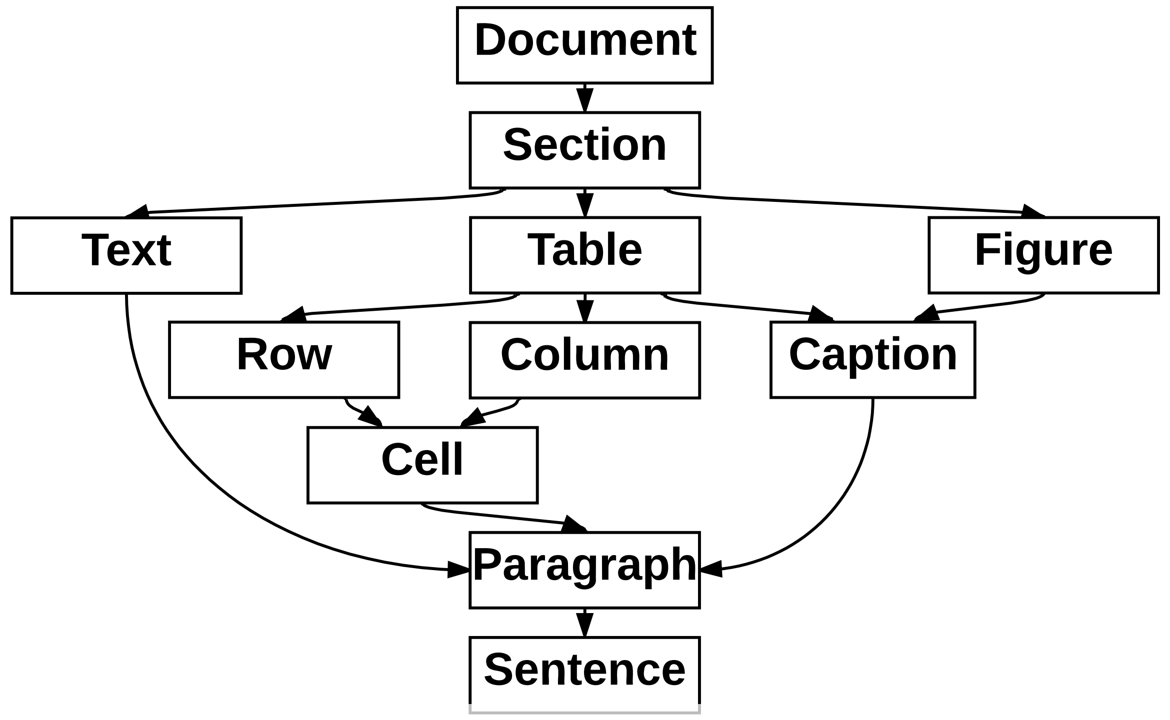

3. Earth system model with parameterizations and predictions that overlap with many different types of empirical data and observations in publications.

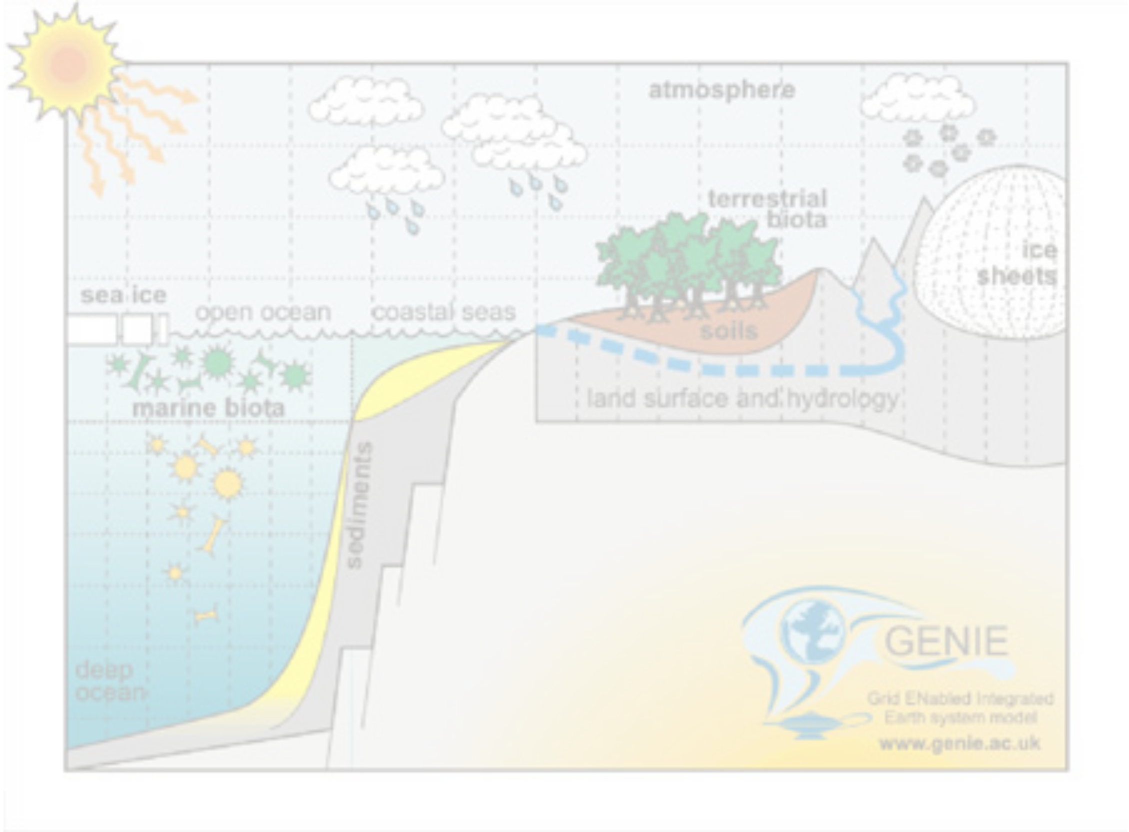

Fonduer: Information Extraction over Richly Formatted Data

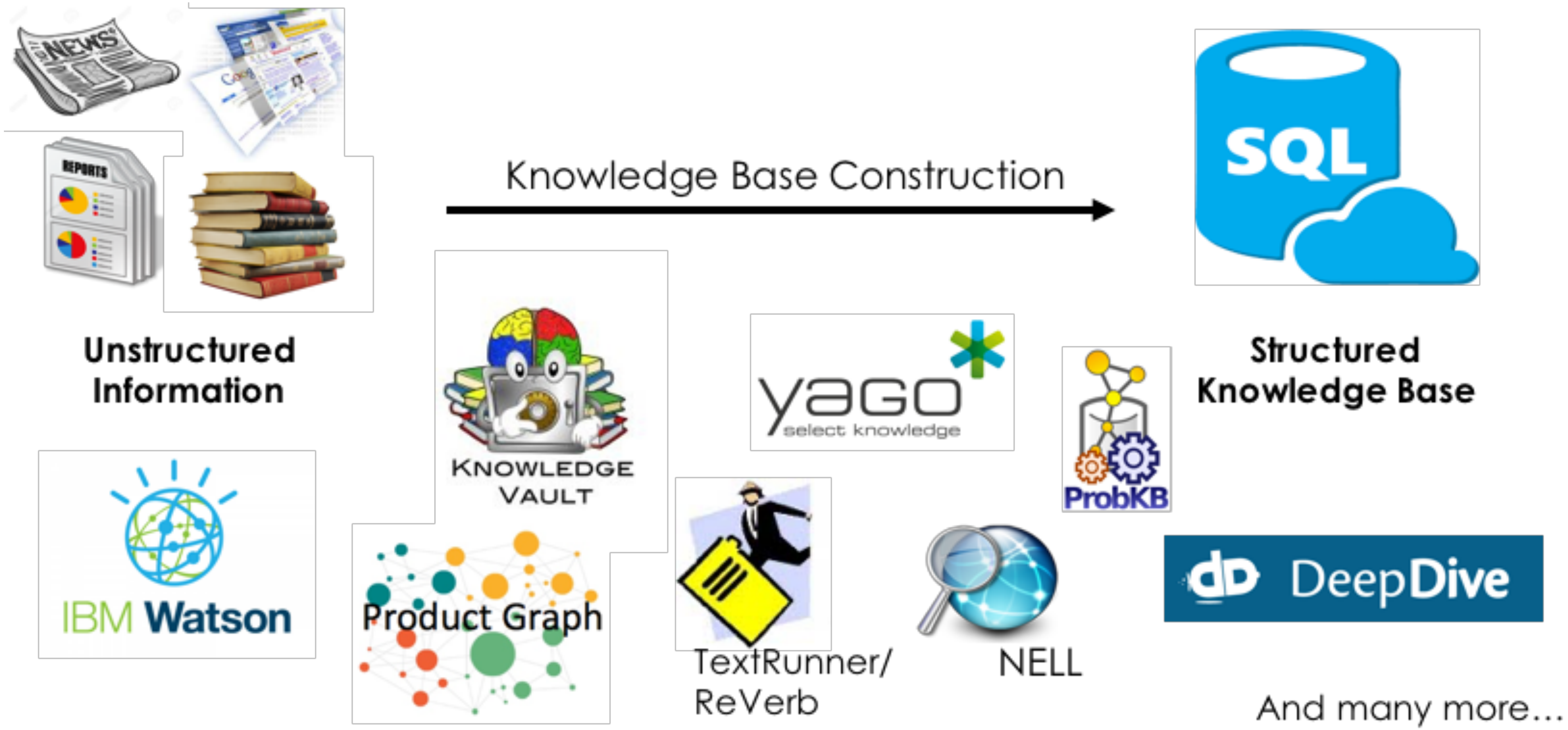

But, troves of "richly formatted" information remains untapped

Fonduer: Information Extraction over Richly Formatted Data

FONDUER

Our collaborators on Fonduer

Sen Wu

Luke Hsiao

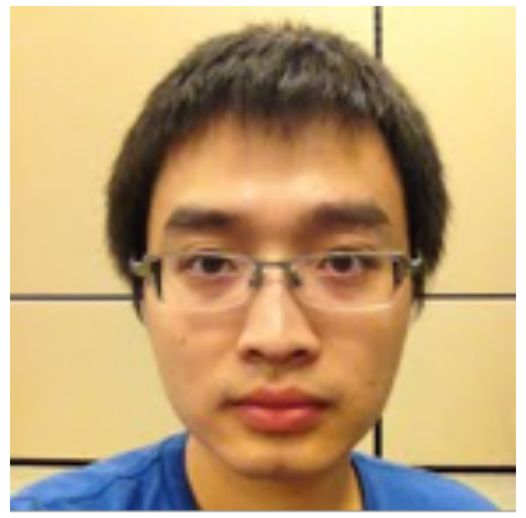

Xiao Cheng

Braden Hancock

Philip Levis

Christopher Ré

Fonduer Users

DARPA MEMEX

accenture

HITACHI Inspire the Next

Stanford MEDICINE

SING

Macrostrat Lab

Alibaba Group

交叉信息研究院 Institute for Interdisciplinary Information Sciences

Richly formatted data

Richly formatted data: information is expressed via textual, structural, tabular, and visual cues.

Transistor Datasheet (PDF)

SMBT3904...MMBT3904

NPN Silicon Switching Transistors

- High DC current gain: 0.1 mA to 100 mA
- Low collector-emitter saturation voltage

Maximum Ratings

Parameter	Symbol	Value	Unit
Collector-emitter voltage	V_{CEO}	40	V
Collector-base voltage	V_{CBO}	60	
Emitter-base voltage	V_{EBO}	6	
Collector current	I_C	200	mA
Total power dissipation	P_{tot}		mV
$T_S \leq 71°C$		330	
$T_S \leq 115°C$		250	
Junction temperature	T_j	150	°C
Storage temperature	T_{stg}	-65 ... 150	

Knowledge base construction from richly formatted data

FONDUER

Goal: extract maximum collector current from transistor datasheets

Transistor Datasheet

SMBT3904...MMBT3904

NPN Silicon Switching Transistors

- High DC current gain: 0.1 mA to 100 mA
- Low collector-emitter saturation voltage

Maximum Ratings

Parameter	Symbol	Value	Unit
Collector-emitter voltage	V_{CEO}	40	V
Collector-base voltage	V_{CBO}	60	
Emitter-base voltage	V_{EBO}	6	
Collector current	I_C	200	mA
Total power dissipation $T_S \leq 71°C$ $T_S \leq 115°C$	P_{tot}	 $_S330_S$ $_S250_S$	mV
Junction temperature	T_j	150	°C
Storage temperature	T_{stg}	-65 ... 150	

HasCollectorCurrent

Transistor Part	Current
SMBT3904	200mA
MMBT3904	200mA

Knowledge Base

Knowledge base construction from richly formatted data

FONDUER

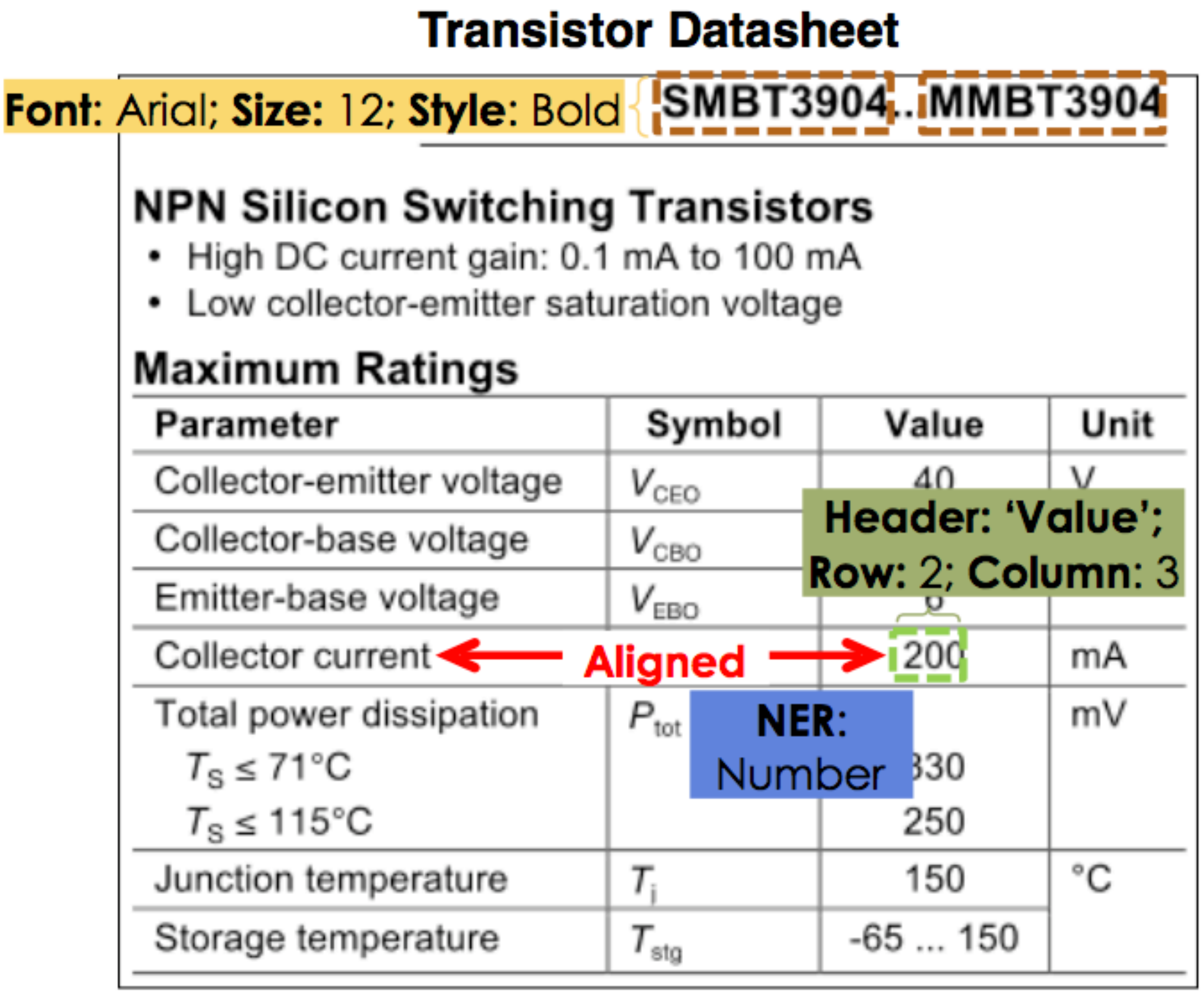

SMBT3904...MMBT3904

NPN Silicon Switching Transistors

- High DC current gain: 0.1 mA to 100 mA
- Low collector-emitter saturation voltage

Maximum Ratings

Parameter	Symbol	Value	Unit
Collector-emitter voltage	V_{CEO}	40	V
Collector-base voltage	V_{CBO}		
Emitter-base voltage	V_{EBO}	6	
Collector current		200	mA
Total power dissipation	P_{tot}		mV
$T_S \leq 71°C$		330	
$T_S \leq 115°C$		250	
Junction temperature	T_j	150	°C
Storage temperature	T_{stg}	-65 ... 150	

In richly formatted data, semantics are expressed in textual, structural, tabular, and visual modalities throughout a document

FONDUER

Knowledge base construction from richly formatted data

Transistor Datasheet

SMBT3904...MMBT3904
NPN Silicon Switching Transistors
High DC current gain: 0.1 mA to 100 mA
Low collector-emitter saturation voltage
Maximum Ratings
Parameter Symbol Value Unit
Collector-emitter voltage VCEO 40 V
Collector-base voltage VCBO 60
Emitter-base voltage VEBO 6
Collector current IC 200 mA
Total power dissipation Ptot mV
TS ≤ 71°C 330
TS ≤ 115°C 250
Junction temperature Tj 150 °C
Storage temperature Tstg -65 ... 150

In richly formatted data, semantics are expressed in textual, structural, tabular, and visual modalities throughout a document

Conventional approach 1: Filter out other modalities besides unstructured text

FONDUER

Knowledge base construction from richly formatted data

Transistor Datasheet

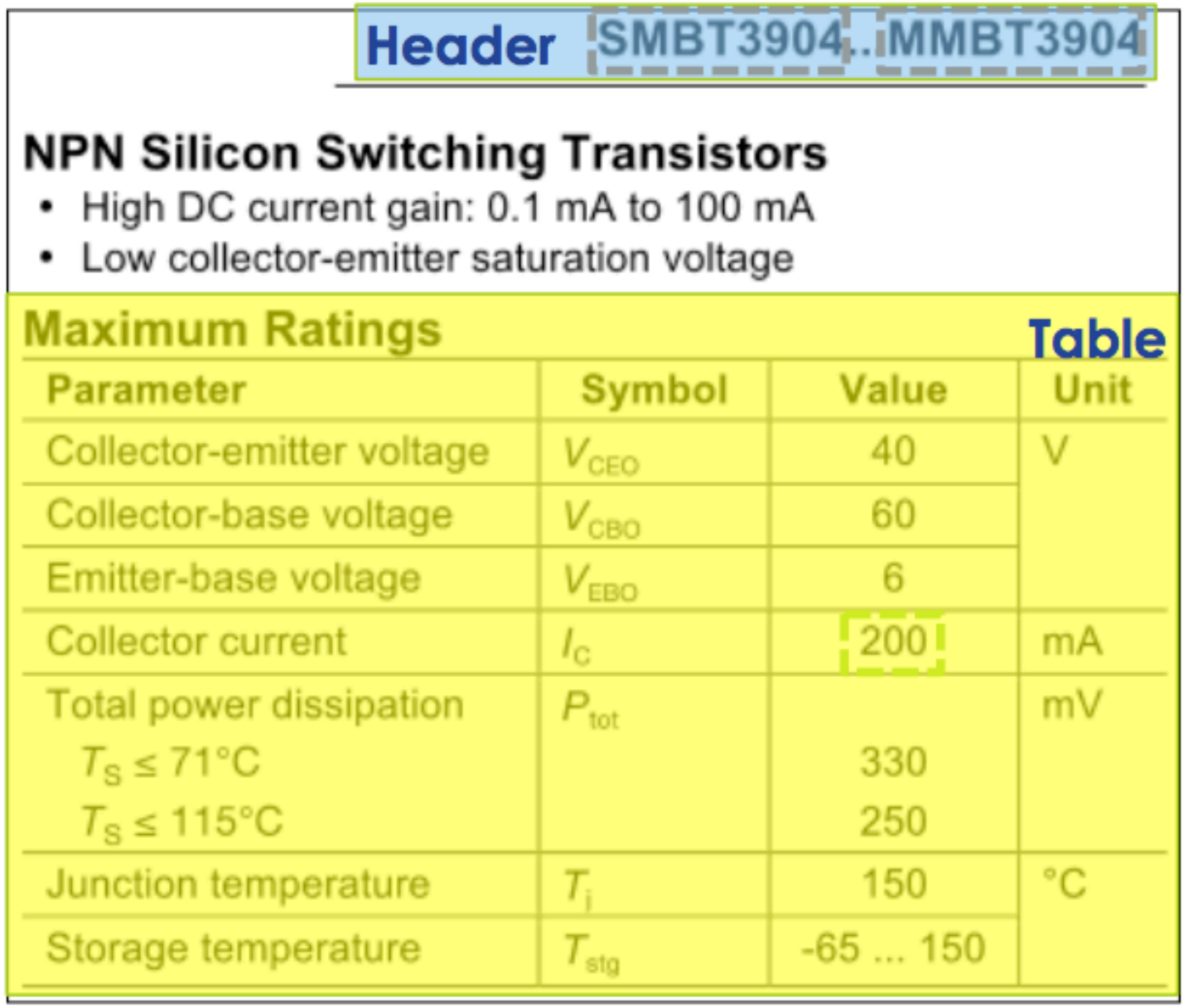
Header SMBT3904...MMBT3904

NPN Silicon Switching Transistors

- High DC current gain: 0.1 mA to 100 mA
- Low collector-emitter saturation voltage

Maximum Ratings Table

Parameter	Symbol	Value	Unit
Collector-emitter voltage	V_{CEO}	40	V
Collector-base voltage	V_{CBO}	60	
Emitter-base voltage	V_{EBO}	6	
Collector current	I_C	200	mA
Total power dissipation	P_{tot}		mV
$T_S \leq 71°C$		330	
$T_S \leq 115°C$		250	
Junction temperature	T_j	150	°C
Storage temperature	T_{stg}	-65 ... 150	

In richly formatted data, semantics are expressed in textual, structural, tabular, and visual modalities throughout a document

Conventional approach 1: Filter out other modalities besides unstructured text

Conventional approach 2: Limit the context scope to sentences or tables.

Problem: Misses important relations if you neglect multimodal information

Fonduer's pipeline

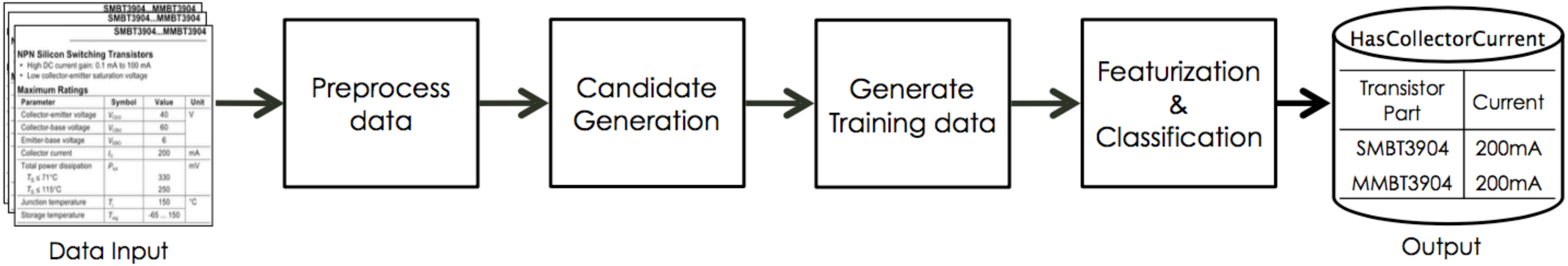

Fonduer is a weakly supervised deep learning framework for knowledge base construction from richly formatted data

FONDUER

Multimodal weak supervision

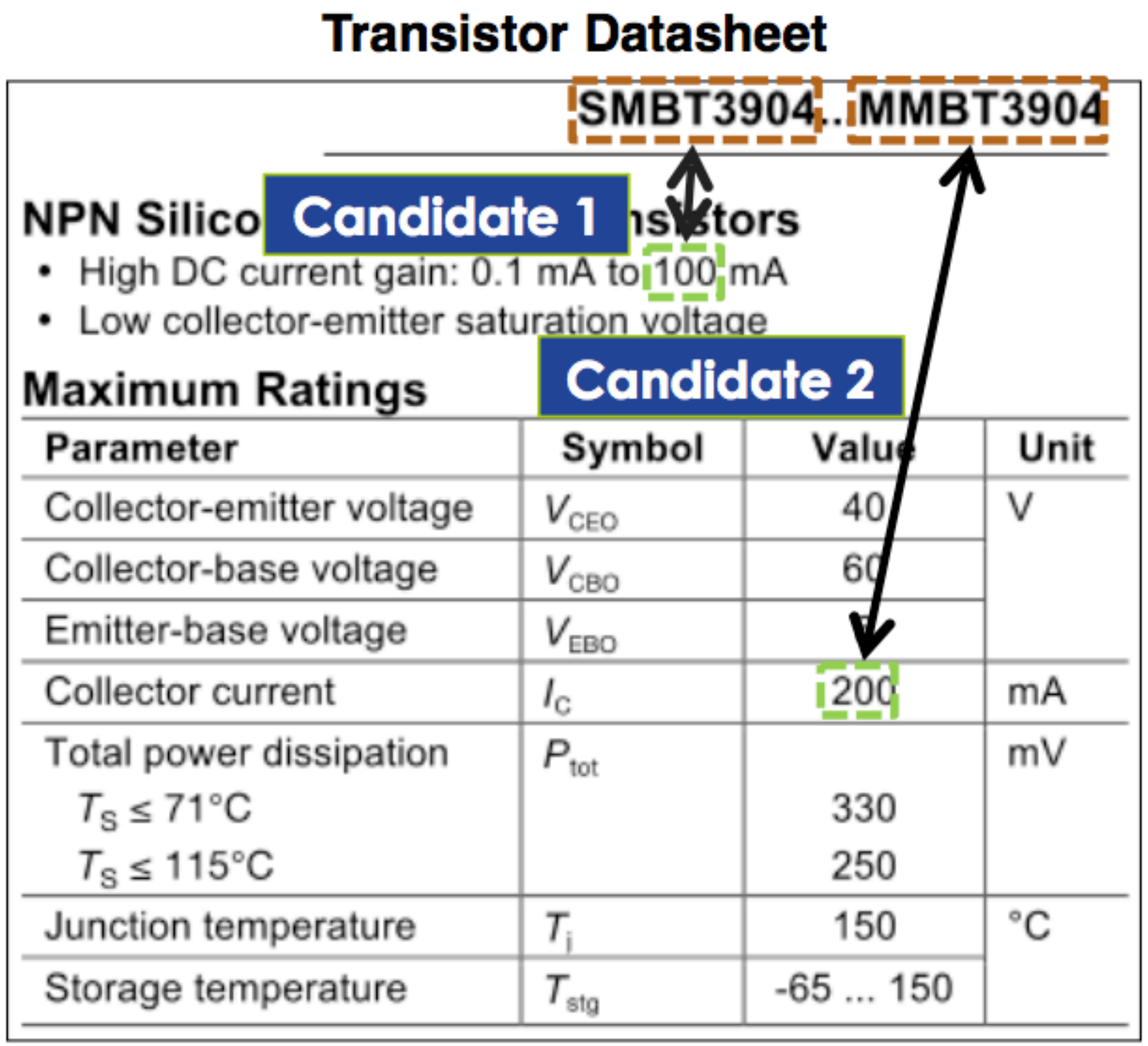

NPN Silicon Switching Transistors

- High DC current gain: 0.1 mA to 100 mA
- Low collector-emitter saturation voltage

Maximum Ratings

Parameter	Symbol	Value	Unit
Collector-emitter voltage	V_{CEO}	40	V
Collector-base voltage	V_{CBO}	60	
Emitter-base voltage	V_{EBO}		
Collector current	I_C	200	mA
Total power dissipation	P_{tot}		mV
$T_S \leq 71°C$		330	
$T_S \leq 115°C$		250	
Junction temperature	T_j	150	°C
Storage temperature	T_{stg}	-65 ... 150	

Doc. level Candidates		Supervision: Manual	Supervision: Labeling function
SMBT3904	100	✗	✗
MMBT3904	200	✓	✓

Weak supervision: express any supervision signal via labeling functions to generate training data

```
# Check if current is in the same row with keyword `collector`
def in_the_same_row_with(candidate):
  if 'collector' in
row_ngrams(candidate.current):
    return 1
  else: return -1
```

Multimodal weak supervision

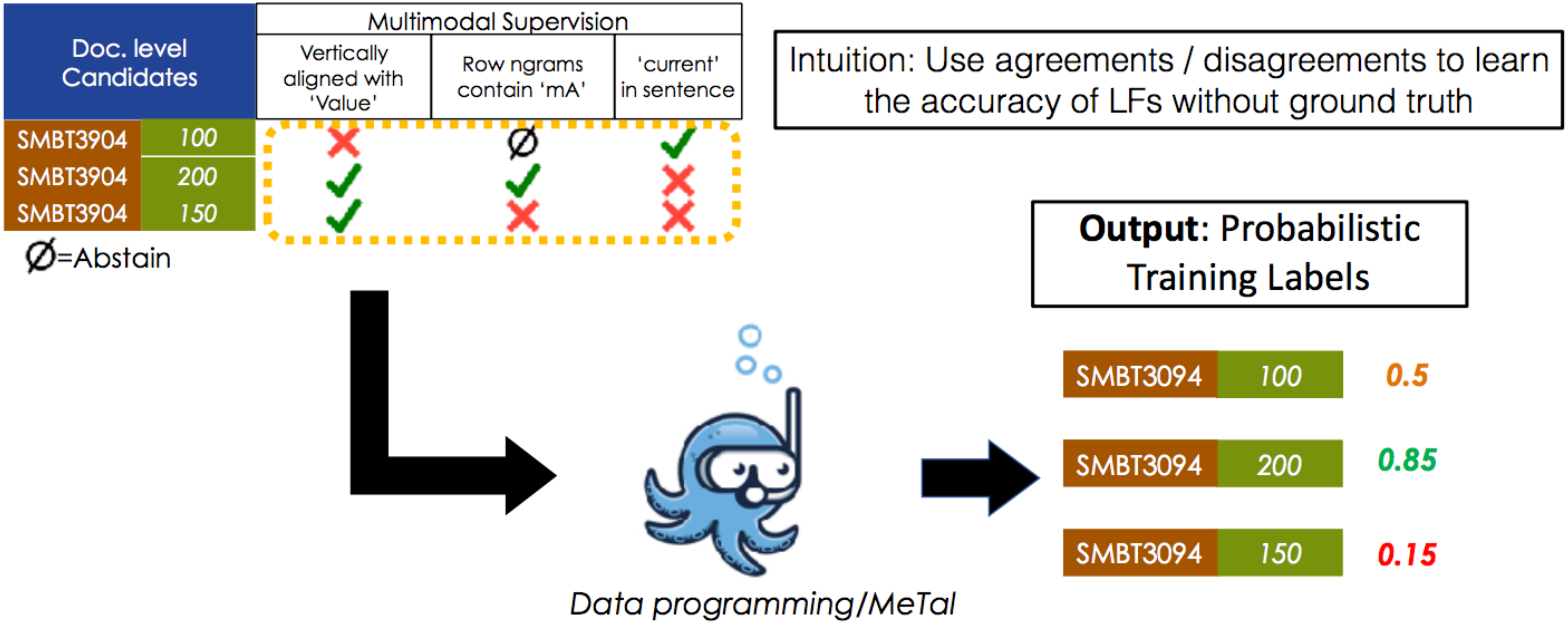

Multimodal supervision is key to quality

For transistor datasheets…

Different supervision resources' effect

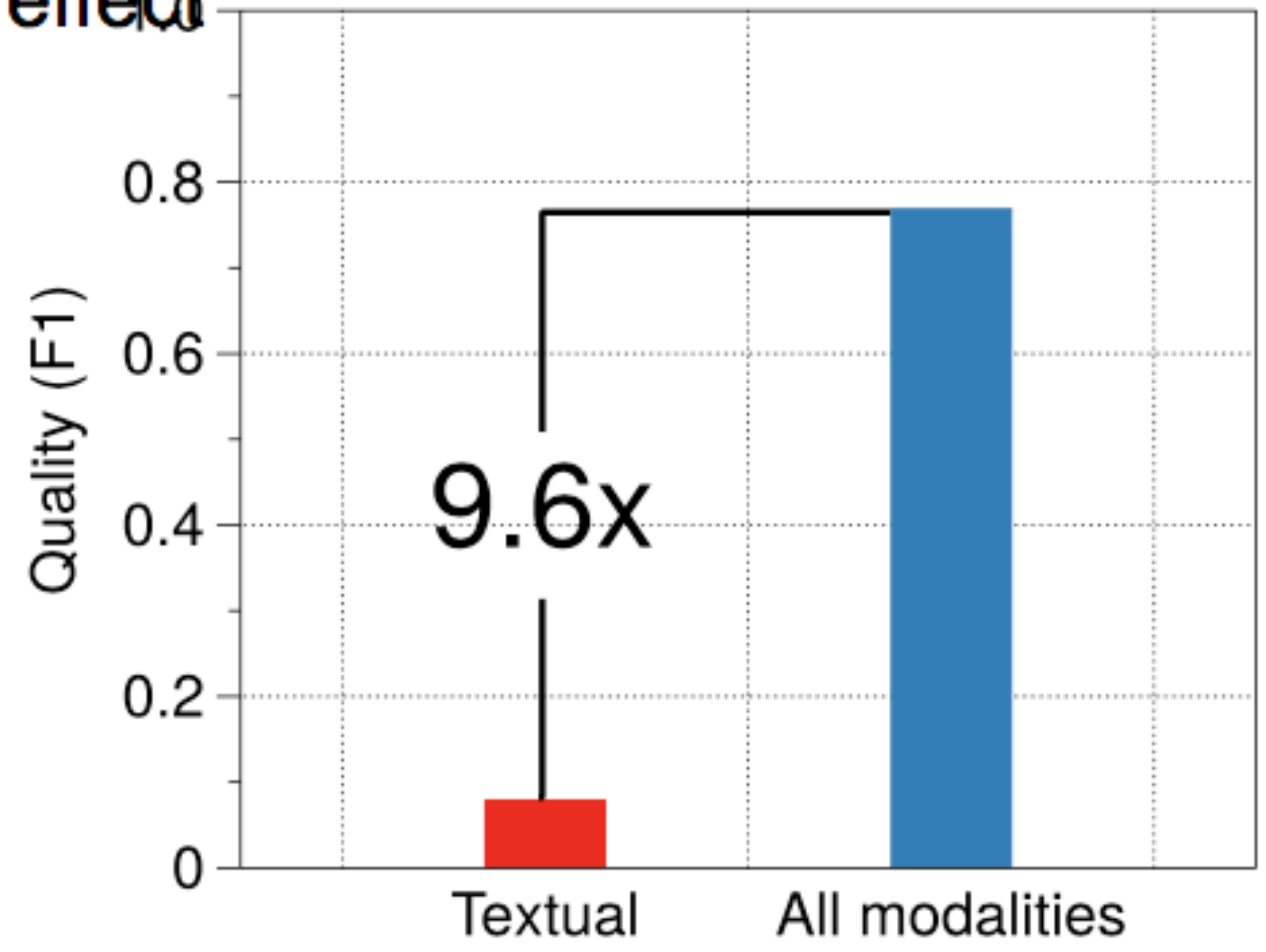

Modality distribution of supervision

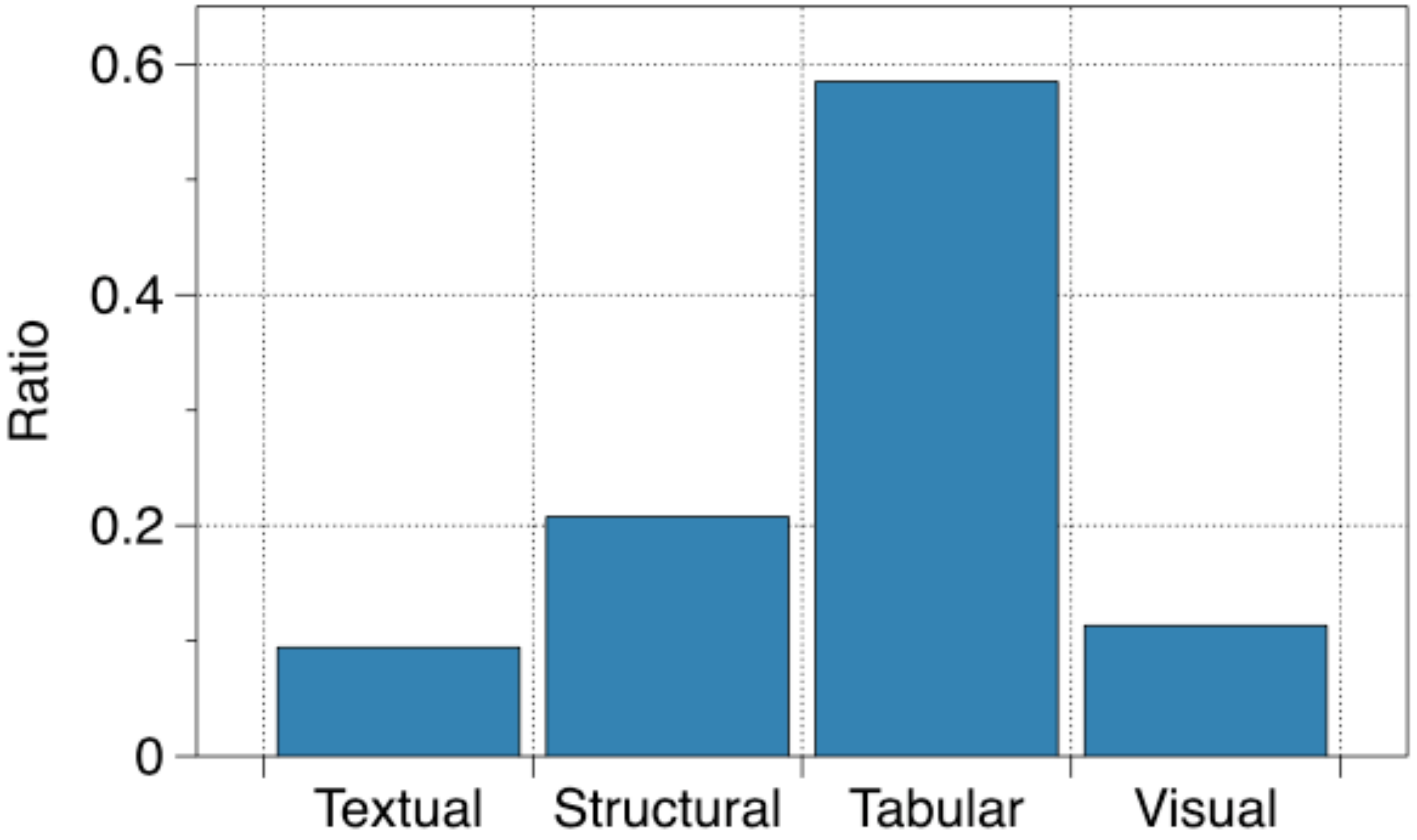

Users intuitively rely on multimodal information for supervision

Fonduer's data model

Richly formatted data

SMBT3904...MMBT3904

NPN Silicon Switching Transistors

- High DC current gain: 0.1 mA to 100 mA
- Low collector-emitter saturation voltage

Maximum Ratings

Parameter	Symbol	Value	Unit
Collector-emitter voltage	V_{CEO}	40	V
Collector-base voltage	V_{CBO}	60	
Emitter-base voltage	V_{EBO}	6	
Collector current	I_C	200	mA
Total power dissipation $T_S \leq 71°C$ $T_S \leq 115°C$	P_{tot}	 330 250	mV
Junction temperature	T_j	150	°C
Storage temperature	T_{stg}	-65 ... 150	

Data model

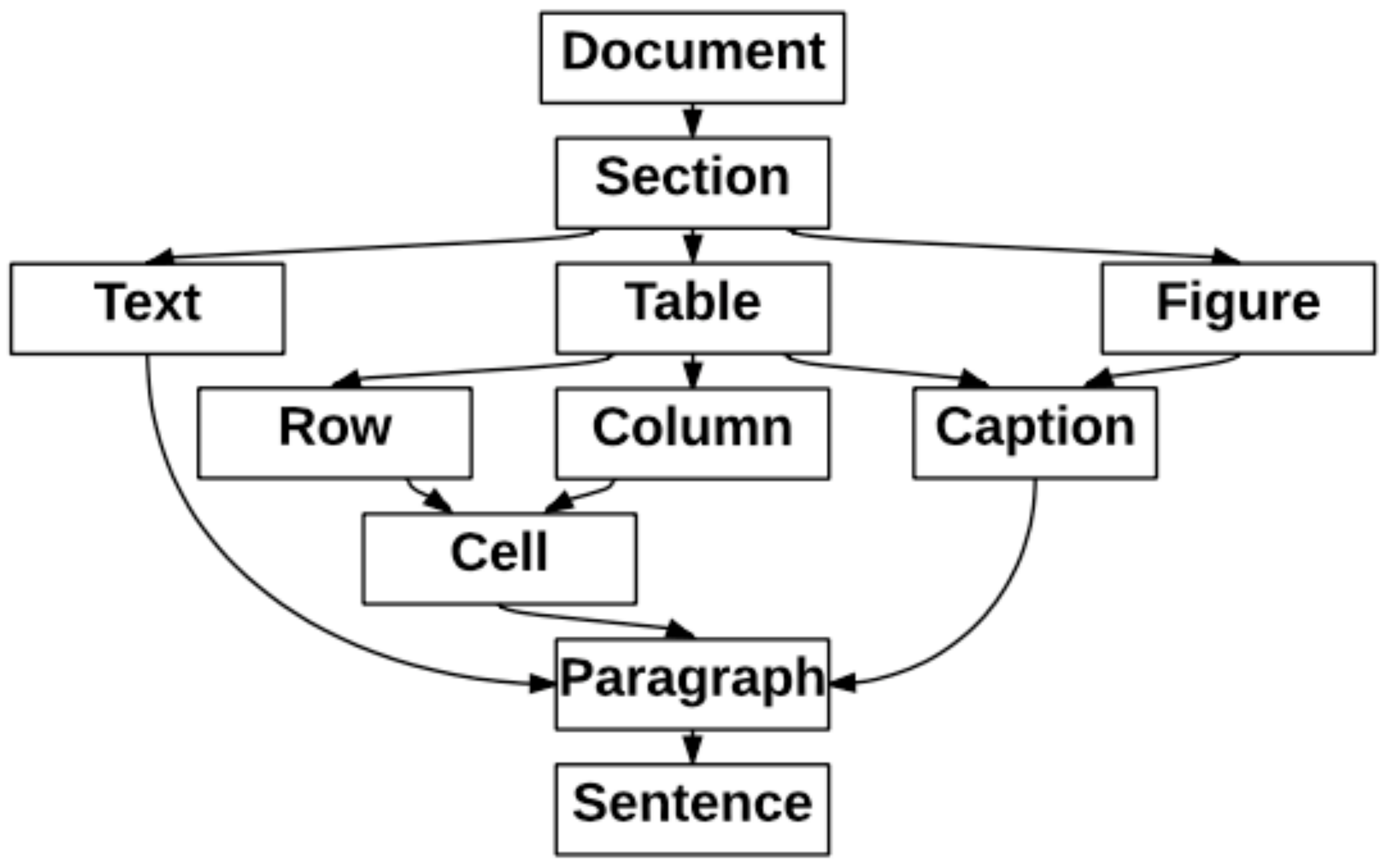

Fonduer automatically parses the richly formatted data into the data model that:

- ❑ Preserves structure/semantics across modalities
- ❑ Unifies a diverse variety of formats and styles
- ❑ Serves as the formal representation in KBC

Weakly Supervised KBC

- Fonduer helps build high-quality KBs from richly formatted data
- Allows users to leverage multimodal signals
- Augments LSTMs with features from each data modality to achieve high quality
- Fonduer is supporting real world applications

From Raw Documents to Fonduer's data model

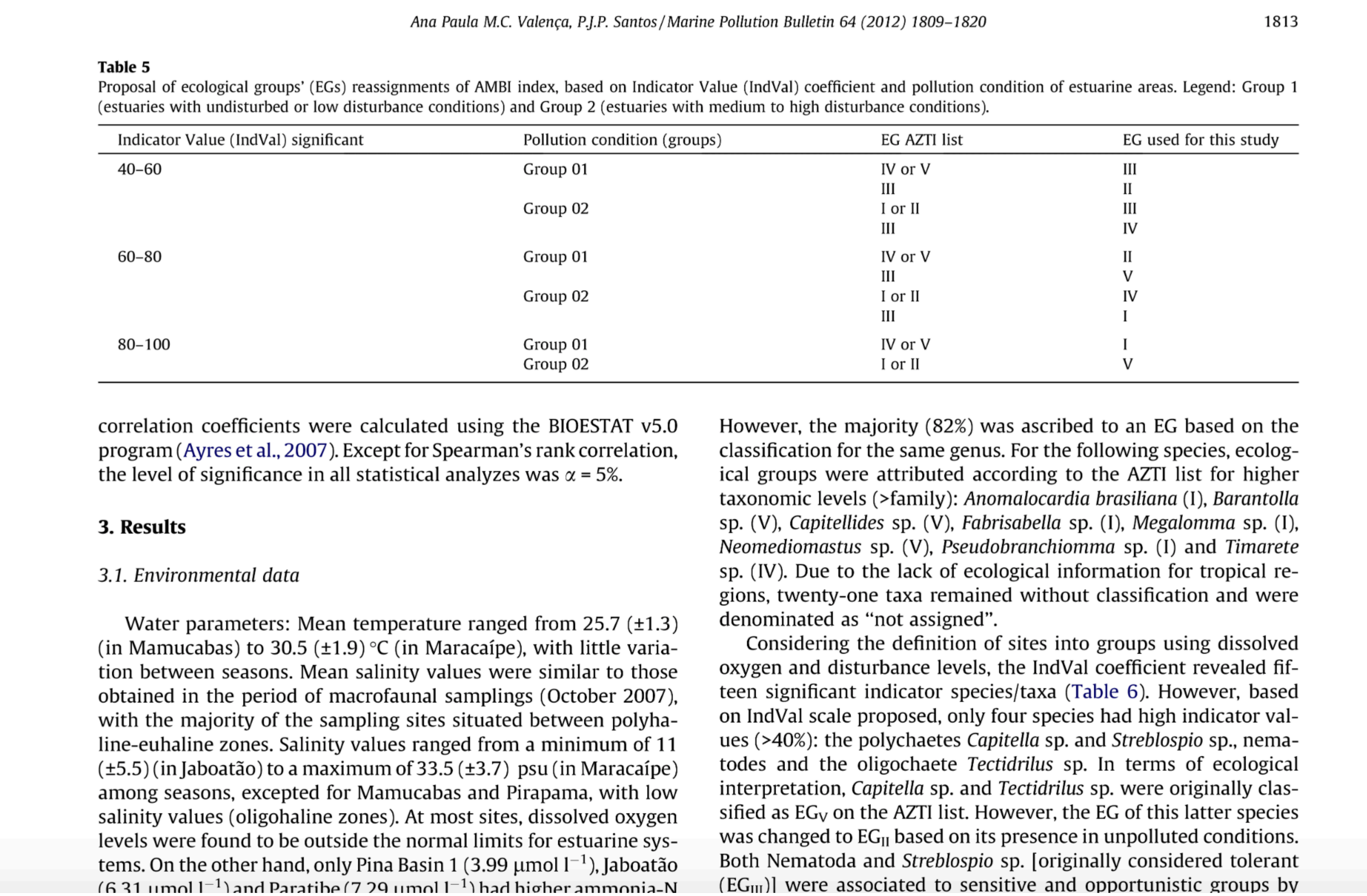

Table 5
Proposal of ecological groups' (EGs) reassignments of AMBI index, based on Indicator Value (IndVal) coefficient and pollution condition of estuarine areas. Legend: Group 1 (estuaries with undisturbed or low disturbance conditions) and Group 2 (estuaries with medium to high disturbance conditions).

Indicator Value (IndVal) significant	Pollution condition (groups)	EG AZTI list	EG used for this study
40–60	Group 01	IV or V	III
		III	II
	Group 02	I or II	III
		III	IV
60–80	Group 01	IV or V	II
		III	V
	Group 02	I or II	IV
		III	I
80–100	Group 01	IV or V	I
	Group 02	I or II	V

correlation coefficients were calculated using the BIOESTAT v5.0 program (Ayres et al., 2007). Except for Spearman's rank correlation, the level of significance in all statistical analyzes was α = 5%.

3. Results

3.1. Environmental data

Water parameters: Mean temperature ranged from 25.7 (±1.3) (in Mamucabas) to 30.5 (±1.9) °C (in Maracaípe), with little variation between seasons. Mean salinity values were similar to those obtained in the period of macrofaunal samplings (October 2007), with the majority of the sampling sites situated between polyhaline-euhaline zones. Salinity values ranged from a minimum of 11 (±5.5) (in Jaboatão) to a maximum of 33.5 (±3.7) psu (in Maracaípe) among seasons, excepted for Mamucabas and Pirapama, with low salinity values (oligohaline zones). At most sites, dissolved oxygen levels were found to be outside the normal limits for estuarine systems. On the other hand, only Pina Basin 1 (3.99 µmol l^{-1}), Jaboatão (6.31 µmol l^{-1}) and Paratibe (7.29 µmol l^{-1}) had higher ammonia-N

However, the majority (82%) was ascribed to an EG based on the classification for the same genus. For the following species, ecological groups were attributed according to the AZTI list for higher taxonomic levels (>family): *Anomalocardia brasiliana* (I), *Barantolla* sp. (V), *Capitellides* sp. (V), *Fabrisabella* sp. (I), *Megalomma* sp. (I), *Neomediomastus* sp. (V), *Pseudobranchiomma* sp. (I) and *Timarete* sp. (IV). Due to the lack of ecological information for tropical regions, twenty-one taxa remained without classification and were denominated as "not assigned".

Considering the definition of sites into groups using dissolved oxygen and disturbance levels, the IndVal coefficient revealed fifteen significant indicator species/taxa (Table 6). However, based on IndVal scale proposed, only four species had high indicator values (>40%): the polychaetes *Capitella* sp. and *Streblospio* sp., nematodes and the oligochaete *Tectidrilus* sp. In terms of ecological interpretation, *Capitella* sp. and *Tectidrilus* sp. were originally classified as EG_V on the AZTI list. However, the EG of this latter species was changed to EG_{II} based on its presence in unpolluted conditions. Both Nematoda and *Streblospio* sp. [originally considered tolerant (EG_{III})] were associated to sensitive and opportunistic groups by

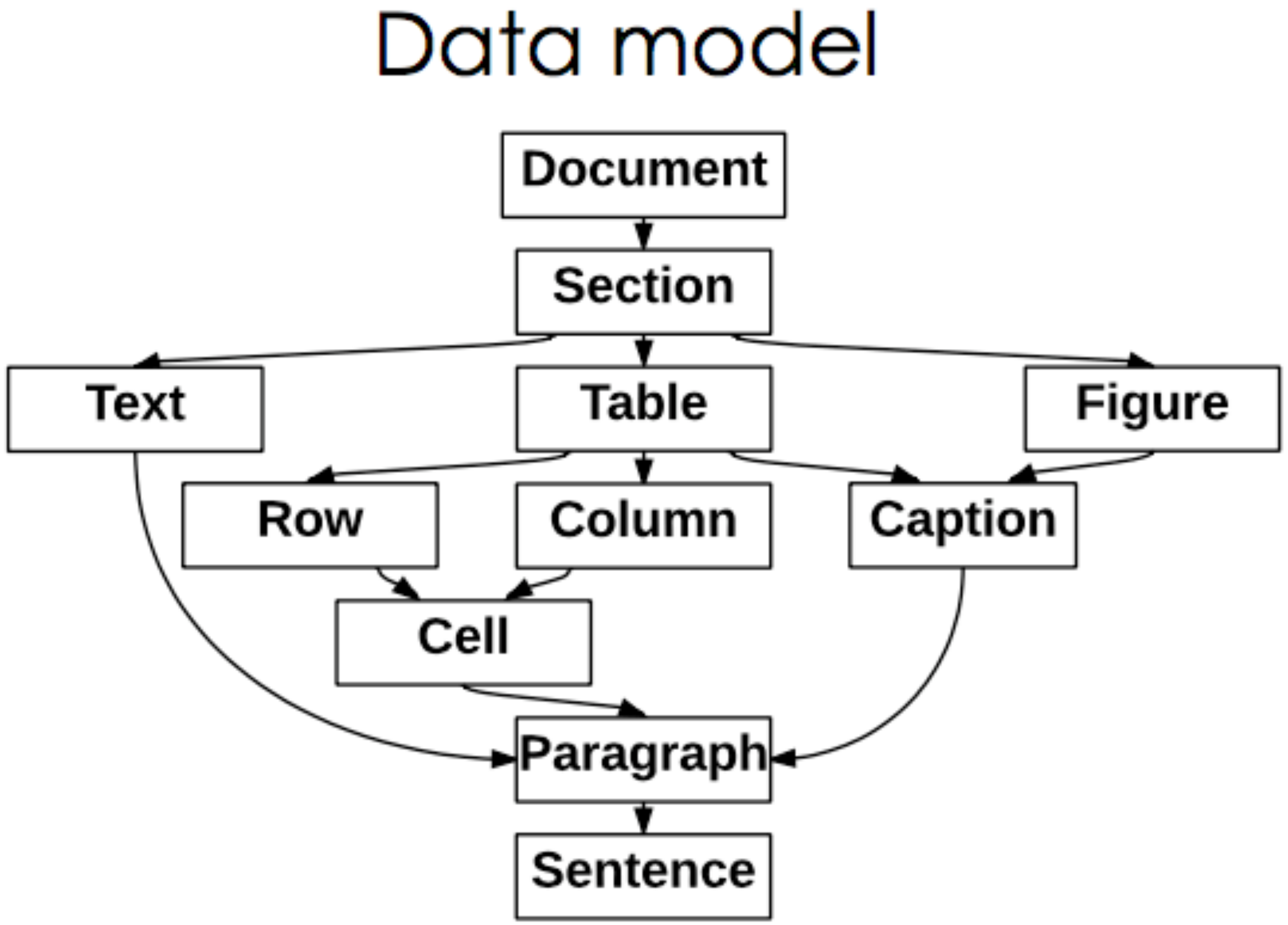

Constructing Fonduer's input requires performing document segmentation.

Typical OCR focuses on text only!

Problem: Text-only segmentation obscures important table structure

Table 1. EnKF calibrated biogeochemical parameters in the GENIE-1 model.

Name	Prior assumptions (mean and range[a])	Posterior mean[b]	Description
$u_0^{PO_4}$	1.65 μmol kg^{-1} yr^{-1} (0.3–3.0)	1.91 μmol kg^{-1} yr^{-1}	maximum PO_4 uptake (removal) rate (Eq. 3)
K^{PO_4}	0.2 μmol kg^{-1} (0.1–0.3)	0.21 μmol kg^{-1}	PO_4 Michaelis-Menton half-saturation concentration (Eq. 3)
r^{POC}	0.05 (0.02–0.08)	0.055	initial proportion of POC export as fraction #2 (Eq. 6)
l^{POC}	600 m (200–1000)	556 m	*e*-folding remineralization depth of POC fraction #1 (Eq. 6)
$r_0^{CaCO_3:POC}$	0.036 (0.015–0.088)[c]	0.022[d]	$CaCO_3$:POC: export rain ratio scalar (Eq. 8)
η	1.5 (1.0–2.0)	1.28	thermodynamic calcification rate power (Eq. 9)
r^{CaCO_3}	0.4 (0.2–0.6)	0.489	initial proportion of $CaCO_3$ export as fraction #2 (Eq. 11)
l^{CaCO_3}	600 m (200–1000)	1055	*e*-folding remineralization depth of $CaCO_3$ fraction #1 (Eq. 11)

[a] the range is quoted as 1 standard deviation either side of the mean
[b] quoted as the mean of the entire EnKF ensemble
[c] assimilation was carried out on a $\log_{10}$ scale
[d] Note that the rain ratio scalar parameter is not the same as the $CaCO_3$:POC export rain ratio as measured at the base of the euphotic zone, because $r_0^{CaCO_3:POC}$ is further multiplied by $(\Omega-1)^\eta$ to calculate the rain ratio, where Ω is the surface ocean saturation state with respect to calcite (see Sect. 2.1). Pre-industrial mean ocean surface Ω is ~5.2 in the GENIE-1 model, so that the global $CaCO_3$:POC export rain ratio can be estimated using the 8-parameter assimilation as being equal to $(5.2\text{–}1)^{1.28} \times 0.022 = 0.14$.

(Table 1). Because we explicitly resolve the individual "components" (i.e., C, ^{13}C, P, ...) of organic matter, the GENIE-1 model can be used to quantify the effect of fractionation

(e.g. Zhang et al., 2001, 2003) or by allowing the tracer transport of negative O_2 concentrations (e.g., Hotinski et al., 2001). We treat the remineralization of dissolved organic

Typical OCR focuses on text only!

Problem: Text-only segmentation obscures important table structure

Solution: Cast document segmentation as a vision problem

Table 1. EnKF calibrated biogeochemical parameters in the GENIE-1 model.

Name	Prior assumptions (mean and range[a])	Posterior mean[b]	Description
$u_0^{PO_4}$	1.65 μmol kg^{-1} yr^{-1} (0.3–3.0)	1.91 μmol kg^{-1} yr^{-1}	maximum PO_4 uptake (removal) rate (Eq. 3)
K^{PO_4}	0.2 μmol kg^{-1} (0.1–0.3)	0.21 μmol kg^{-1}	PO_4 Michaelis-Menton half-saturation concentration (Eq. 3)
r^{POC}	0.05 (0.02–0.08)	0.055	initial proportion of POC export as fraction #2 (Eq. 6)
l^{POC}	600 m (200–1000)	556 m	*e*-folding remineralization depth of POC fraction #1 (Eq. 6)
$r_0^{CaCO_3:POC}$	0.036 (0.015–0.088)[c]	0.022[d]	$CaCO_3$:POC: export rain ratio scalar (Eq. 8)
η	1.5 (1.0–2.0)	1.28	thermodynamic calcification rate power (Eq. 9)
r^{CaCO_3}	0.4 (0.2–0.6)	0.489	initial proportion of $CaCO_3$ export as fraction #2 (Eq. 11)
l^{CaCO_3}	600 m (200–1000)	1055	*e*-folding remineralization depth of $CaCO_3$ fraction #1 (Eq. 11)

[a] the range is quoted as 1 standard deviation either side of the mean
[b] quoted as the mean of the entire EnKF ensemble
[c] assimilation was carried out on a $\log_{10}$ scale
[d] Note that the rain ratio scalar parameter is not the same as the $CaCO_3$:POC export rain ratio as measured at the base of the euphotic zone, because $r_0^{CaCO_3:POC}$ is further multiplied by $(\Omega-1)^{\eta}$ to calculate the rain ratio, where Ω is the surface ocean saturation state with respect to calcite (see Sect. 2.1). Pre-industrial mean ocean surface Ω is ~5.2 in the GENIE-1 model, so that the global $CaCO_3$:POC export rain ratio can be estimated using the 8-parameter assimilation as being equal to $(5.2-1)^{1.28} \times 0.022 = 0.14$.

(Table 1). Because we explicitly resolve the individual "components" (i.e., C, ^{13}C, P, …) of organic matter, the GENIE-1 model can be used to quantify the effect of fractionation between the components of organic matter during remineral-

(e.g. Zhang et al., 2001, 2003) or by allowing the tracer transport of negative O_2 concentrations (e.g., Hotinski et al., 2001). We treat the remineralization of dissolved organic matter in an analogous manner if O_2 availability is insuffi-

Mask-RCNN (He et al. 2018)

- State of the art image segmentation model
- Performs instance segmentation
- Identifies regions of interest (ROI) followed by object detection, classification, and mask detection in parallel
- We set mask to the bounding box with intention to refine bounding box

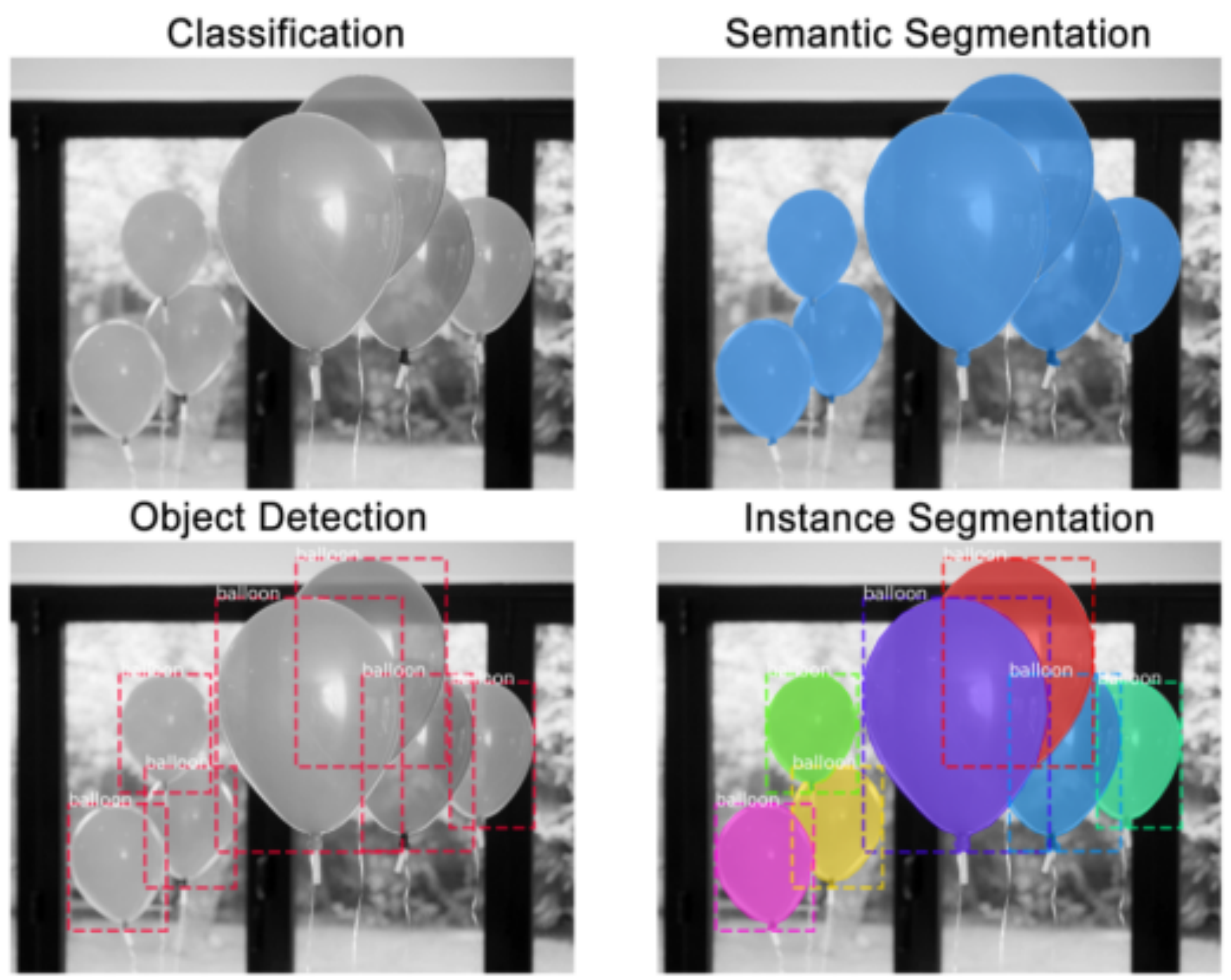

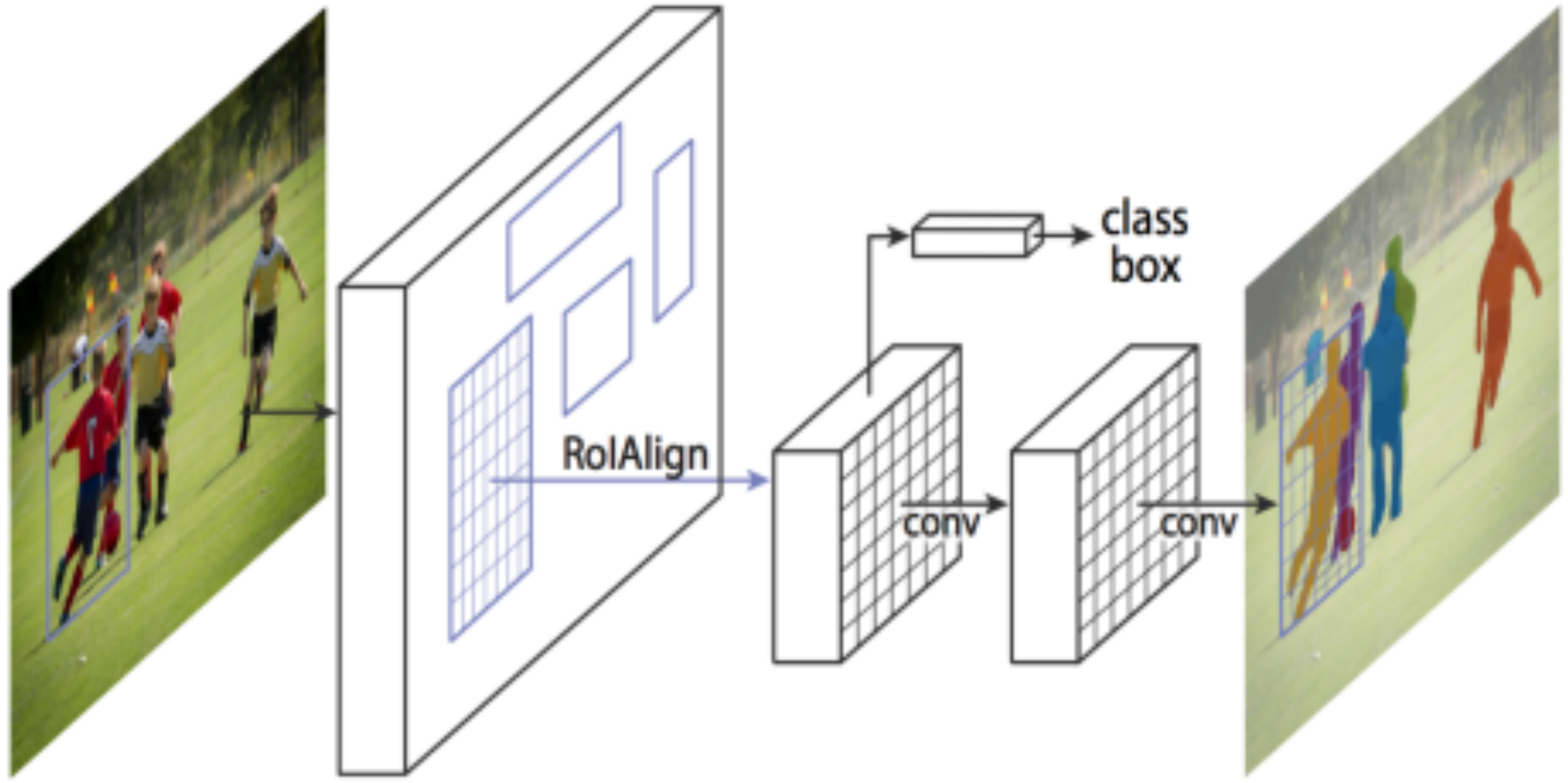

Mask R-CNN framework. Source: https://arxiv.org/abs/1703.06870

Data annotation: In-house labeler

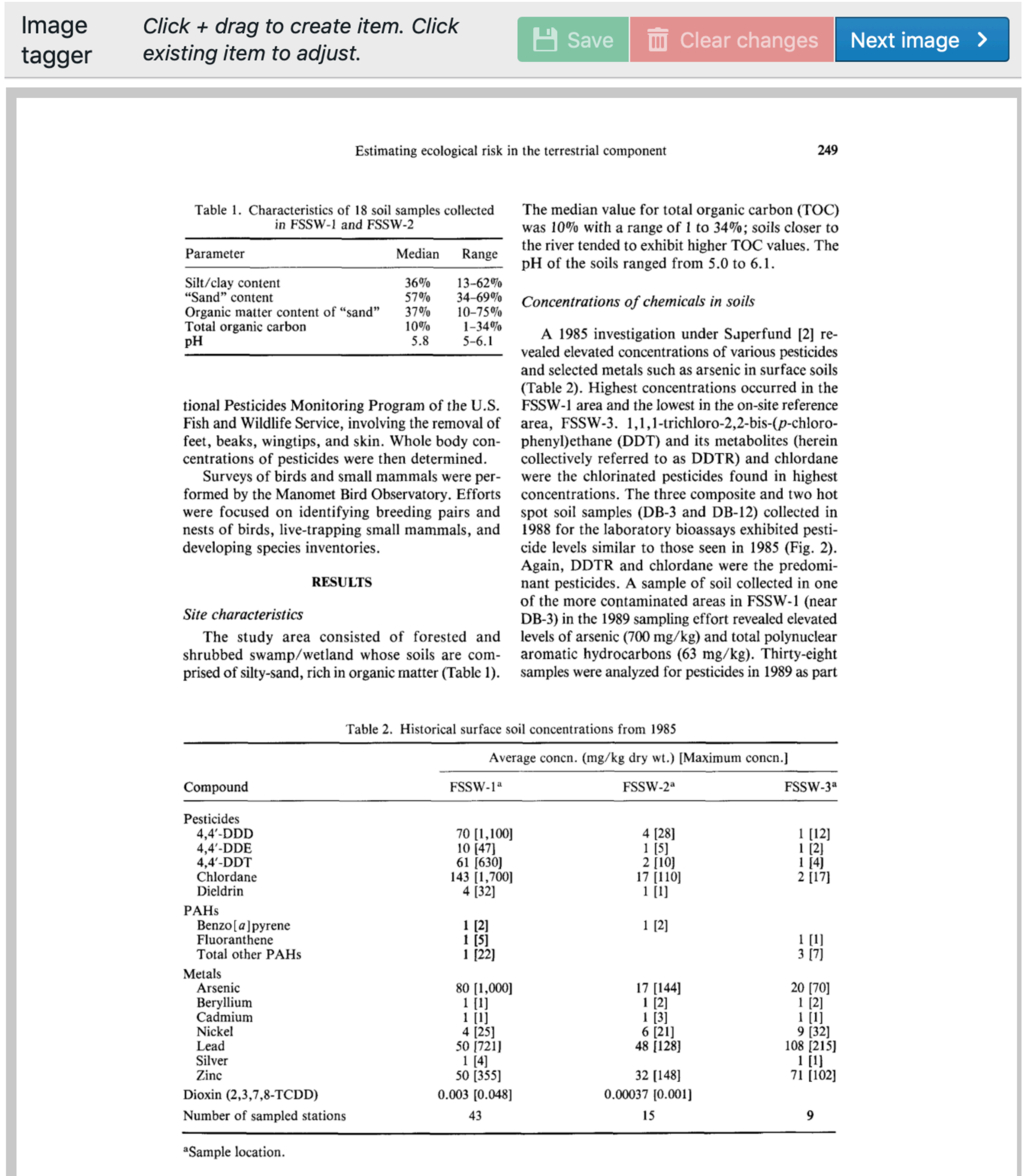

Estimating ecological risk in the terrestrial component 249

Table 1. Characteristics of 18 soil samples collected in FSSW-1 and FSSW-2

Parameter	Median	Range
Silt/clay content	36%	13–62%
"Sand" content	57%	34–69%
Organic matter content of "sand"	37%	10–75%
Total organic carbon	10%	1–34%
pH	5.8	5–6.1

tional Pesticides Monitoring Program of the U.S. Fish and Wildlife Service, involving the removal of feet, beaks, wingtips, and skin. Whole body concentrations of pesticides were then determined.

Surveys of birds and small mammals were performed by the Manomet Bird Observatory. Efforts were focused on identifying breeding pairs and nests of birds, live-trapping small mammals, and developing species inventories.

RESULTS

Site characteristics

The study area consisted of forested and shrubbed swamp/wetland whose soils are comprised of silty-sand, rich in organic matter (Table 1). The median value for total organic carbon (TOC) was 10% with a range of 1 to 34%; soils closer to the river tended to exhibit higher TOC values. The pH of the soils ranged from 5.0 to 6.1.

Concentrations of chemicals in soils

A 1985 investigation under Superfund [2] revealed elevated concentrations of various pesticides and selected metals such as arsenic in surface soils (Table 2). Highest concentrations occurred in the FSSW-1 area and the lowest in the on-site reference area, FSSW-3. 1,1,1-trichloro-2,2-bis-(*p*-chlorophenyl)ethane (DDT) and its metabolites (herein collectively referred to as DDTR) and chlordane were the chlorinated pesticides found in highest concentrations. The three composite and two hot spot soil samples (DB-3 and DB-12) collected in 1988 for the laboratory bioassays exhibited pesticide levels similar to those seen in 1985 (Fig. 2). Again, DDTR and chlordane were the predominant pesticides. A sample of soil collected in one of the more contaminated areas in FSSW-1 (near DB-3) in the 1989 sampling effort revealed elevated levels of arsenic (700 mg/kg) and total polynuclear aromatic hydrocarbons (63 mg/kg). Thirty-eight samples were analyzed for pesticides in 1989 as part

Table 2. Historical surface soil concentrations from 1985

	Average concn. (mg/kg dry wt.) [Maximum concn.]		
Compound	FSSW-1[a]	FSSW-2[a]	FSSW-3[a]
Pesticides			
4,4′-DDD	70 [1,100]	4 [28]	1 [12]
4,4′-DDE	10 [47]	1 [5]	1 [2]
4,4′-DDT	61 [630]	2 [10]	1 [4]
Chlordane	143 [1,700]	17 [110]	2 [17]
Dieldrin	4 [32]	1 [1]	
PAHs			
Benzo[*a*]pyrene	1 [2]	1 [2]	
Fluoranthene	1 [5]		1 [1]
Total other PAHs	1 [22]		3 [7]
Metals			
Arsenic	80 [1,000]	17 [144]	20 [70]
Beryllium	1 [1]	1 [2]	1 [2]
Cadmium	1 [1]	1 [3]	1 [1]
Nickel	4 [25]	6 [21]	9 [32]
Lead	50 [721]	48 [128]	108 [215]
Silver	1 [4]		1 [1]
Zinc	50 [355]	32 [148]	71 [102]
Dioxin (2,3,7,8-TCDD)	0.003 [0.048]	0.00037 [0.001]	
Number of sampled stations	43	15	9

[a]Sample location.

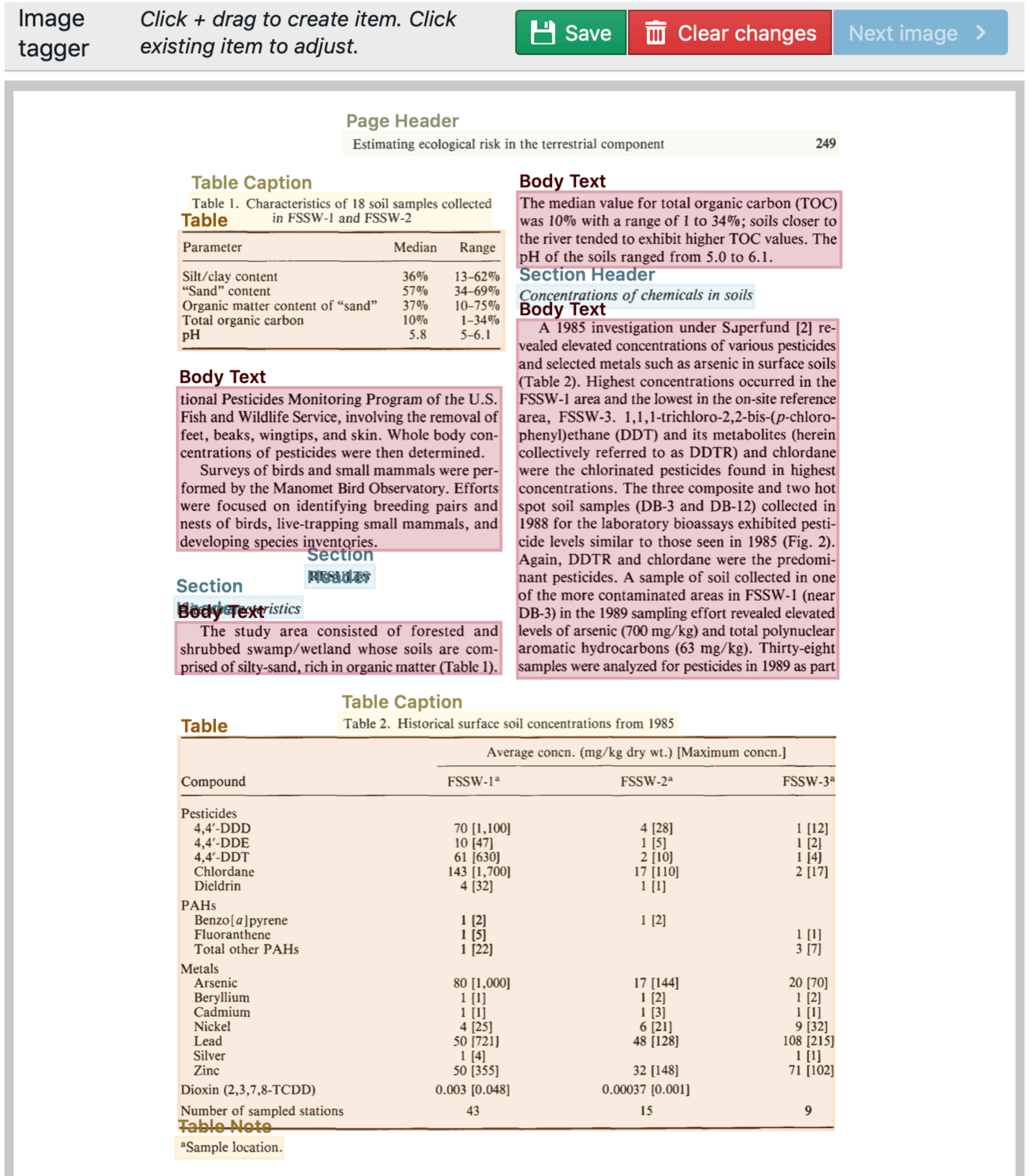

Qualitative Results

Prediction
Ground Truth

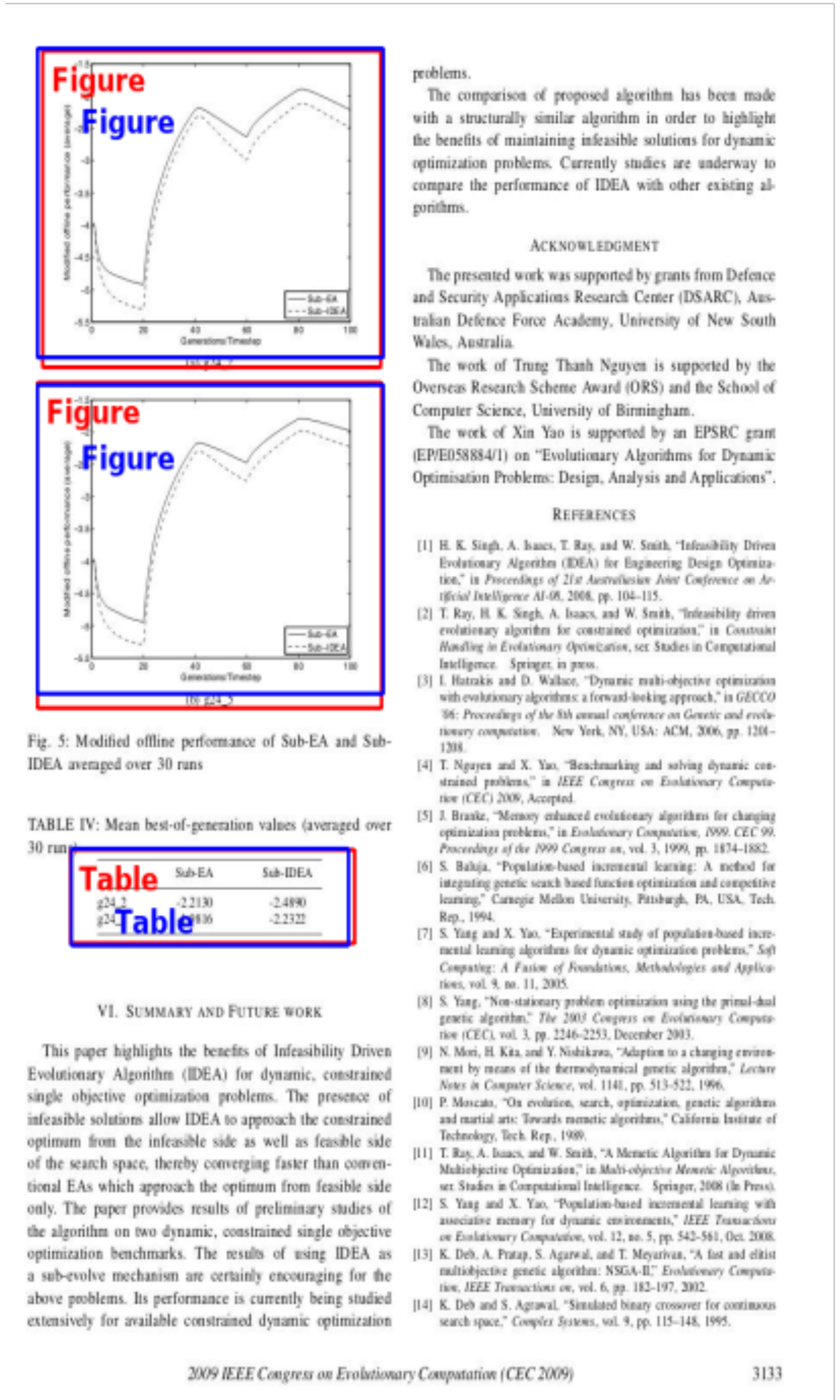

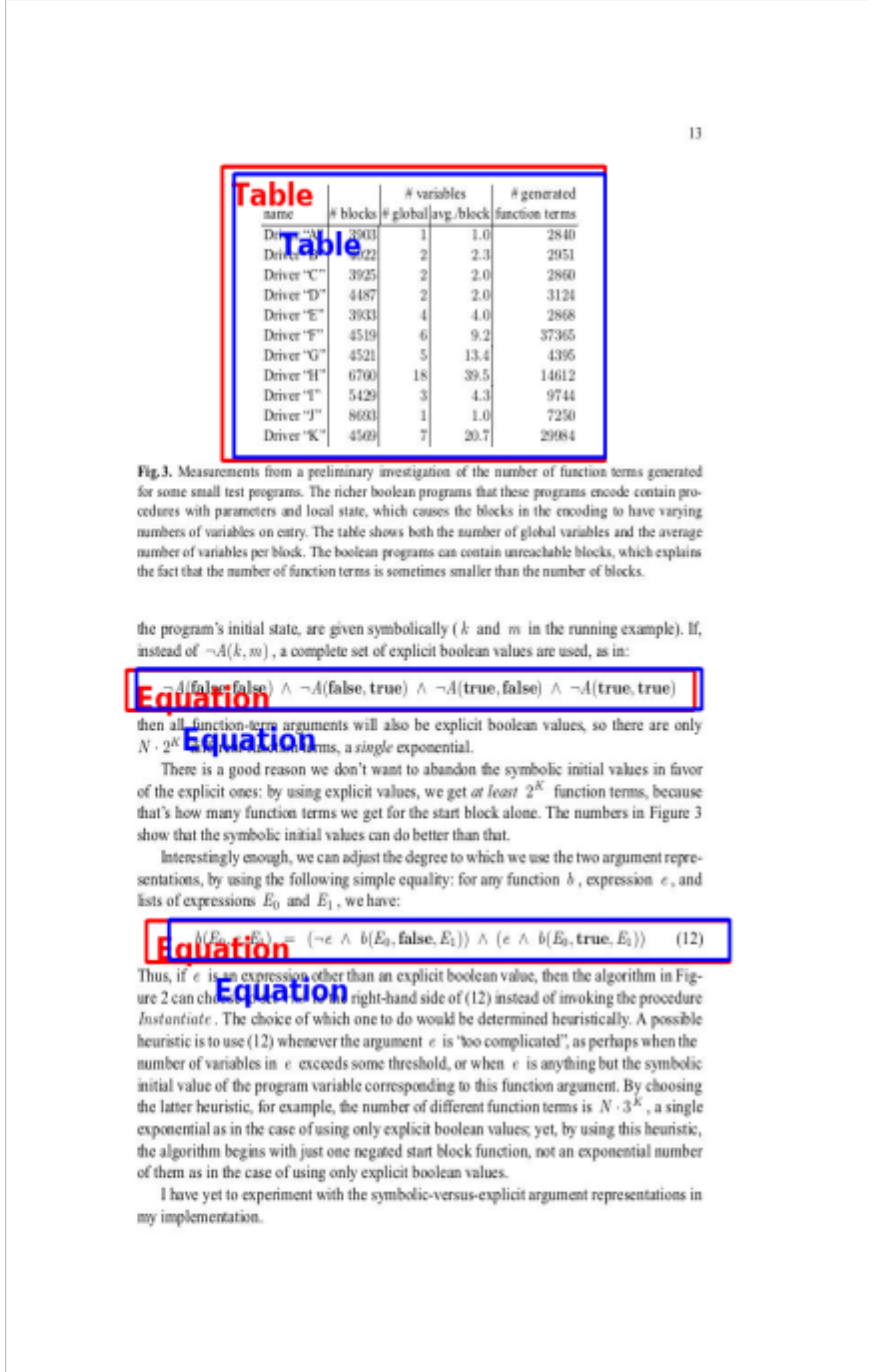

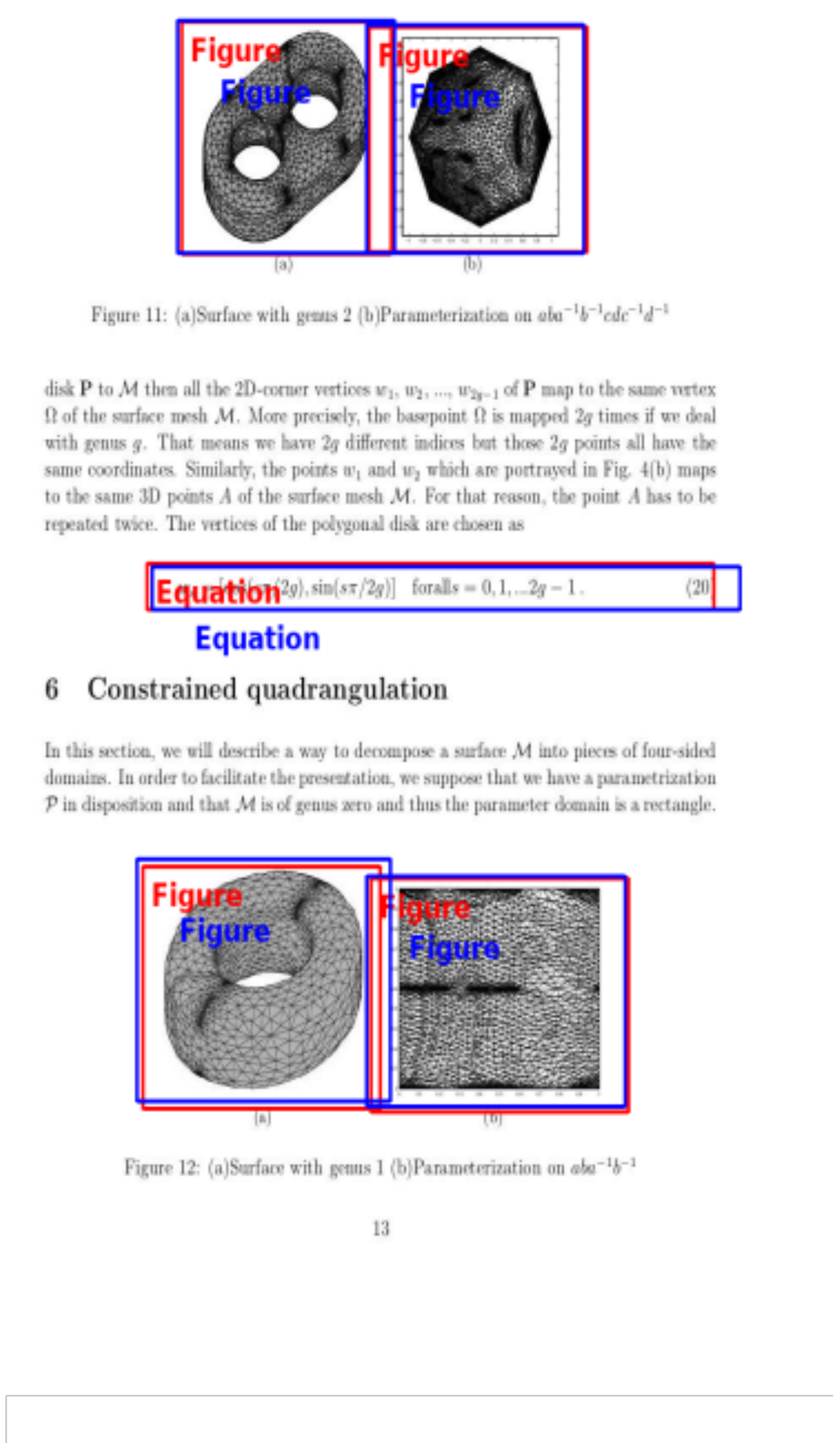

Qualitative Results

Prediction

Ground Truth

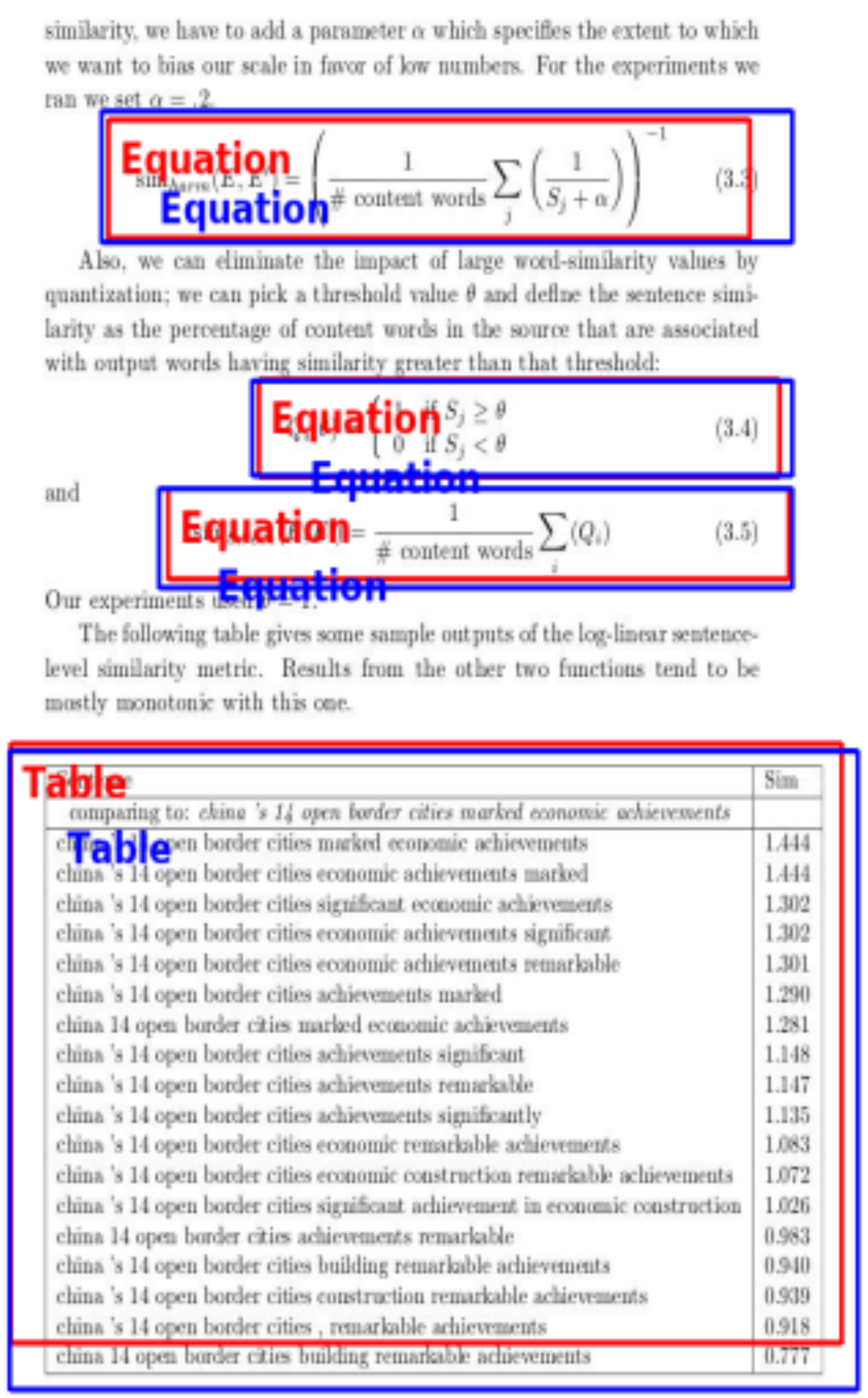

Truncation

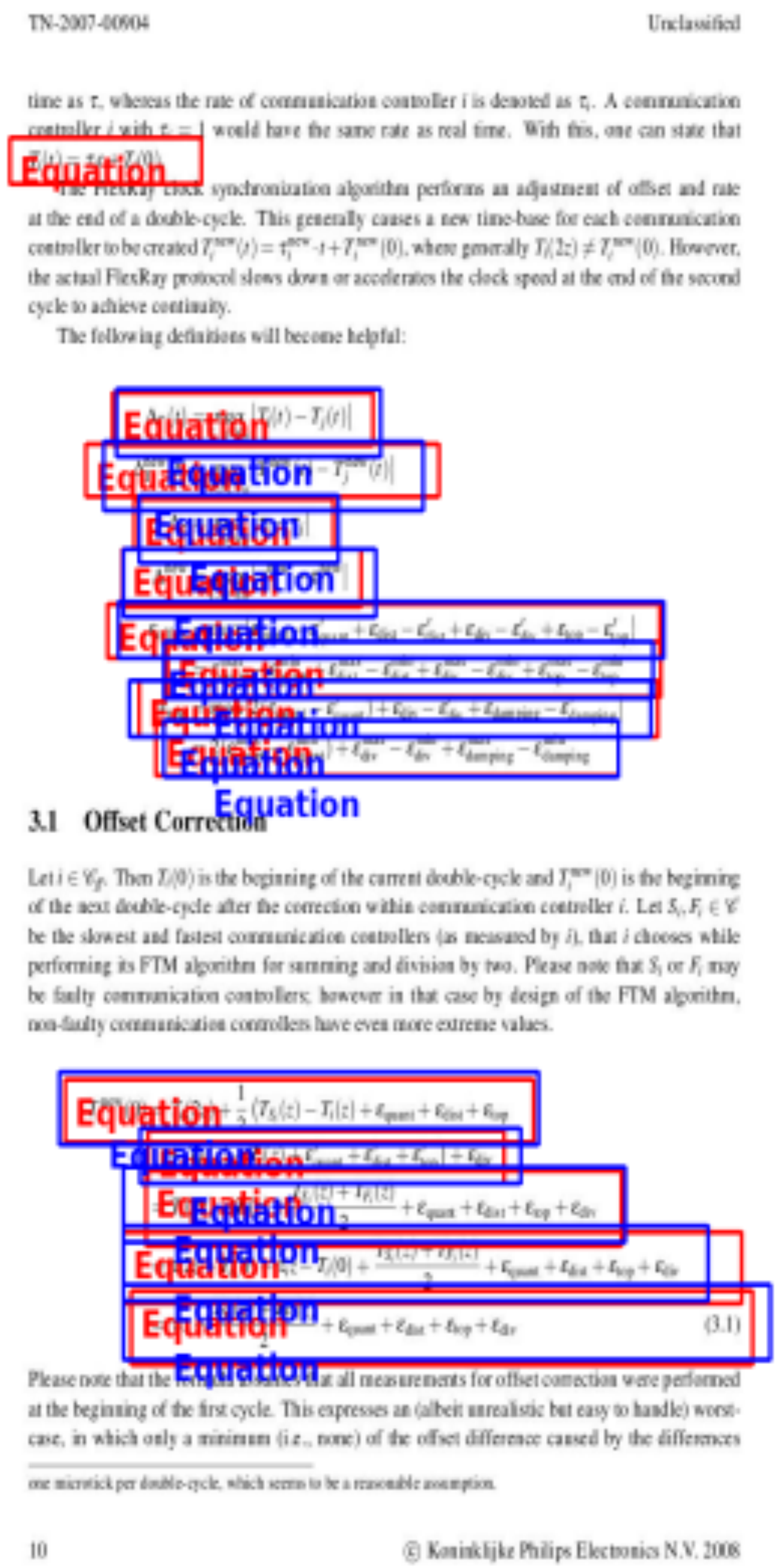

In-line equations

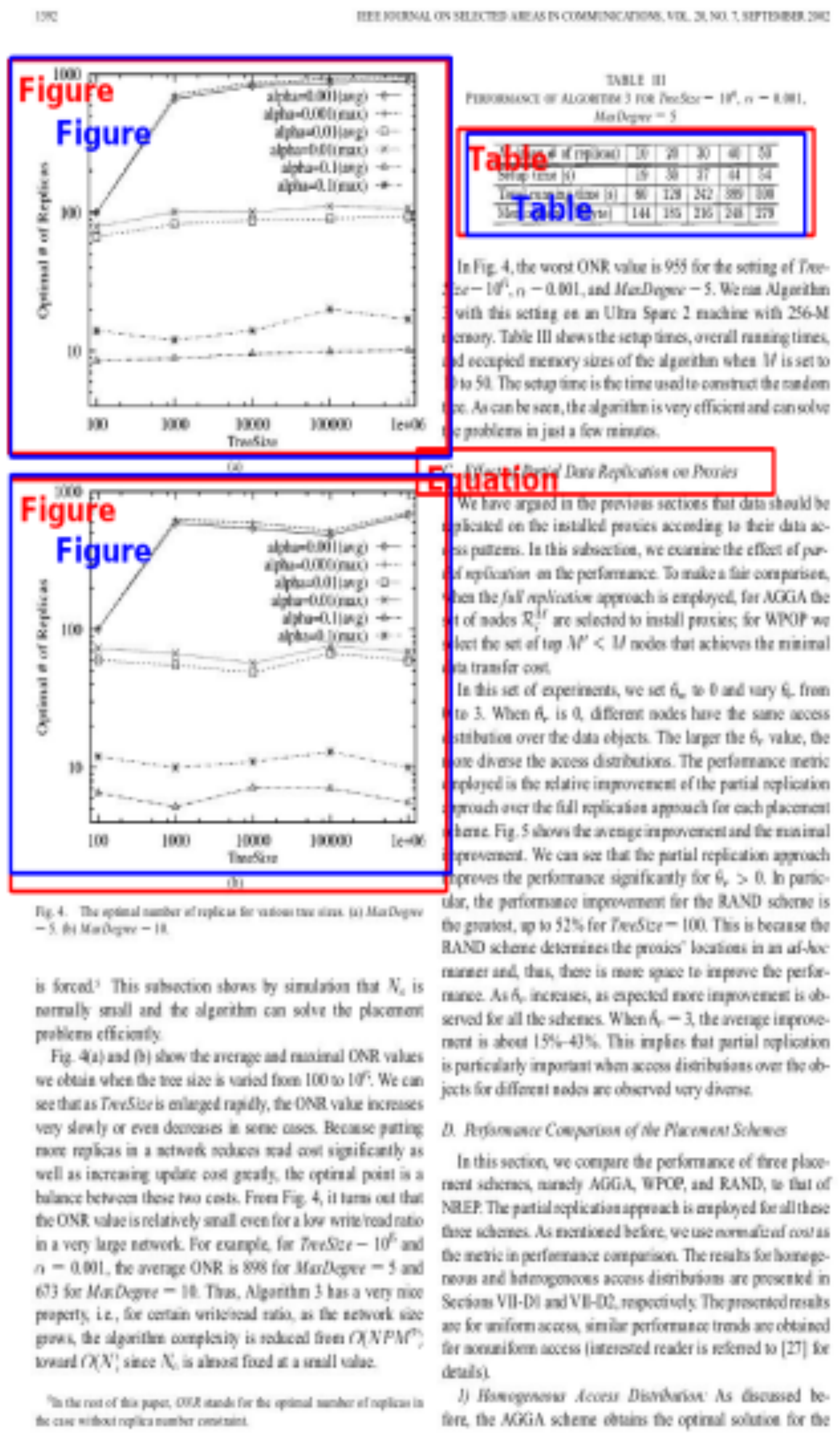

Inaccurate areas of interest

Quantitative Results

IoU = TP / (TP + FP + FN) (segmentation metric)

Average Precision (AP) -- TP / TP + FP
(classification metric)

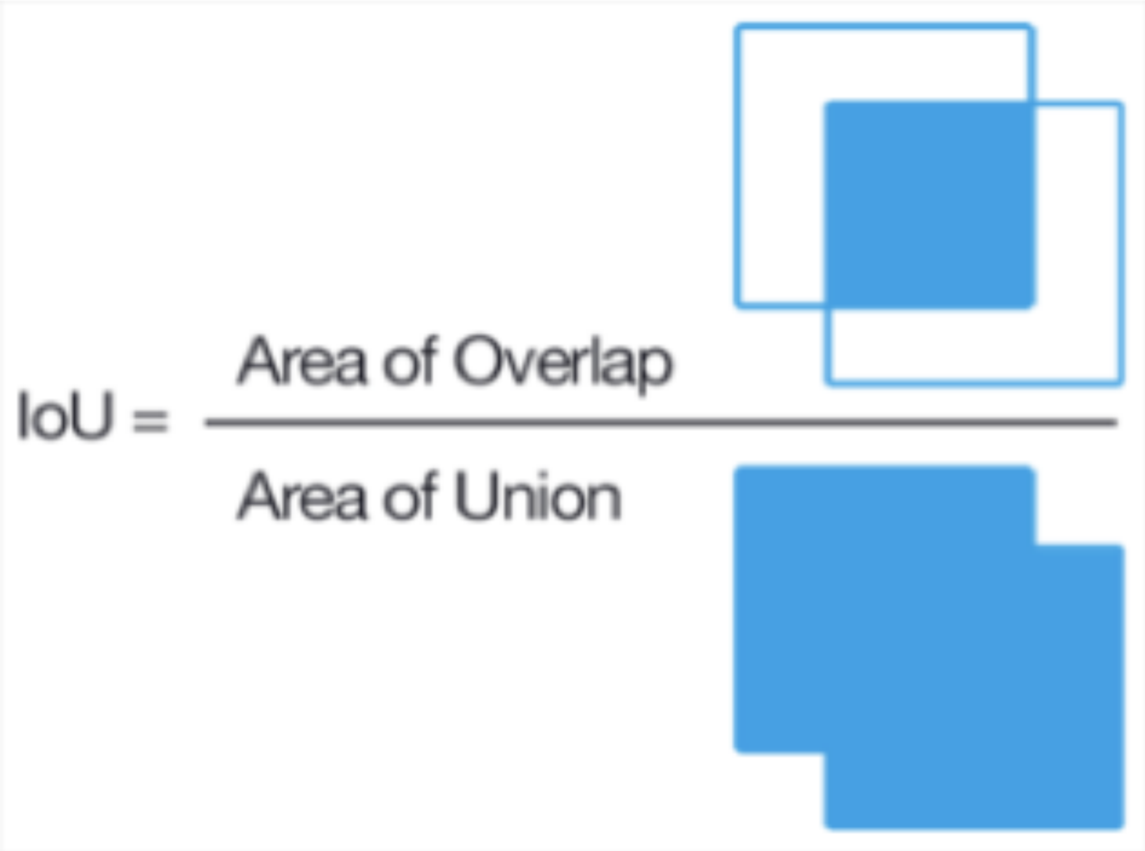

Class Specific

Formula AP: 0.723
Formula IoU: 0.750

Figure AP: 0.734
Figure IoU: 0.768

Table AP: 0.888
Table IOU: 0.877

Next Steps: Improve Segmentation

- Multi-modal segmentation
  - Core insight: we are not utilizing the actual text information in the document we're processing
    - IE: If a body text contains the word abstract, it's the abstract
  - Proposed solution:
    - When a region is proposed in the region proposal network, run OCR on the region and pass the text results to the next layer
- Better attention mechanism for document classification
  - Core insight: tradition segmentation is done in a rich pixel environment -- the background corresponds simply to non labelled objects (think a self driving car on the road)
  - Background in a document corresponds to null space. Partitioning null space is a challenge because there are many possible ways to validly partition it
  - Proposed solution:
    - Compensate for a lack of internal ROI info by providing additional context to an ROI
    - Attend to areas directly surrounding the ROI, then feed that output to the head.

Next Steps: OCR within individual segments

Name	Prior assumptions (mean and range[a])	Posterior mean[b]	Description
$u_0^{PO_4}$	1.65 μmol kg^{-1} yr^{-1} (0.3–3.0)	1.91 μmol kg^{-1} yr^{-1}	maximum PO_4 uptake (removal) rate (Eq. 3)
K^{PO_4}	0.2 μmol kg^{-1} (0.1–0.3)	0.21 μmol kg^{-1}	PO_4 Michaelis-Menton half-saturation concentration (Eq. 3)
r^{POC}	0.05 (0.02–0.08)	0.055	initial proportion of POC export as fraction #2 (Eq. 6)
l^{POC}	600 m (200–1000)	556 m	*e*-folding remineralization depth of POC fraction #1 (Eq. 6)
$r_0^{CaCO_3:POC}$	0.036 (0.015–0.088)[c]	0.022[d]	$CaCO_3$:POC: export rain ratio scalar (Eq. 8)
η	1.5 (1.0–2.0)	1.28	thermodynamic calcification rate power (Eq. 9)
r^{CaCO_3}	0.4 (0.2–0.6)	0.489	initial proportion of $CaCO_3$ export as fraction #2 (Eq. 11)
l^{CaCO_3}	600 m (200–1000)	1055	*e*-folding remineralization depth of $CaCO_3$ fraction #1 (Eq. 11)

Extract text modality to construct Fonduers data model

From Raw Documents to Fonduer's data model

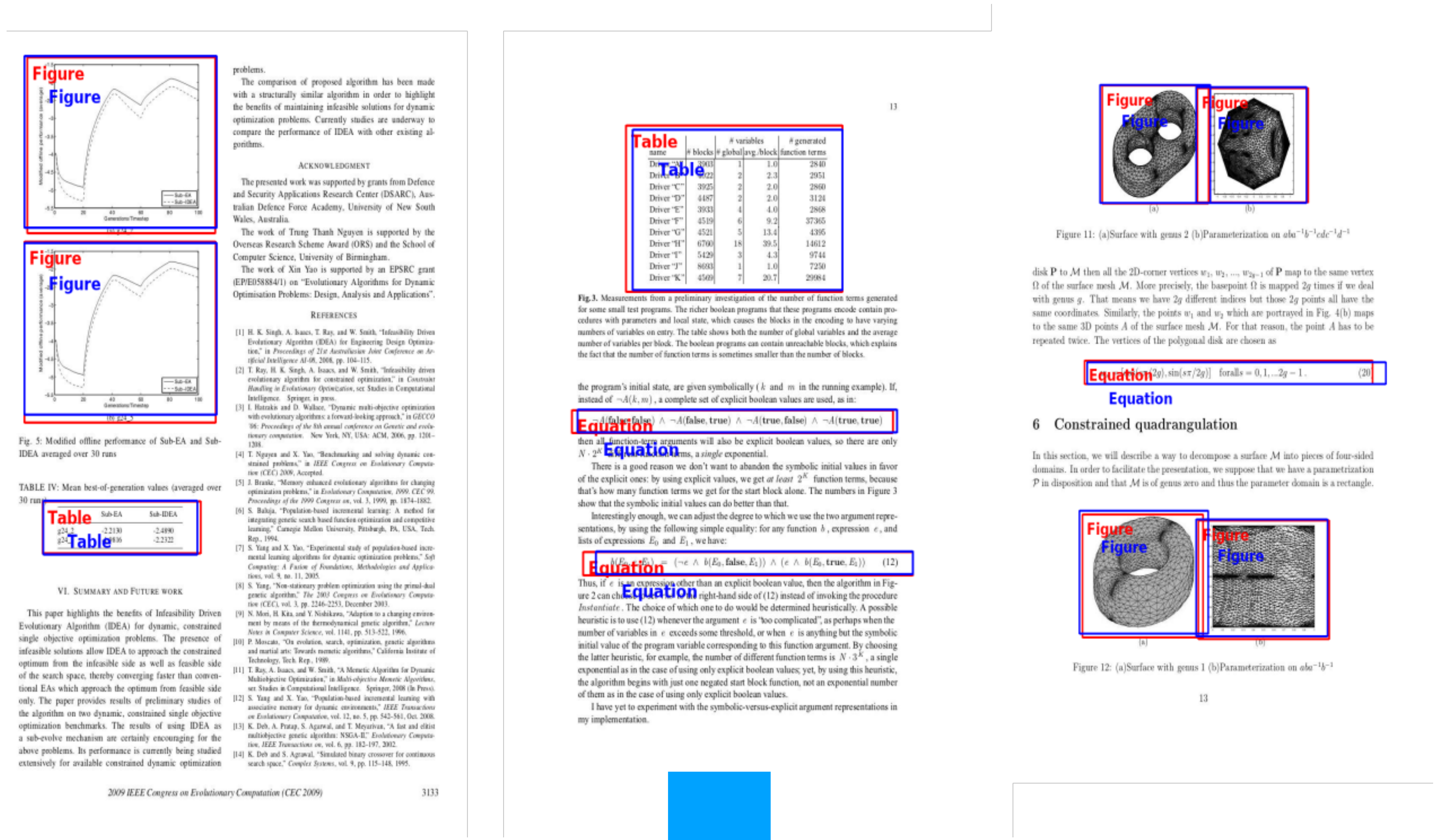

Name	Prior assumptions (mean and range[a])	Posterior mean[b]	Description
$u_0^{PO_4}$	1.65 μmol kg^{-1} yr^{-1} (0.3–3.0)	1.91 μmol kg^{-1} yr^{-1}	maximum PO_4 uptake (removal) rate (Eq. 3)
K^{PO_4}	0.2 μmol kg^{-1} (0.1–0.3)	0.21 μmol kg^{-1}	PO_4 Michaelis-Menton half-saturation concentration (Eq. 3)
r^{POC}	0.05 (0.02–0.08)	0.055	initial proportion of POC export as fraction #2 (Eq. 6)
l^{POC}	600 m (200–1000)	556 m	*e*-folding remineralization depth of POC fraction #1 (Eq. 6)
$r_0^{CaCO_3:POC}$	0.036 (0.015–0.088)[c]	0.022[d]	$CaCO_3$:POC: export rain ratio scalar (Eq. 8)
η	1.5 (1.0–2.0)	1.28	thermodynamic calcification rate power (Eq. 9)
r^{CaCO_3}	0.4 (0.2–0.6)	0.489	initial proportion of $CaCO_3$ export as fraction #2 (Eq. 11)
l^{CaCO_3}	600 m (200–1000)	1055	*e*-folding remineralization depth of $CaCO_3$ fraction #1 (Eq. 11)

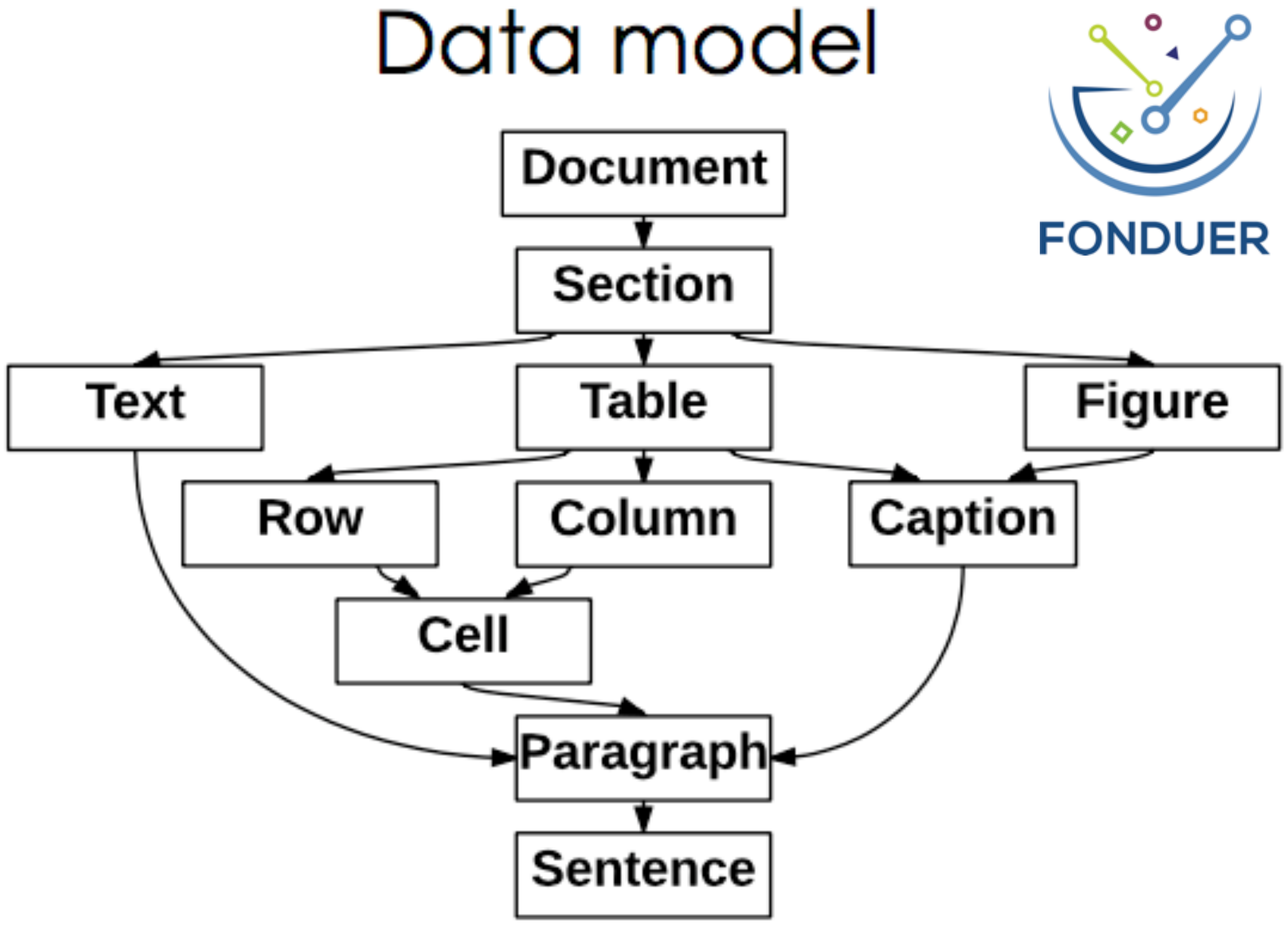

FONDUER

COSMOS: required components

1. Principled, automated access to scientific publications and the computing capacity and infrastructure required to repeatedly analyze them.

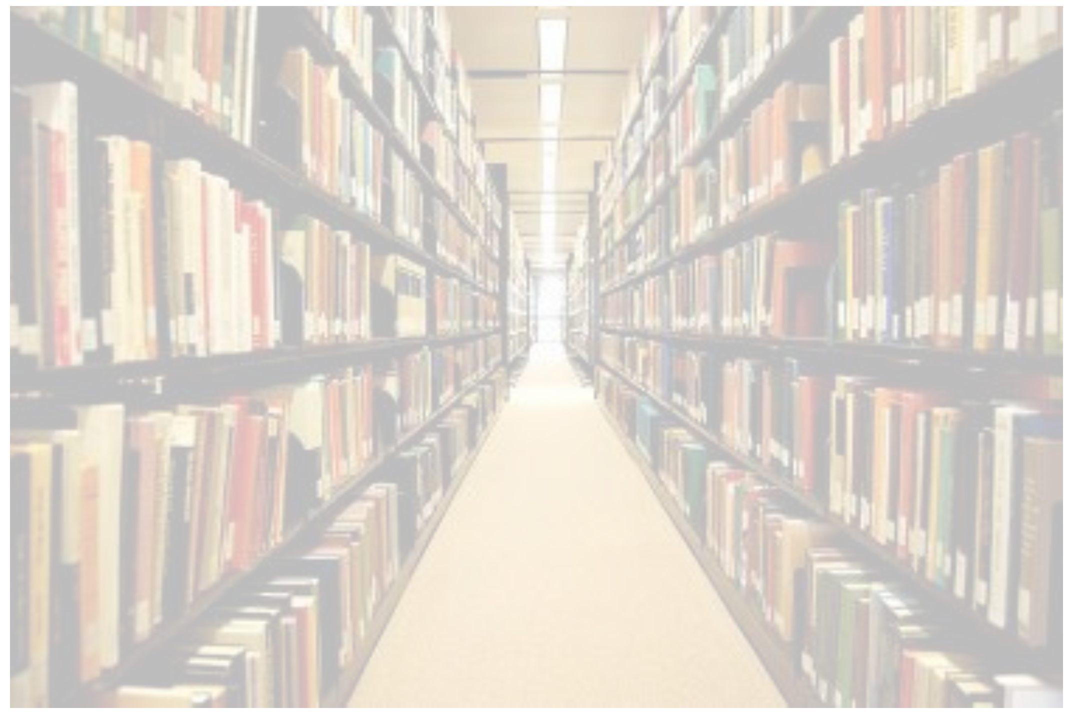

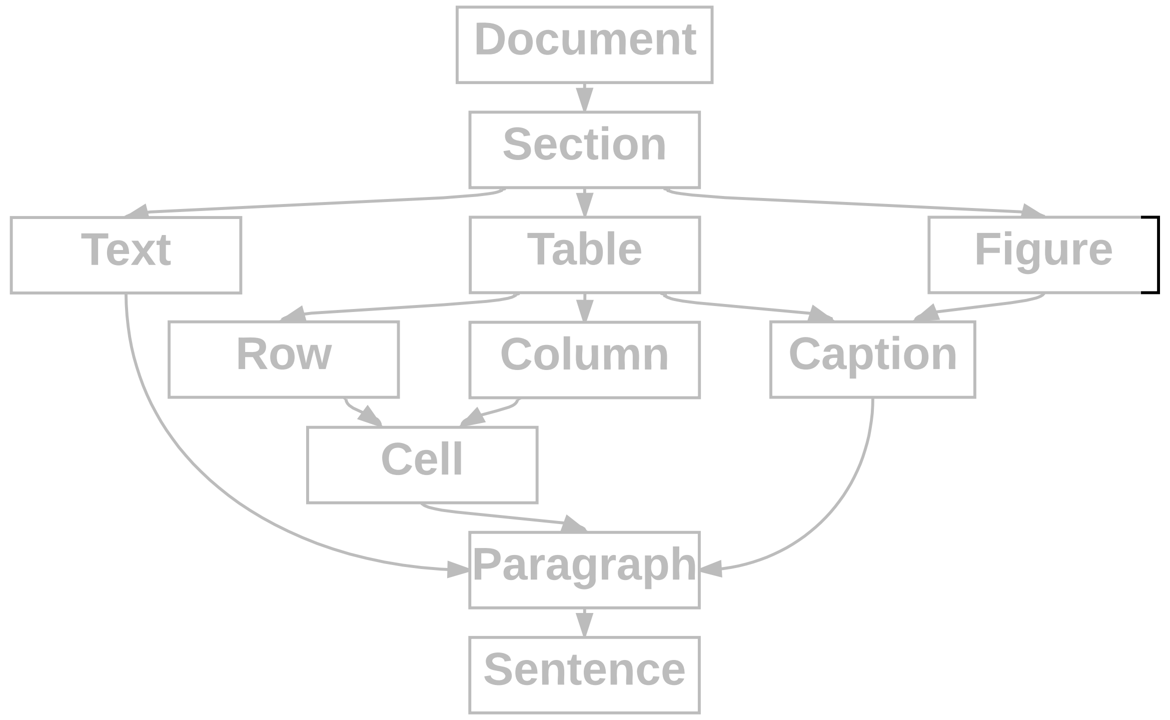

2. Models and techniques to represent and capture multi-modal data within publications.

3. Earth system model with parameterizations and predictions that overlap with many different types of empirical data and observations in publications.

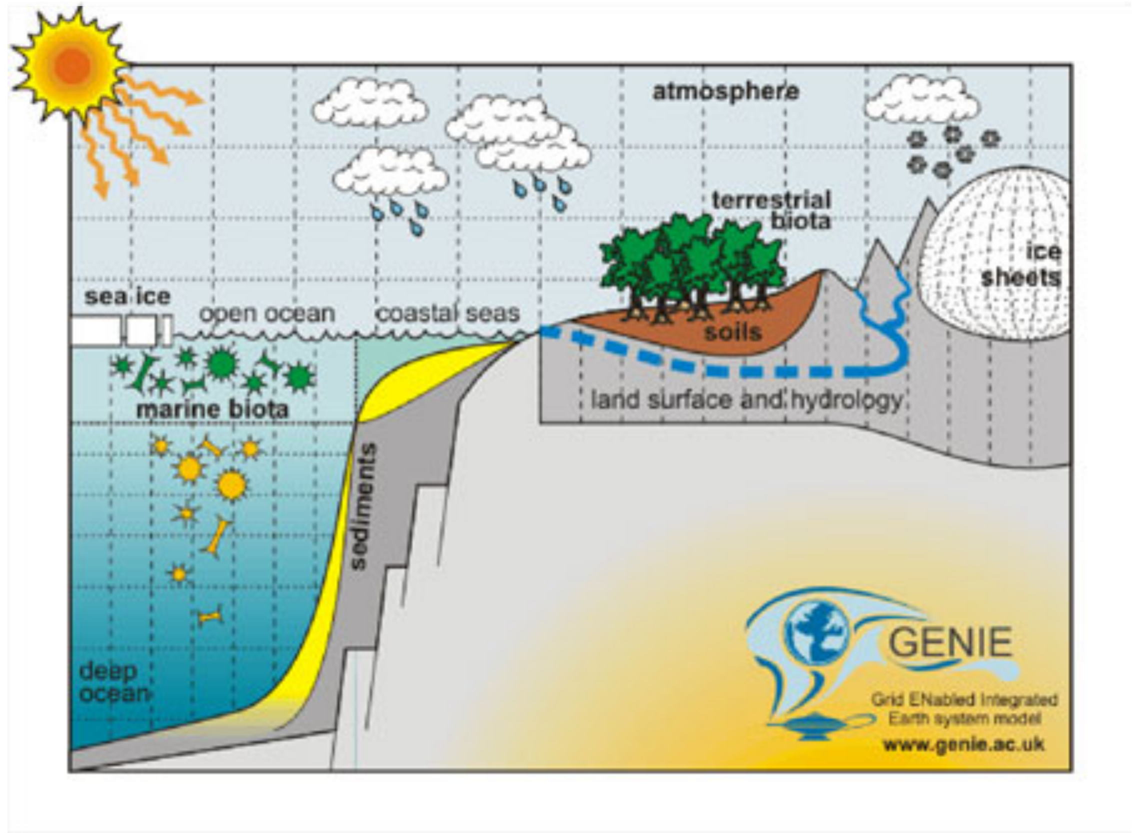

GENIE:
Grid ENabled Integrated Earth system model

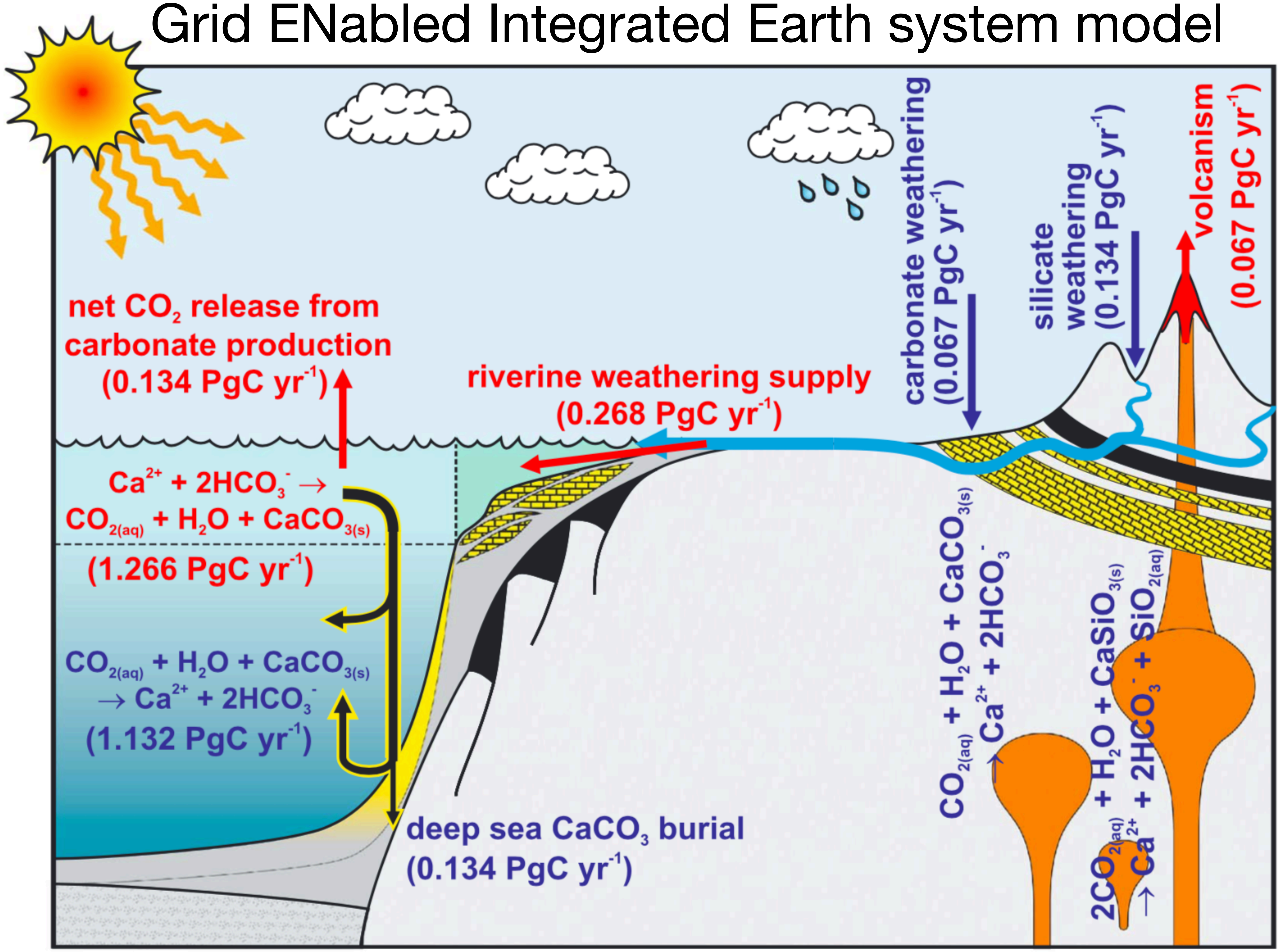

Figure 1. Illustration of the long-term (geological) carbon cycle fluxes. Shown are the long-term fluxes in the GENIE model at steady state. In red are sources of CO_2 to the atmosphere or ocean, and in dark blue are sinks of CO_2.

Colburn et al. (2015)

- Earth system model of intermediate complexity
  - highly parameterized; processes operating over small spatial and temporal scales aggregated into high-level parameterizations
  - more processes can be modeled and integrated over longer periods of model time, but increased uncertainty
- Includes both first-principle physics and empirical observations
- Makes predictions (e.g., stable C isotopic composition of limestone) that can be assessed with samples in field.

Example: cGENIE-predicted sea surface temperature 60 Myr ago

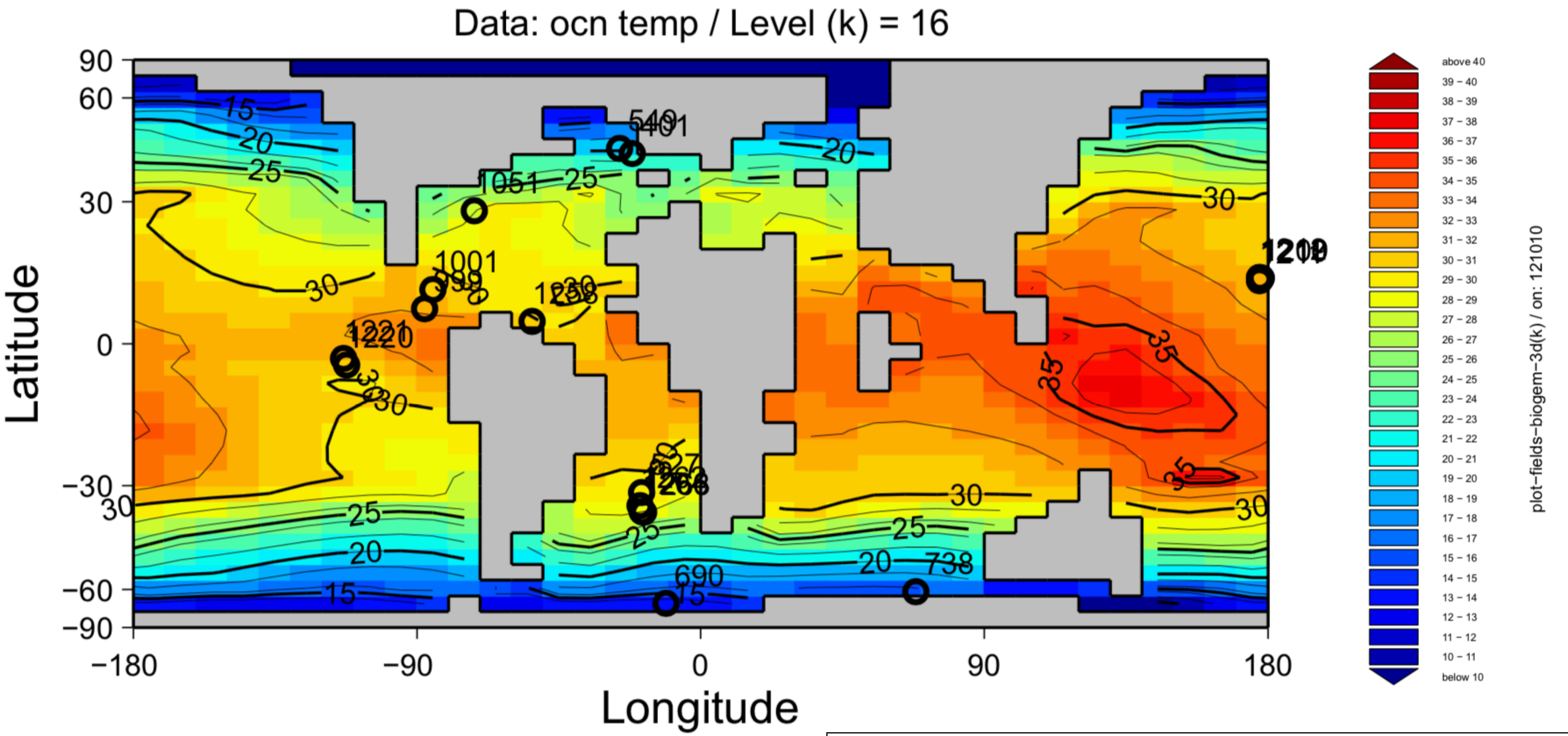

Ridgwell cGENIE user-manual (2017)

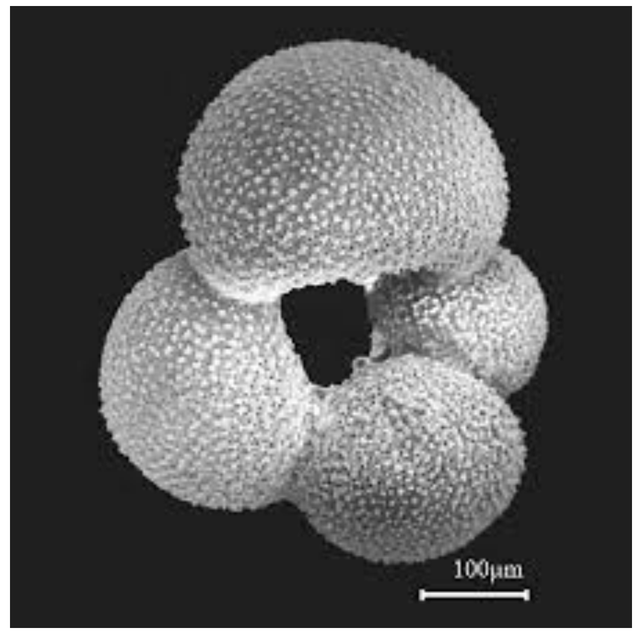

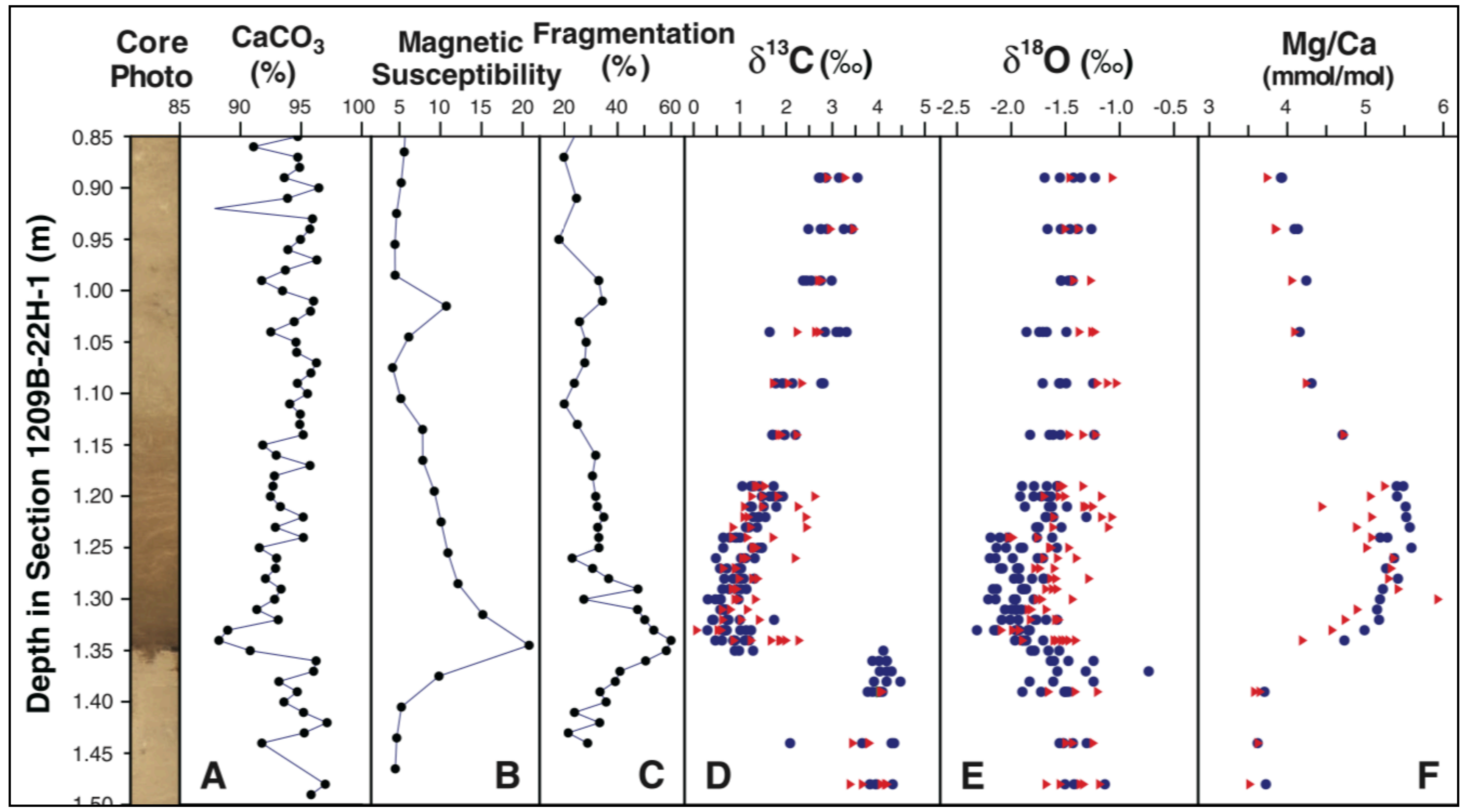

Paleotemperature proxy records
(Saleska et al., 2003)

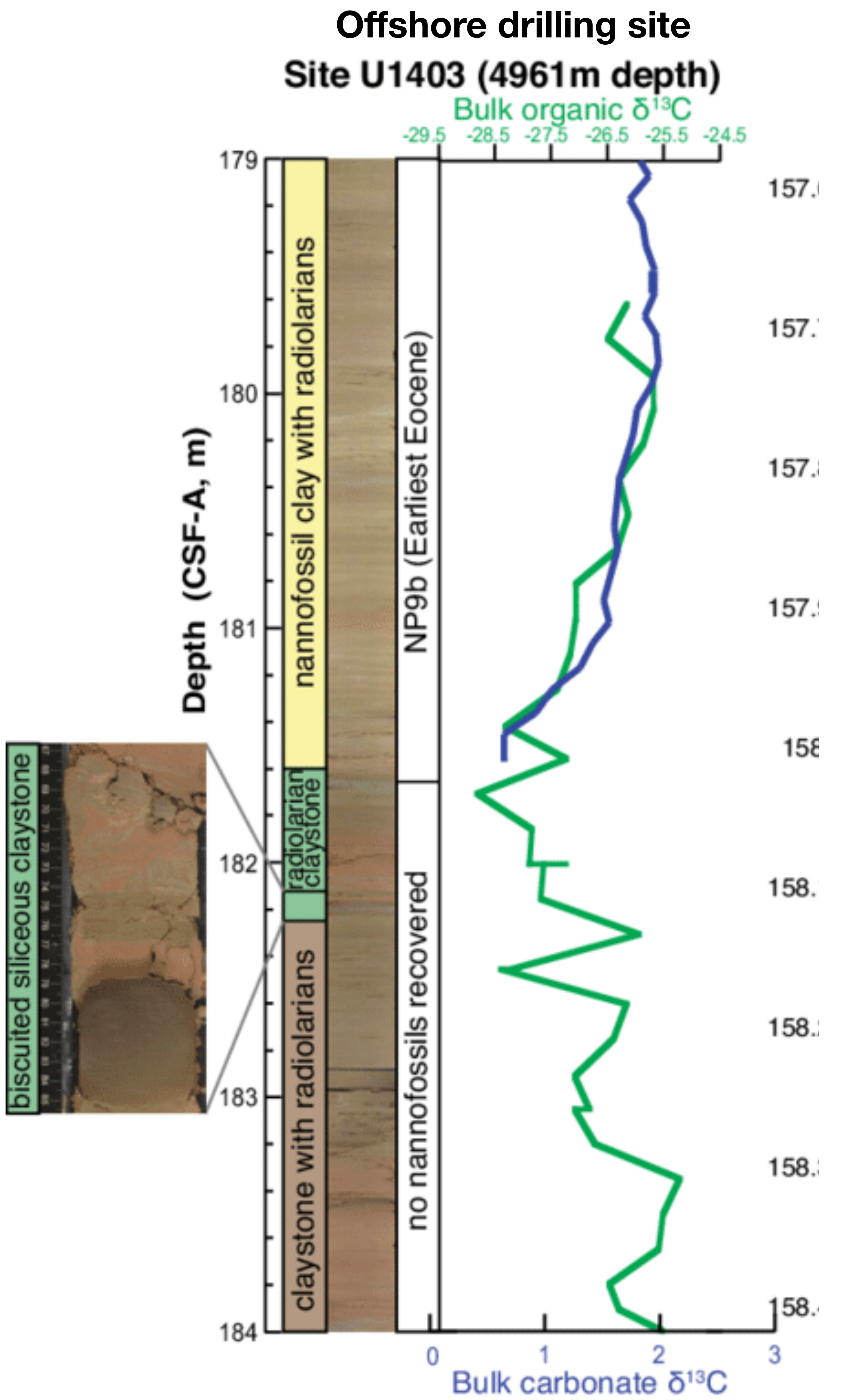

GENIE:
Grid ENabled Integrated Earth system model

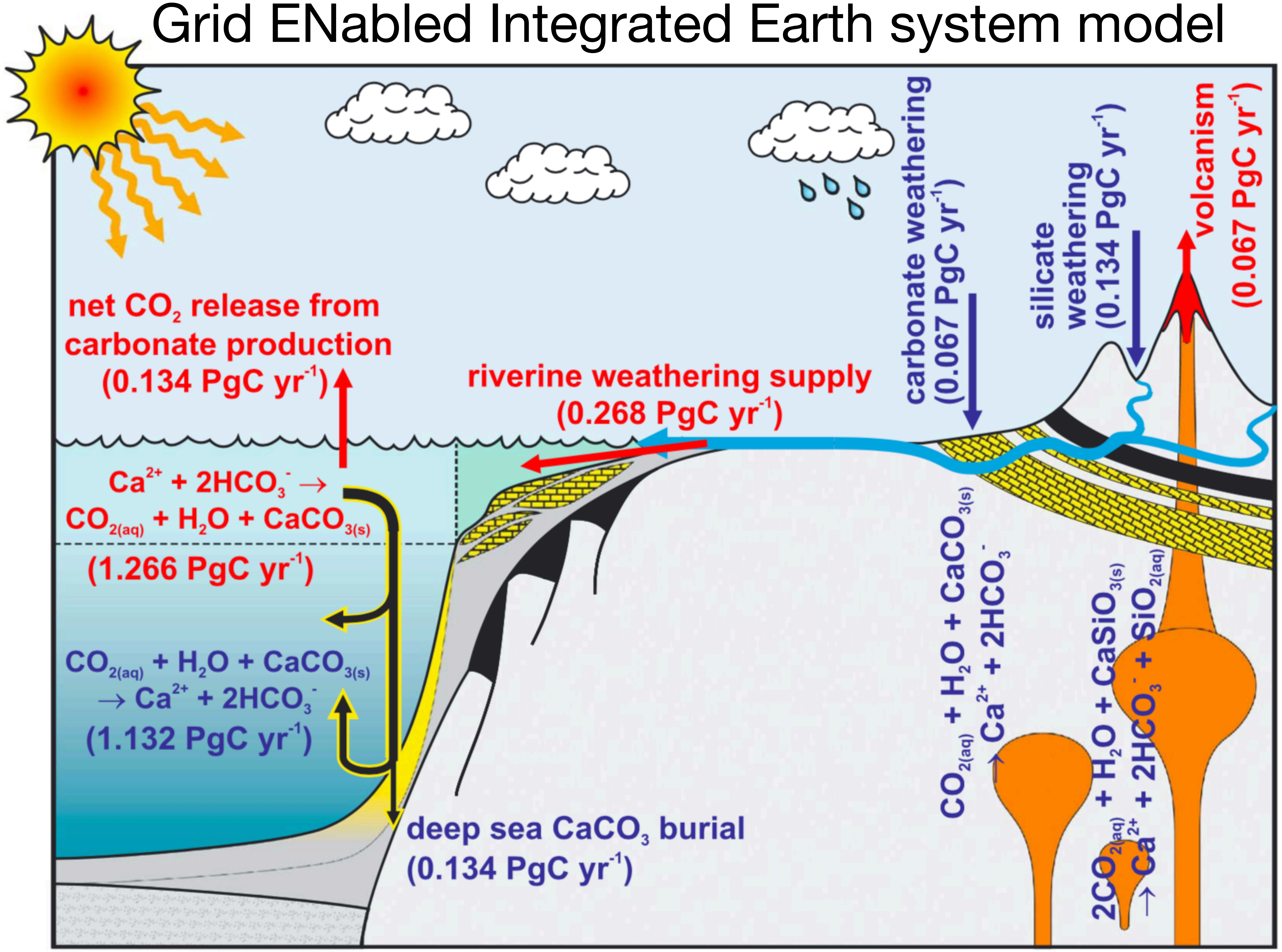

Figure 1. Illustration of the long-term (geological) carbon cycle fluxes. Shown are the long-term fluxes in the GENIE model at steady state. In red are sources of CO_2 to the atmosphere or ocean, and in dark blue are sinks of CO_2.

Colburn et al. (2015)

Phase II

Collaborator Seth Finnegan
UC Berkeley


User Community
user-generated software
GENIE
Grid ENabled Integrated Earth system model
ES model
Application Layer
{ api }
high performance machines to power API and run model curation queries
model code
ASKE COSMOS Layer
Fonduer Layer
Weakly supervised knowledge base construction
High Throughput Computing Layer
storage/backup
NLP/OCR/tool output
table/figure extracts
vocabulary labeling/tuples
HTCondor
High Throughput Computing
encrypted documents, binaries
XML
derived data products
DAGMan Job Q.
Building Block
GeoDeepDive Layer
Digital Library Layer
storage/backup
document metadata storage
secure document storage
~10K/day
Pub.Crawlers
Libraries
UNIVERSITY OF WISCONSIN-MADISON
publisher contracts
Canadian Science Publishing
ELSEVIER
WILEY
GeoDeepDive